การออกแบบเสาค้ำยันที่เหมาะสมสำหรับแหล่งแร่โปแตชของแอ่งโคราช ตะวันออกเฉียงเหนือ ประเทศไทย

นายพิสิทธ เมา

วิทยานิพนธ์นี้เป็นส่วนหนึ่งของการศึกษาตามหลักสูตรปริญญาวิศวกรรมศาสตรมหาบัณฑิต
สาขาวิชาวิศวกรรมทรัพยากรธรณี ภาควิชาวิศวกรรมเหมืองแร่และปิโตรเลียม
คณะวิศวกรรมศาสตร์ จุฬาลงกรณ์มหาวิทยาลัย
ปีการศึกษา 2558

Optimization of Pillar Design for Potash Deposits of Khorat Basin, Northeast Thailand

Mr. Pisith Mao

A Thesis Submitted in Partial Fulfillment of the Requirements
for the Degree of Master of Engineering Program in Georesources Engineering
Department of Mining and Petroleum Engineering
Faculty of Engineering
Chulalongkorn University
Academic Year 2015

Thesis Title	Optimization of Pillar Design for Potash Deposits of Khorat Basin, Northeast Thailand
By	Mr. Pisith Mao
Field of Study	Georesources Engineering
Thesis Advisor	Pipat Laowattanabandit, Ph.D.

Accepted by the Faculty of Engineering, Chulalongkorn University in Partial Fulfillment of the Requirements for the Master's Degree

....Dean of the Faculty of Engineering

(Associate Professor Supot Teachavorasinskun, D.Eng.)

THESIS COMMITTEE

....Chairman

(Associate Professor Dawan Wiwattanadate, Ph.D.)

....Thesis Advisor

(Pipat Laowattanabandit, Ph.D.)

....Examiner

(Assistant Professor Tanate Srisirirojanakorn, Ph.D.)

....External Examiner

(Associate Professor Pornkasem Jongpradist, Ph.D.)

พิสิทธ เมา : การออกแบบเสาค้ำยันที่เหมาะสมสำหรับแหล่งแร่โปแตชของแอ่งโคราชตะวันออกเฉียงเหนือ ประเทศไทย (Optimization of Pillar Design for Potash Deposits of Khorat Basin, Northeast Thailand) อ.ที่ปรึกษาวิทยานิพนธ์หลัก: ดร. พิพัฒน์ เหล่าวัฒนบัณฑิต, 83 หน้า.

แอ่งโคราชเป็นแอ่งหินเกลือที่ใหญ่ที่สุดในประเทศไทย เป็นบริเวณที่มีแร่โปแตชขนาดใหญ่ใต้พื้นที่นี้ โปรแตชในแอ่งโคราชตั้งอยู่ในหน่วยหินมหาสารคามอยู่เหนือเกลือชั้นล่างซึ่งมีความลึกมากกว่า 100 เมตร วิธีการทำเหมืองใต้ดินแบบ “ห้องว่างสลับเสาค้ำยัน” เป็นวิธีการที่เหมาะสมทีสุดวิธีการหนึ่งในการขุดแร่โปแตช อย่างไรก็ตามยังไม่มีการศึกษาการออกแบบเสาค้ำยันอย่างจริงจังสำหรับแร่โปแตชของประเทศไทย

งานวิจัยนี้นำเสนอวิธีการกำหนดขนาดของเสาค้ำยันที่เหมาะสมสำหรับการทำเหมืองแร่โปแตชต้ดินในประทศไทยโดยเฉพาะใต้แอ่งโคราช ซึ่งจะให้สมดุลที่ดีที่สุดระหว่างสัดส่วนการขุดได้และความมั่นคง การออกแบบสำหรับทั้งเสาค้ำยันปกติและเสาค้ำยันผนังกั้น การศึกษาได้ประยุกต์ใช้ทั้งการวิเคราะห์เชิงประจักษ์และเชิงตัวเลข สมการของ Obert และ Duvall ที่ใช้ในการหาความแข็งแรงของเสาค้ำยันในเหมืองถ่านหินใต้ดินได้ถูกนำมาปรับเปลี่ยนในกรณีศึกษาเชิงประจักษ์ซึ่งได้ปรับแก้ด้วยวิธีการเชิงตัวเลขด้วยโปรแกรม FLAC3D คุณสมบัติเชิงกลศาสตร์ของแร่โปแตชจากแอ่งโคราชถูกเลือกนำมาใช้เป็นพารามิเตอร์ในการศึกษา

ผลลัพท์ของขนาดที่เหมาะสมของเสาค้ำยัน ถูกนำเสนอในรูปแบบขอบเขตความปลอดภัยซึ่งได้จากการใช้ ผลลัพท์จากการวิเคราะห์เชิงตัวเลข ขอบเขตความปลอดภัยแสดงให้เห็นการลดลง 10% ของอัตราส่วนขุดได้เมื่อความลึกเพิ่มขึ้นจาก 200 เมตร เป็น 300 เมตร ตามคาคล่วงหน้าสมการเชิงประจักษ์ยังไม่เหมาะสมสำหรับการประมาณความแข็งแรงของเสาค้ำยัน การศึกษาค่าคงที่ของสัดส่วนอ้วนสูงคือกุญแจสำหรับการปรับปรุงแก้ไขสมการดังกล่าวเพื่อให้สามารถใช้ได้กับแร่โปแตชในประเทศไทย ในที่สุดแล้วผลลัพท์ที่ได้แสดงให้เห็นความสามารถของสมการที่แก้ไขแล้วในการประเมินความแข็งแรงเสาค้ำยันอย่างมีประสิทธิผล

ภาควิชา	วิศวกรรมเหมืองแร่และปิโตรเลียม	ลายมือชื่อนิสิต	....
สาขาวิชา	วิศวกรรมทรัพยากรธรณี	ลายมือชื่อ อ.ที่ปรึกษาหลัก	....
ปีการศึกษา	2558		

5770490321 : MAJOR GEORESOURCES ENGINEERING
KEYWORDS: FLAC3D / NUMERICAL MODELLING / PILLAR DESIGN / POTASH UNDERGROUND MINING / ROOM AND PILLAR

PISITH MAO: Optimization of Pillar Design for Potash Deposits of Khorat Basin, Northeast Thailand. ADVISOR: PIPAT LAOWATTANABANDIT, Ph.D., 83 pp.

Khorat Basin is the biggest evaporite basin of Thailand where there is a huge potash deposit underneath this basin. Potash in Khorat Basin is located in Maha Sarakham formation overlying the lower rock salt which have the depth of more than hundred meters. Underground mining method called 'Room and Pillar' is one of the most suitable methods to extract potash. However, there is no intensive study on pillar design for potash of Thailand yet.

This work offers a procedure to determine the optimal dimension of pillar for underground potash mine in Thailand, especially under Khorat, which in turn provides the best balance between extraction ratio and stability. The design is focused on both regular pillar and barrier pillar. The study has been carried out using both empirical and numerical analysis. Obert and Duvall relation equation, for estimation the pillar strength in an underground coal mine, is adapted in empirical case studies which is then calibrated with numerical modeling by using FLAC3D. Mechanical properties of potash from Khorat Basin are chosen as the input parameters of the study.

The result of optimal dimension of pillar is represented by safety envelop which is constructed utilizing simulated result from numerical analysis. The safety envelops illustrate the decrease of 10% in extraction ratio when the depth is increased from 200m to 300m. As expected, the empirical equation is not suitable for estimating strength of potash in Thailand yet. The study of slenderness constants is the key for modifying the equation above to be applicable for potash in Thailand. The result finally shows the capability of modified formulas for effectively estimated pillar strength.

Department:	Mining and Petroleum Engineering	Student's Signature	....
		Advisor's Signature	....
Field of Study:	Georesources Engineering		
Academic Year:	2015		

ACKNOWLEDGEMENTS

Firstly, I would like to express my greatest gratitude to AUN/SEED-Net program from JICA who provided a full financial support for me during the time of my master degree. I also would like to thank Chulalongkorn University, especially department of Mining and Petroleum Engineering for giving me the admission to study my master degree.

Secondly, I am grateful to acknowledge my advisor, Dr. PIPAT LAOWATTANABANDIT, for his hard work in guiding and advising me during my research. He also provided me the needed field data that make this research possible.

Thirdly, I would like to pay highly respect to all the lecturers in Mining and Petroleum Engineering Department for proving me a great background in geo-resources engineering which give me enough capability for doing this research. A big thank to Ms. SIRILUCK SANGLAOR for solving any problems regarding to the administration and providing the all the access to department facilities.

I am really appreciated to all my friends and seniors from all the nation for their support and contribution of making my student life in Thailand better.

Finally, I would like to express my warmest gratitude and love to my parents and family for their loves, believes, supports and encouragements which giving me enough strength to fight with any problems that I faced in life.

CONTENTS

Page

Page

Page

LIST OF FIGURES

LIST OF TABLES

CHAPTER 1

INTRODUCTION

1.1. Background

Thailand is the country that hosts two giant formations of evaporite basins which were formed in Cretaceous age. According to Garrett [1], the potash deposits are divided into two main areas, the northern area which is called Sakhon Nakhon Basin, covering 21,000 km^2 and the southern area which is called Khorat Basin, covering 40,000 to 50,000 km^2 as shown in Figure 1-1.

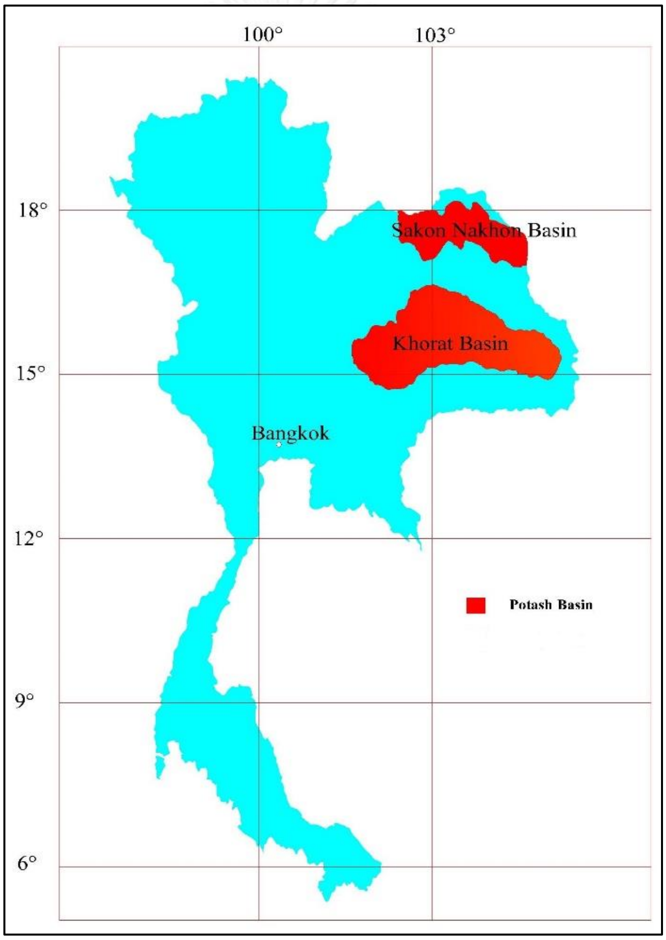

Figure 1-1 Location Map of Evaporite Basins

Even though there is not a clear agreement on depositional model for potash, there are a lot of evidences showed that marine evaporite environment should be considered to be the most common formation of potash deposits [1]. Based on the study of Suwanich [2], Khorat group has three main formations: Khok Kruat formation, Maha Sarakham formation and Phutok formation as illustrated in Table 1-1. In Maha Sarakham formation, there are three main layers of rock salt. Potash deposits of Thailand are located in Maha Sarakham formation overlying the lower rock salt. In the potash zone, two types of potash mineral are found. Carnallite ($KMgCl_3.6H_2O$) is formed as primary deposits. It is the most common potash mineral which has the equivalent K_2O about 15 to 20%. Sylvite (KCl) is an altered form of carnallite resulted from slowly leaching by groundwater in the secondary deposits. It is the best potash mineral since it has high content of K_2O around 20 to 30%.

Table 1-1 General Stratigraphy of Khorat Group [2]

Group	Formation	Member
Khorat		Topsoil
	Phutok	Upper Clastic
	Maha Sarakham	Upper Salt
		Middle Clastic
		Middle Salt
		Lower Clastic
		Potash Zone
		Lower Salt
		Basal Anhydrite
	Khok Kruat	Conglomerate, Sandstone

He also found out the identical correlation between both evaporite basins of Thailand. This evident proves the two basins are one big basin before the development of Phu Phan Range which separated them into two basins nowadays. Figure 1-2 shows general structure of rock salt in Maha Sarakham formation. In addition, Japakasetr and Workman [3] had drawn a detail general stratigraphy of the Khorat Basin which is illustrated in the Figure 1-3.

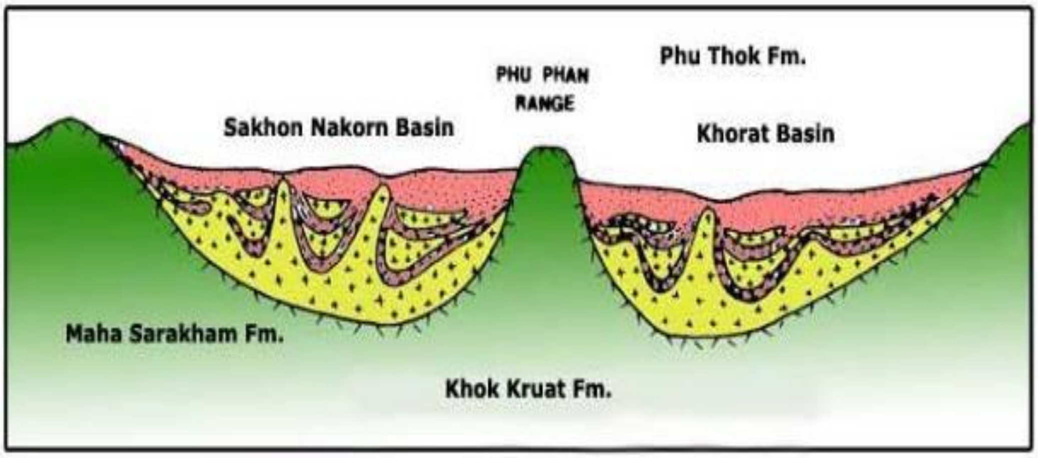

Figure 1-2 Structure of salt rock in Maha Sarakham Formation [2]

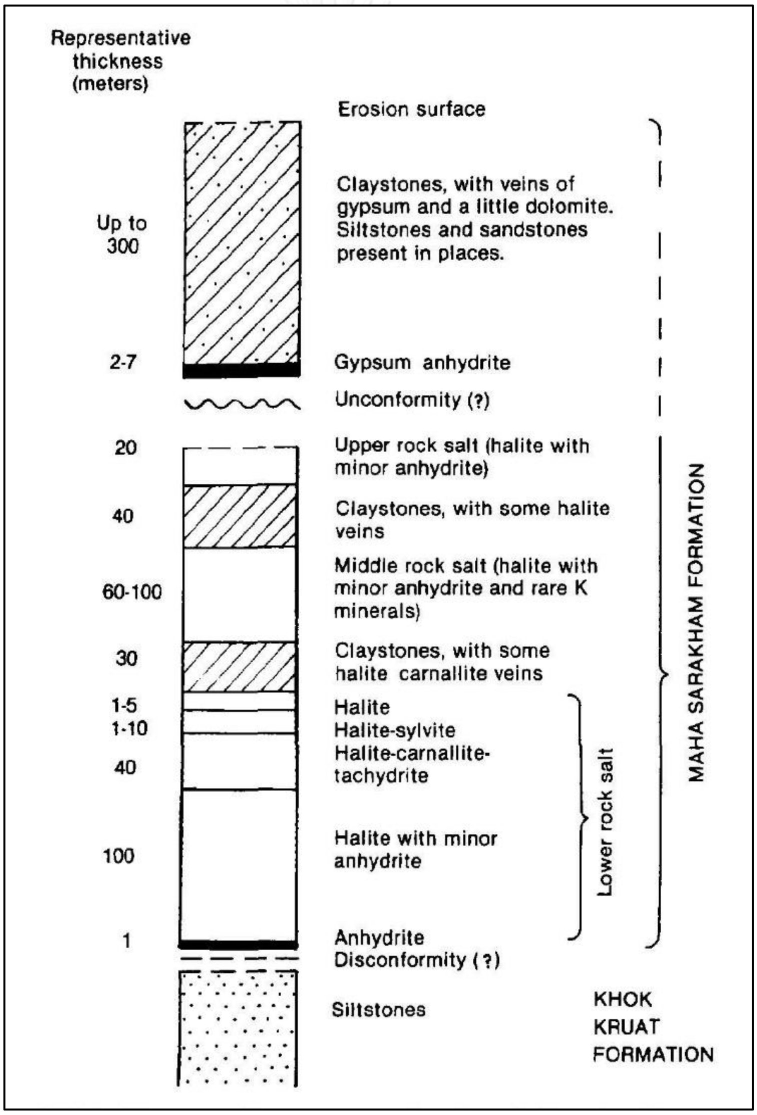

Figure 1-3 General stratigraphy of the Khorat Basin [3]

In terms of potash mining, there are two most common methods which have been successfully used and have been developed for many decades. The first method is called solution mining, which according to [4], it is defined by all terms of ore extraction method that inject heated water into the ore deposit to leach or dissolve the ore. After the ore is dissolved, the solution is recovered back to the surface for further ore processing. The second one is much safer in terms of stability which is known as room and pillar. This method is referred to as a type of underground mining method which left some part of the ore as pillar to support the stress generated from the upper ground [5]. The horizontal and small angle bed structure of the potash formation in Thailand, provides a suitable condition to develop this underground mining technique, called “Room and Pillar”.

Mine design will take an important role at the beginning stage of resources extraction. A good design provides an optimum profit during mining operation. The maximum extraction of the ore is a goal of every mining activity including potash mining. However, it should not be the only main factor that should be considered in selecting and designing underground mine. In addition, this decision should be made by considering many other main factors which include mine stability and safety of the mine.

1.2. Problem Statement

Underground mining is one of the most complicated method to take out the mineral ore from the earth. Potash underground mining is not different. Keeping the stability of the mine while excavating high proportion of potash from the ground is a big challenge for mine design. Underground mine opening and pillar size play an important role for this challenge. The problem is that this factor has a close relationship with mechanic properties and the depth of the potash deposit. Potash from different country has different properties and have different depth. As a result, this factor is really flexible depend on where the potash came from. A new research need to be conducted in order to develop a new suitable opening as well as optimum pillar size for potash underground mine for Thailand to kreep the mine stable while maximizing the recovery of potash from the ground.

1.3. Objectives of the Study

The objectives of this research are:

- Optimize underground mine pillar design by defining the most suitable pillar dimensions based upon
    - Mechanic properties of potash from Khorat basin
    - Depth of the deposit
    - Other local factors
- Develop formulas that are capable of effectively estimating pillar strength for both pillar and barrier pillar in underground pillar design for potash deposit of Thailand in Khorat basin.

CHAPTER 2
CONCEPT AND THEORY

2.1. Room and Pillar Design

The Layout of room and pillar is fairly simple in underground mining. The ore is only mined in the room stope. The ore that left out in a series for supporting in the mine is considered as the pillar (Figure 2-1). The layout of the mine is separated into panels as the layout system required the stress relief for the benefit during excavation operation [1]. Panels system also provides a great advantage for preventing the failure of the whole mine. In the condition where a panel is collapsed for some reasons, the excavation operation of ore is still possible for other panels. All panels are separated by the barrier pillar.

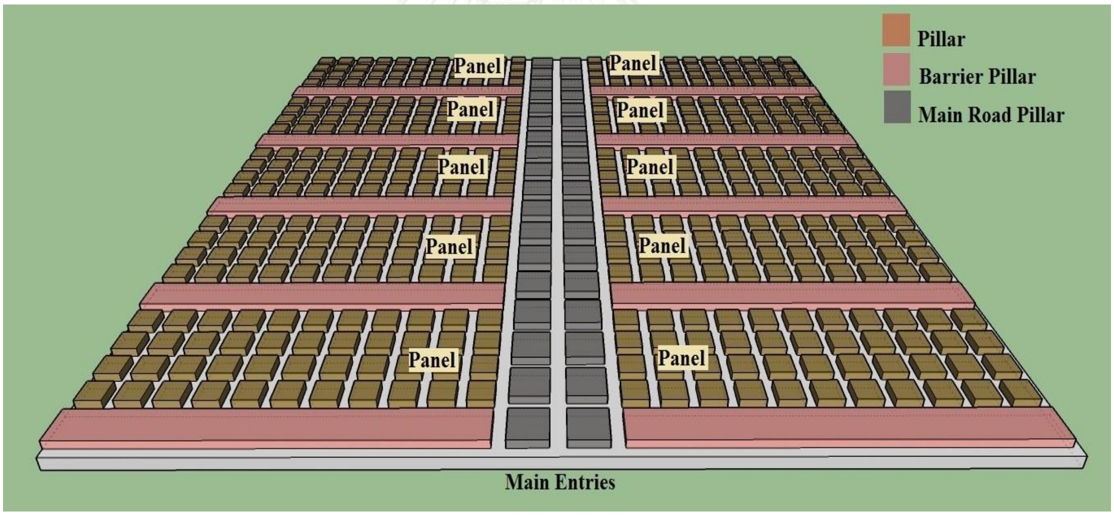

Figure 2-1 Basic Layout of underground mine “Room and Pillar”

Pillar dimension, mining height and depth of potash seam are the keys criteria that affect mine production and stability. This research will study on the relationship between these key criteria in order to optimize pillar design for potash underground room and pillar.

2.2. Pillar Stress Estimation

According to Livingstone et. al. [6], the average pillar stress in underground mine design is the weight of the overburdens rock. The following Equation 2-1 is used to represent the average pillar stress for rectangular pillar shape where γ is represent the unit weight of the rock mass, the depth of overburden is h as well as e is the percentage of extraction which are illustrated in the Figure 2-2. According to Lau [7], the extraction ratio can be calculated using the Equation 2-2 which is related to the room width w_R and pillar width w. Figure 2-3 demonstrated the top view of the barrier pillar. By applying the same concept of extraction ratio for barrier pillar with the length l, extraction ratio for barrier pillar can be calculated using Equation 2-3.

$$\sigma_{APS} = \frac{\gamma \times h}{1-e} \qquad \textit{Equation 2-1}$$

$$e = \frac{(w_R + w)^2 - w^2}{(w_R + w)^2} \qquad \textit{Equation 2-2}$$

$$e = \frac{\left((w_{Pn} + w_B)\times 1\right) - \left(w_B \times l\right)}{\left((w_{Pn} + w_B)\times 1\right)} = \frac{w_{Pn}}{(w_{Pn} + w_B)} \qquad \textit{Equation 2-3}$$

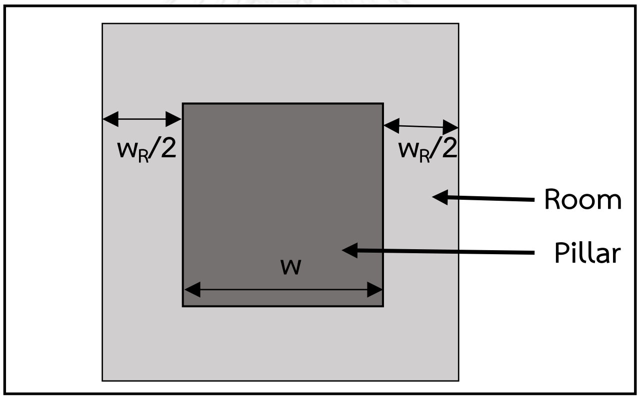

Figure 2-2 Top view of the pillar

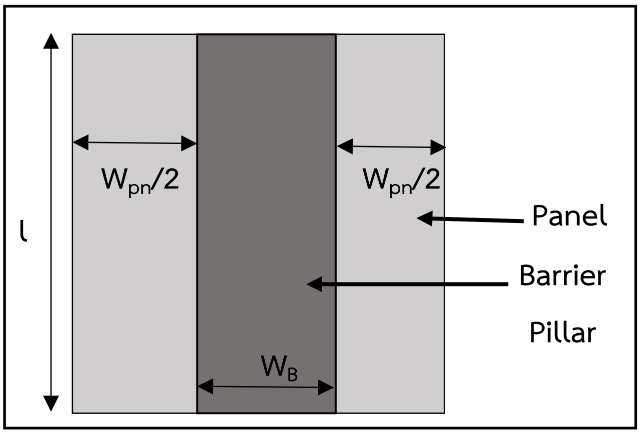

Figure 2-3 Top view of the barrier pillar

2.3. In-situ Stress

In situ stress is the stress that already presents in initial state of rock mass before any excavation begins. These stress present in both vertical, σ_v and horizontal, σ_h which cause by gravity, geological structure and many other tectonic activities [8]. The vertical in situ stress can be simply presented by the multiplication between the depth *H* and unit weight of the material γ . For multiple seam formation this stress can be generalized into Equation 2-4.

$$\sigma_v = \sum_{i=1}^{n} H_i \gamma_i \qquad \textit{Equation 2-4}$$

The relation between vertical and horizontal in situ stress is associated with a constant *K* which represented in Equation 2-5. From his study, this relationship can be expressed in Equation 2-6 which is a relation between elastic constants, *E* and υ coefficient of thermal expansion, *β* geothermal gradient, *G*. However, if the thermal effect is overlooked the horizontal in situ stress can be presented as Equation 2-7.

$$K = \frac{\sigma_h}{\sigma_v} \qquad \textit{Equation 2-5}$$

$$\sigma_h = \frac{\nu}{1-\nu}\sigma_v + \frac{\beta E G}{1-\nu}(H + 1000) \qquad \textit{Equation 2-6}$$

$$\sigma_h = \frac{\nu}{1-\nu}\sigma_v \qquad \textit{Equation 2-7}$$

2.4. Pillar Strength Estimation

Pillar strength is also known as the maximum resistance of how tough the pillar is able to withstand and support the stress resulted from the weight of the overburden rock in order to keep the whole underground mining structure in stable condition [9]. The study of Zipf [10] had shown pillar strength formulation which is based on the Obert and Duvall relation. The formula of pillar strength can be expressed in the Equation 2-8 in which σ_p represent pillar strength and σ_S is the strength of the rock sample. The width and height of the pillar is symbolized respectively by W and H. The constant α and β are developed from the effect of pillar shape.

$$\sigma_P = \sigma_S(\alpha + \beta \frac{w}{h}) \qquad \textit{Equation 2-8}$$

According to Jeremic [11], the size of the sample spacimen has an effect on the its compressive strength which leads to an error in defining the pillar strength. In order to demonstrate the effect of size on pillar strength, various sizes of the cubic samples are run under the unconfined compressive strength. Based on the size effect theory, the bigger size of the sample spacimen, the lower compressive strength it will be. This variation of strength of the material will become stable when the size of the sample reaches the critical size limit. Above the critical size limit the contant compressive strength is equal to σ_S. In order to generated an effectively estimation on pillar strength, there is a requirement to define the strength of material at a critical size limit.

Slenderness of the sample is also another factor that is influent on pillar strength estimation the same as the concept of shape effect [12]. Shape effect on pillar strength is represented by slenderness constants which can be estimated from the study of UCS strength of various w/h ratios. The study in underground coal mine by Bieniawski [13] had drawn the attention to slenderness constants. The result from his study reached to the conclusion that the value of slenderness constants α and β are 0.64 and 0.36 respectively for estimating strength of square pillar. These values are used to modified the Equation 2-8 to a new Bieniawski formula that is suitable for estimating coal pillar strength as show in Equation 2-9.

$$\sigma_P = \sigma_S (0.64 + 0.36 \frac{w}{h}) \qquad \textit{Equation 2-9}$$

Mark, Chase [14] have extended the study of the slenderness constants for estimating strength of rectangular pillar in high-wall coal mining. In the case where the length of the pillar much longer that width of the pillar, slenderness constants α and β are 0.64 and 0.54 respectively which lead to the formation of Mark and Bieniawski formula of pillar strength estimation for long length pillar as shown in Equation 2-10. The formula in Equation 2-9 and 2-10 are used for pillar and barrier pillar strength estimation respectively in empirical analysis of this research.

$$\sigma_P = \sigma_S (0.64 + 0.54 \frac{w}{h}) \qquad \textit{Equation 2-10}$$

2.5. Strength Parameters and Piecewise Function for Strain Softening

This section will discuss the relationship between UCS strength with cohesion and friction angle. Some previous researches stress that cohesion can be estimated from UCS strength with internal friction angle. The research by Vermeer and De Borst [15] provided this relation in an equation as shown in the Equation 2-11.

$$c = \frac{\sigma_c (1 - \sin\phi)}{2\cos\phi}$$ *Equation 2-11*

Mohan, Sheorey [16]had generated a piecewise function from strain softening material which is represented as the change of shear strain compare with cohesion and internal friction angle. This relation can be found in Table 2-1. The residual cohesion is equal to zero while residual internal friction is equal to internal friction angle minus five degrees.

Table 2-1 Change of cohesion and friction angle vs. shear strain

Shear Strain	Cohesion (MPa)	Friction Angle (Degree)
0.000	c	ϕ
0.005	c/5	ϕ-2.5
0.010	0	ϕ-5
0.050	0	ϕ-5

2.6. Safety Factor

Safety factor is main factor consideration in designing the pillars system for stability concern. It can be expressed by the division of the strength of the pillar with the average stress of the pillar as shown in the Equation 2-12. [9].

$$FOS = \frac{\sigma_P}{\sigma_{APS}}$$ *Equation 2-12*

Based on Jeremic [11], factor of safety of all the pillar design is recommended to approximately 1.1 for temporary pillar support, 1.3 for intermediate pillar support and 1.6 for the long term support. These value of safety factors are the most widely accept in designing underground pillar support.

CHAPTER 3
LITERATURE REVIEW

3.1. Numerical Estimation of Pillar Strength in Coal Mine

The research of Mohan, Sheorey [16] which study numerical estimation strength in coal mine, had compared pillar strength estimation from both empirical and numerical simulation. Two group of pillar cases, failed and stable cases, is taken from Indian coal fields for this study. This study use Equation 3-1 and 3-2 for empirical estimation of pillar strength and stress respectively.

$$S = 0.27\sigma_C h^{-0.36} + \left(\frac{H}{250}+1\right)\left(\frac{w}{h}-1\right) \qquad \textit{Equation 3-1}$$

$$P = 0.025H\frac{(w+w_R)^2}{w^2} \qquad \textit{Equation 3-2}$$

Mohan, Sheorey [16] used FLAC3D for numerical simulation of pillar strength estimation. In situ stresses and other input parameter are pre-estimated before the simulations. Strength parameters are estimated using Sheorey's empirical rock failure criteria. In order to save simulated time, only a quarter of the pillar model is used for the simulation. For numerical analysis only the pillar strengths are simulated. Stresses were taken from empirical. A series of FLAC code and Fish function were coded in order to define the peak stress with the strain. The results from both methods were compared together. The outcome from this research can be concluded that numerical modeling with stain softening is a better alternative to other pillar strength estimation. Most of empirical formulation is concerned with both size and w/h ratio separately. However, Mohan, Sheorey [16] found out that for coal the size effect on the strength can be eliminated after size of 1.5m.

3.2. Numerical Estimation of the Strength of St. Peter Sandstone Pillars

Arthur and Ge [17] draw our attention to the study of numerical modeling of St. Peter sandstone pillar in Iowa. The purpose of this study is to improve and develop a new empirical formulation from the previous empirical method which had been develop in the past three decades as this old empirical method provided a very challenging in designing room and pillar underground mining for this St. Peter sandstone. There are 32 cases study of sable pillar in Iowa for this research. The methods used in this research is to use numerical simulation of the stable pillar to modify the empirical formula for pillar strength estimation. Both strength and stress of the pillar were estimated using empirical and numerical analysis. There are two empirical formulas for estimating the strength of the pillar including Obert and Duvall formula and Salamon and Munro formula which are shown in Equation 3-3 and 3-4. Empirical stress estimation is performed using Equation 3-2.

$$\sigma_P = \sigma_S \left(0.778 + 0.22 \times \frac{w}{h}\right) \qquad \textit{Equation 3-3}$$

$$\sigma_P = \sigma_S \frac{w^{0.5}}{h^{0.75}} \qquad \textit{Equation 3-4}$$

$$\sigma_P = \frac{228}{h^{1.24}}\left(0.778 + 0.22 \times \frac{w}{h}\right) \qquad \textit{Equation 3-5}$$

FLAC3D is used in this study for simulating the strength and stress of the pillar. The strength of the pillar is coded and taken out from the peak of average stress of the pillar with the pillar strain. Pillar stress is also coded and define as the residual stress. After comparing the result from both methods, it can be concluded that the utilization of Equation 3-3 provided a similar result to the numerical estimation but not totally satisfactory agreement. So there is a requirement of modifying this equation. Equation 3-4 on the other hand, provided a highly differentiated result of strength estimation which lead to underestimating the St. Peter sandstone pillar strength. The result from the study of the size effect provide a key to modify Equation 3-3 into an effective empirical formula for estimation pillar strength for this kind of material. The result comparison between modified formula in Equation 3-5 provided a good agreement in estimated the pillar strength for St. Peter sandstone pillar.

3.3. Empirical Approached for Design of Web Pillar in Highwall Mining

Verma, Porathur [18] had reviewed and analyzed empirical approached for design web pillars in highwall mining. This investigation used three difference empirical approaches for estimating pillar strength from Mark_Bieniawski in Equation 2-10, CSIRO (Australia) in Equation 3-6 and CIMFR (Sheorey's) in Equation 3-1.

$$\sigma_P = \sigma_S \left(0.64 + 0.36 \times \left(0.69 + 0.44 \frac{w}{h} \right) \frac{w}{h} \right) \qquad \textit{Equation 3-6}$$

Many case studies from India had been adopted with difference criteria from many locations. The results from these empirical approaches are compared with numerical simulation in FLAC3D which used model strain softening. From this study, this empirical approaches can be used for pillar strength estimation with high confident. It also come to a conclusion that highlight the utilization of CIMFR equation can be used in a wider range of strength estimation compare to the other two equations as it considers the depth of the cover and UCS. Strength estimation between the three approached are consistent from the moderated depth. In contrast for the shallow depth, there is a noticeable different strength value between them.

CHAPTER 4
THESIS METHODOLOGY

4.1. Preliminary Study

The purpose of this research is to define the optimum pillar design and modify the empirical analysis using numerical simulation. However, some preliminary studies need to be made in order to provide some key components to the main study approaches. The preliminary studies include adopted pillar dimension, mesh sensitivity, estimating input parameters and size effect of the material. For model of the pillar, square pillar is adopted for the regular pillar while rectangular pillar is adopted for barrier pillar. Varieties of value dimension parameters are selected in order to identify the effect of each parameter as well as their relationships which lead to the demonstration of optimum pillar design for potash underground mine. After selecting the adopted pillar dimensions, mesh sensitivity is studied. This study can be performed by running some simulation on same dimension model with different mesh size. The mesh size was decreased until the simulated result become constant. Because of the limitation of input parameters, some of the unknown parameters are simulated by using FLAC3D. The procedure of this estimation is described in details in the next section. Because the main focus of this research is about pillar dimension, the effect of pillar size need to be studied and eliminated.

4.2. Model Simulation

The basic procedure in simulating pillar model in FLAC3D involved a series of code writing which include:

- Constructing Model Geometry
- Selecting constitutive model and required rock properties
- Setting the boundary conditions
- Applying in-situ stresses/overburden load (in case the model is just a part of the real dimension condition)
- Fishing code for defining output parameters

- Plotting history to show the results

The main concerns of this thesis research are focused on mine stability and the material extraction. The simulation for pillar design are divided into two main model simulations which included the model for estimating the pillar stress and model for estimating the pillar strength. For stress estimation the floor and roof materials are also included in the modeling with the pillar. In contrast, pillar strength estimation is modelled without the floor and roof material. The initial in situ stress both in vertical and horizontal direction are applied into both pillar models.

4.3. Complementary Study

In pillar design, the purpose of complementary study is to minimize the simulated cases by eliminating cases which gave the same results. In order to minimize the number of cases for estimation the stress in numerical simulation, it required some study on the behavior of stress which is the relationship between extraction ratio and pillar load. Based on the equation for estimating pillar stress mentioned above, it cans be perceived that the load exerted on pillar tend to be associated with the extraction ratio. In theoretical point of view, the same extraction ratio will give the same pillar load regardless the pillar dimension. In order to provide a better evidence for this problem, some random case studies are selected for simulating to define pillar load. Selecting criteria would be the case that have the same extraction ration but have different dimension (height, w/h ratio, etc.). This finding is also adopted for barrier pillar design.

As the shape of barrier pillar is rectangular with long length, only some part of the pillar length is simulated in the model. The complementary study for barrier pillar design is to learn about the effect of barrier pillar length on its strength. This study is aimed to reduce the model size into minimum by defining the length that will not affect the barrier pillar strength estimation. The study took cases where barrier pillar has mining height of 5m with the width of 5m. The length is varied from 5 to 100m. The strength is simulated using FLAC3D. The results will be plotted together and discussed to demonstrate the value of barrier pillar length that is suitable for model.

4.4. Formula Modification

Before any modification of the equation, the results of pillar strength estimation from this equation are compared with the results from numerical simulation. Based on this comparison, it will confirm the capability of the previous equation on estimation the pillar strength of potash in Thailand. In case the previous equation is not suitable, the equation is required some modification in order to fit with potash properties of Thailand. The reasons behind this error might be that the slenderness constant α and β of the previous equation are usually optimized for coal mine.

As mentioned above, the procedure of formula modification is aimed to define slenderness constants which is suitable for properties of potash in Thailand. These constants can be defined from the study of potash slenderness. In order to find these slenderness constants, series of same height pillar strength models with different width are simulated. The results from this study are plotted for each series. Slenderness constant is calculated from trendline's equations of the all the series model.

4.5. Safety Envelope

The optimum pillar design is represented by safety envelope which is the optimum correlation between pillar dimension and extraction ratio. For constructing this safety envelope, the safety factor is needed to be fixed into an acceptable value. Many cases of pillar dimension with different extraction are taken in the study. The analytical method of each case have simulated both pillar stress and strength. Safety factor of each case was calculated from the simulation results. The correlation between safety factors and w/h ratio are plotted in a series of extraction ratio. The optimum correlation between extraction ratio with w/h can be demonstrated by selecting the combination of extraction ratio with w/h ratio which give the safety factors 1.3. Safety envelope is presented by series of optimum value of correlation between extraction ratio and w/h ratio which in the plot can generate a curve under which the safety zone is located.

CHAPTER 5
MODEL DESCRIPTION

5.1. Model Dimensions

The purpose of underground mine pillar design is to identify the effect of the pillar dimension on strength and stress of the pillar. As the matter of fact, few dimension parameter are studied by varying the values in order to demonstrate that effect. For this research, there are 4 dimension parameters that are varied into a wide-range of values. These parameters are including depth of the seam *H,* mining height *h*, width to height ratio *w/h* and extraction ratio *e.* Because there are two type of pillar for this research which included pillar and barrier pillar, model dimension parameters are divided into two main groups. Table 5-1 and 5-2 shows summary of dimension parameters for normal pillar and barrier pillar respectively. The effect of barrier pillar length will be studied in order to demonstrate a suitable length that can eliminate this effect to the minimum.

Table 5-1 Dimension parameters for pillars

Depth of Seam *H* (m)	**Height *h* (m)**	**Width to Height Ratio *w/h* (-)**	**Extraction Ratio *e* (-)**
200	5	1.0	0.4
250	10	1.5	0.5
300	15	2.0	0.6
(-)	20	2.5	0.7
(-)	(-)	3.0	0.8
(-)	(-)	3.5	(-)
(-)	(-)	4.0	(-)
(-)	(-)	4.5	(-)
(-)	(-)	5.0	(-)

Table 5-2 Dimension parameters for barrier pillars

Depth of Seam *H* (m)	Height *h* (m)	Width to Height Ratio w_B/h (-)	Extraction Ratio *e* (-)
200	5	1.0	0.60
250	10	1.5	0.65
300	15	2.0	0.70
(-)	20	2.5	0.75
(-)	(-)	3.0	0.80
(-)	(-)	3.5	0.85
(-)	(-)	4.0	(-)
(-)	(-)	4.5	(-)
(-)	(-)	5.0	(-)
(-)	(-)	5.5	(-)
(-)	(-)	6.0	(-)
(-)	(-)	6.5	(-)
(-)	(-)	7.0	(-)

Table 5-3 Thickness of Rock Strata

Rock Types	Thickness
Upper halite	15m
Claystone	5m
Roof (potash)	1m
Pillar (potash)	5m, 10m, 15m, 20m
Floor (potash)	1m
Lower halite	20m

By understanding the concept of symmetry geometry, pillar simulation is modeled only a quarter of the real pillar and barrier pillar model is simulated only half of the real dimension as shown in Figure 5-1 and 5-2. This particular type of simulation is chosen as it decreased the time of simulating while maintained the same result of the simulation. The model is simplified into 4 main strata: upper halite, claystone, potash and lower halite. The thickness of each strata is presented in Table 5-3. Around 20 meters of the roof and floor material is considered to have a significant effect from the room excavation.

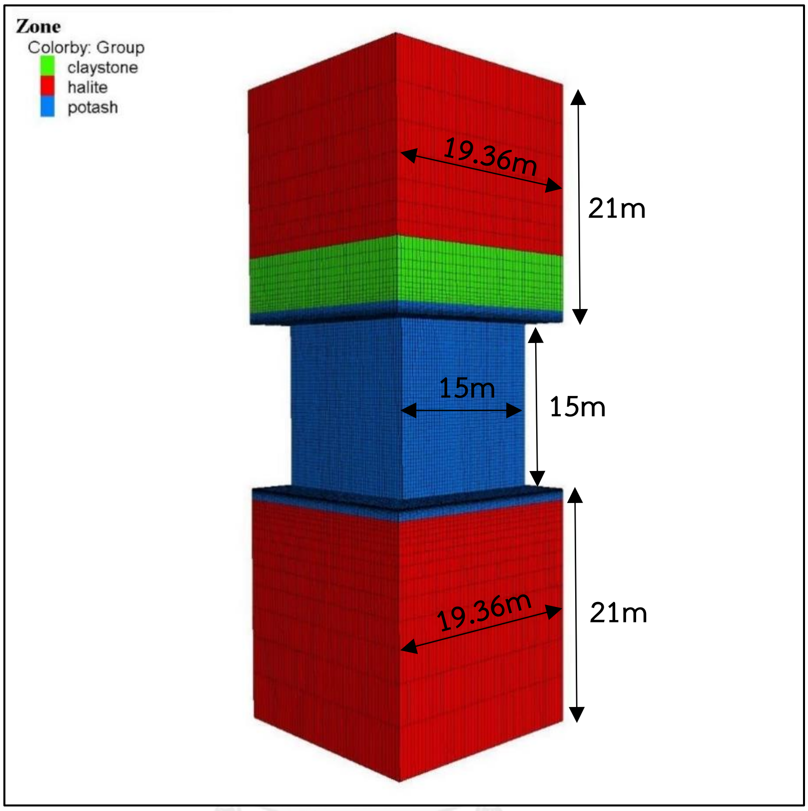

Figure 5-1 Model dimension of pillar (w/h=2, e=0.4)

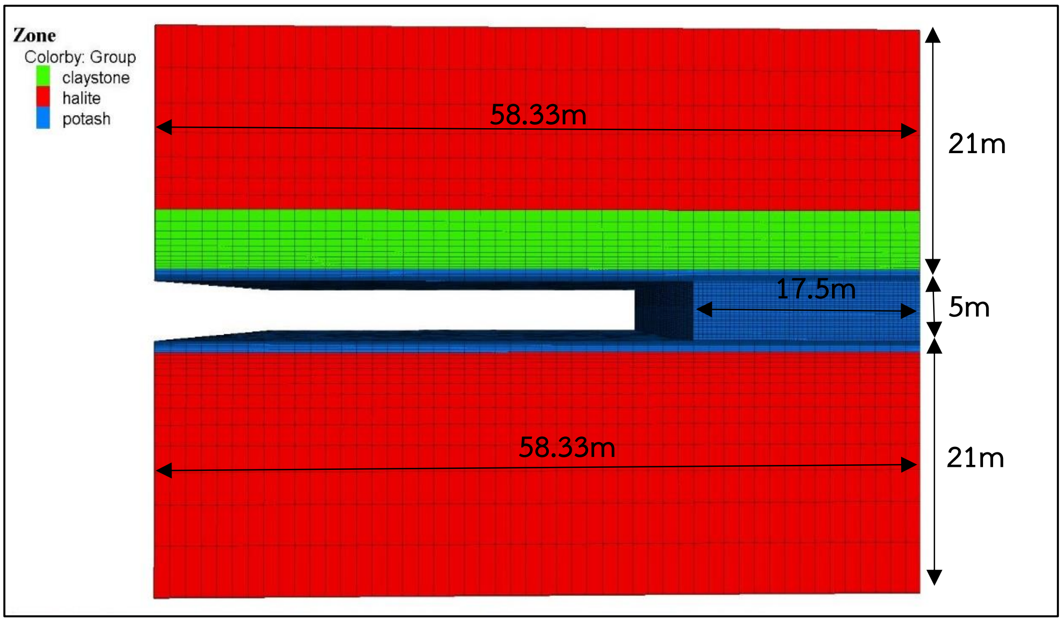

Figure 5-2 Model dimension of barrier pillar (w_B/h=7, e=0.7)

5.2. Mesh Sensitivity

The model in FLAC3D is composed of many brick zones. The size of the zone will affect the results of the simulation. In order to obtain the results of the simulation as accurate as possible, mesh sensitivity need to be studied for this software. For demonstrating the sensitivity of the mesh in FLAC3D, some simulations need to be made. The examination of mesh sensitivity is divided into two main dimensional groups due to the significant different of size. The first group is for any geometry with less than 5m and the second group is for any geometry from 5m and above. The procedure of determination mesh sensitivity was performed using simulation of UCS test on cube sample by FLAC3D. Different values of dimension in the group range is simulated with different mesh to obtain the strength from this UCS test. The strengths of different mesh from each dimension were plotted in the graph to define the maximum mesh scale that the strength become constant. For group less than 5m, there are 4 values of cube dimensions 1m, 2m, 3m and 4m whereas cube dimensions of group from 5m and above are 5m, 10m, 15m and 20m.

5.3. Input Parameters

The essential rock mechanic properties for strain-softening model in FLAC3D requires 4 main properties including Young's Modulus (E), Possion's ratio (υ), cohesion (c) and friction angle (ϕ). Potash core samples from Khorat basin are executed under UCS test. The result from these tests can define the average value of E and υ. Table 5-4 summarize the results from UCS test in the laboratory. Tensile strength σ_t is estimated to be equal to 1/10 of UCS strength.

Table 5-4 Mechanic Properties of rock strata from laboratory

Rock Type	UCS (MPa)	E (GPa)	υ	σ_t (MPa)
Halite	29.00	19.11	0.41	2.9
Claystone	2.12	0.48	0.33	0.21
Potash	8.74	10.48	0.36	0.87

Due to the shortage of information about c and ϕ, it is compulsory to perform back analysis in FLAC3D to obtain these two mechanical properties. According to some previous work of Kolano and Flisiak [19], friction angle of the pink rock salt ,which has similar properties to our carnallite, are equal to 35 degree. The procedure of determination utilizes the real dimension of 5 core samples to simulate in the software. Varieties of friction angles are applied to each sample for testing. Cohesion can be calculated using Equation 2-11 which is the relationship between friction angle and ultimate strength from the real UCS test [17].

The ultimate strengths from this simulated model are used to compare with the strength from the real UCS test. The decision of selected friction angle and cohesion for each core sample are based on the closest value of ultimate strength of the real UCS test. The selected friction angle and cohesion from each sample are calculated to be the average value which can be represented as the universal ϕ and c of Thailand potash.

5.4. Size Effect

Theoretically, the size of material has an effect on the estimation of pillar strength. The bigger material sizes the lower strength material is. This strength reduction of material is resulted from the fact that bigger size material tends to have more fractures and other discontinuities. The effect of material size can be estimated using model simulation in FLAC3D. The procedure of identification the size effect of potash material is performed by simulated UCS test on cubic samples. Many different size of cubic potash samples, which the size ranges from 1m to 20m, are modelled in FLAC3D. Properties of Thailand's potash are input into the model. The process of model simulation of UCS test will be discussed in the next section in pillar strength estimation. The strength of potash cubic sample is expected to become constant, starting from a certain material size called critical size limit, above which the effect of the material size will no longer have any effect on the strength of the pillar. By study this effect, the accuracy of the result from this study will be increased.

5.5. In Situ Stresses

There are seven potash exploration drilled-holes available for this research. Theses drilled-holes are categorized based on the depth of the potash seam. Vertical in-situ stress σ_v is obtained directly from analyzing drilled-hole data by using Equation 2-4.

Table 5-5 Drilled-hole data of hole number 1

DH1				
Rock Strata	**Density (Kg/m^3)**	**Thickness (m)**	**Unit Weight (kN/m^3)**	**Stress (MPa)**
Topsoil	1600	2.5	15.70	0.039
Siltstone	2000	48.5	19.62	0.952
Claystone	2100	36.8	20.60	0.758
Anhydrite	2400	6.2	23.54	0.146
Halite	2110	91.5	20.70	1.894
Claystone	2100	22.3	20.60	0.459
Halite	2110	4.4	20.70	0.091
Total Depth		212.2	**Total Stress**	4.34

Table 5-5 shows analyzed information of a drilled-hole. Information of other drilled-holes can be found in the *appendix A*. After obtain vertical in situ stress, Equation 2-7 is utilized to define horizontal in situ stress σ_h because of limitation of information about thermal expansion and geothermal gradient.

5.6. Simulation of Pillar Stress

In an attempt to estimate the stress loading on each pillar for different cases, the size of the pillar and overburden are coded into FLAC3D. The model is divided into rock seams based on the thickness that is mentioned in the previous section. The load σ_v is applied on the top of the model in order to compensate the load of the overburden load due to the fact that the pillar model is simulated with only 20m overburden rock.

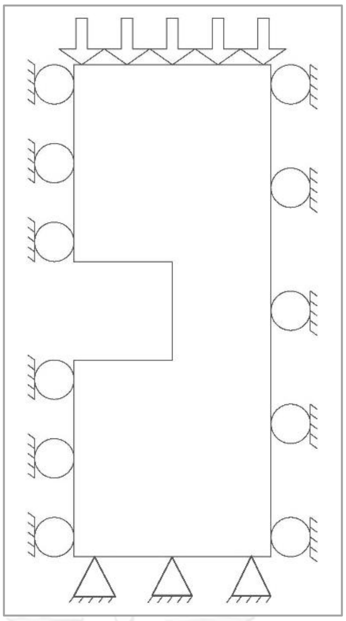

Figure 5-3 Boundary conditions of pillar stress

After selecting the constitutive model for numerical model and applying the mechanical properties, the base of model is fixed in *z* and the 4 sides of the model are restricted in *x* and *y* respectively for horizontal directions as illustrated in Figure 5-3. The next step is setting initial state in both vertical and horizontal stress. Fish function was coded to define the average stress acting on pillar. The outcome result is plotted as shown in Figure 5-4 for pillar and Figure 5-5 and 5-6 for barrier pillar.

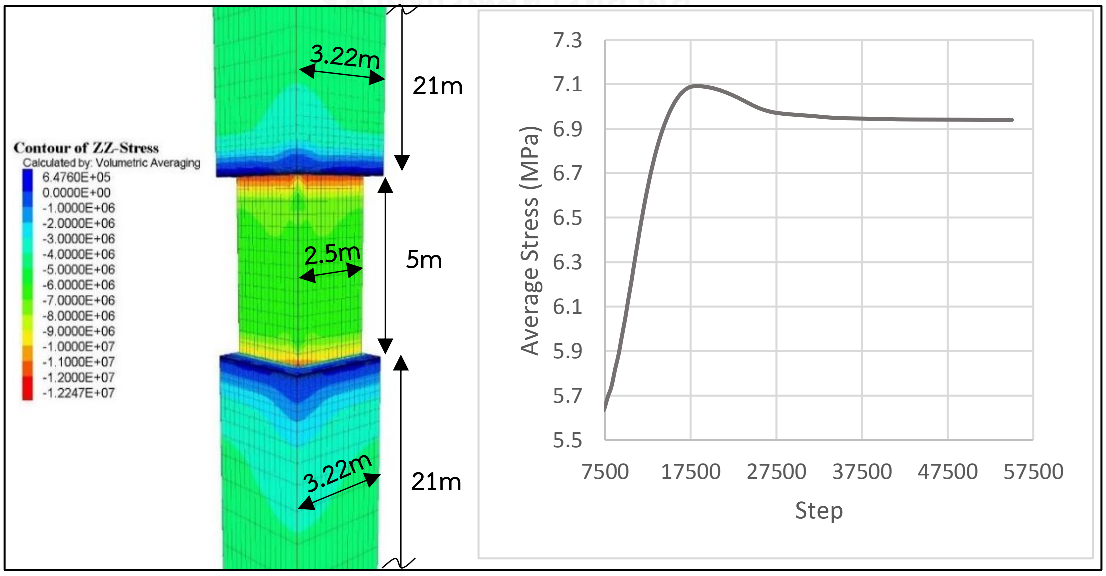

Figure 5-4 Result of pillar stress estimation (w/h=1, e=0.4)

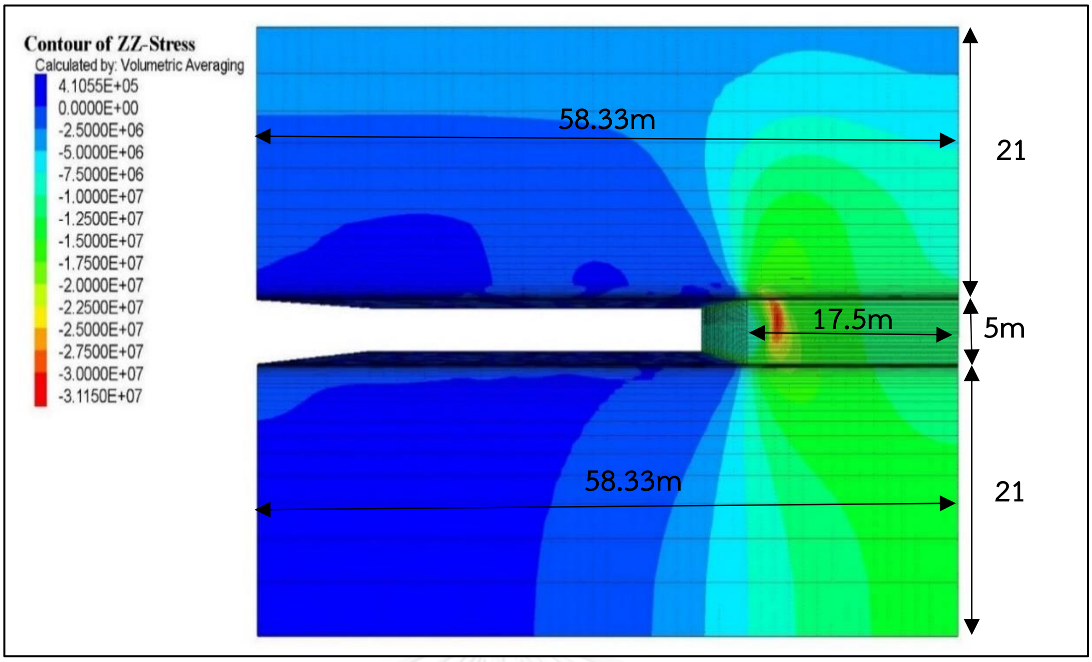

Figure 5-5 Model result of barrier stress estimation (w_B/h=7, e=0.7)

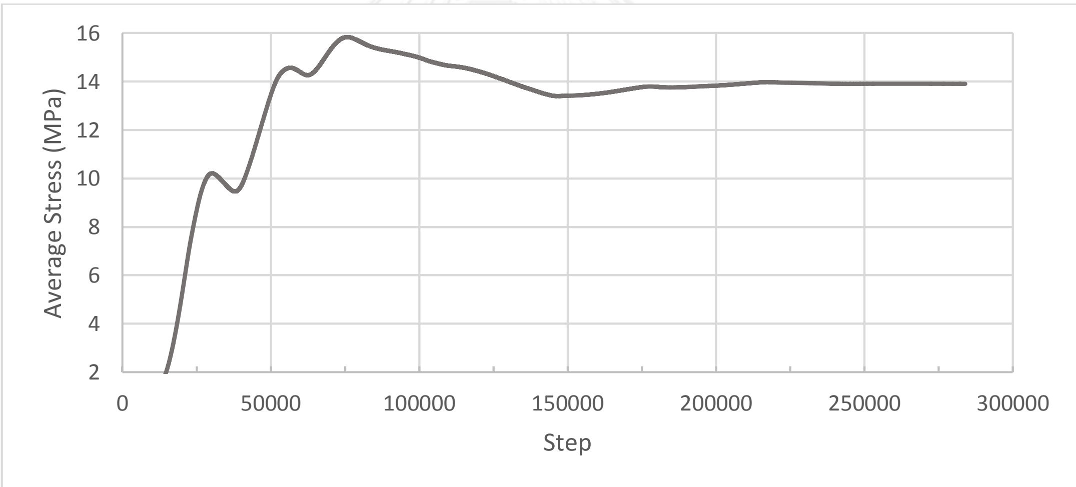

Figure 5-6 History plot result of barrier pillar stress estimation

5.7. Simulation of Pillar Strength

Pillar strength simulation is performed similarly to the UCS test in the real laboratory with the additional present of real initial state of stress added into the model. The full size of the pillar is modeled in the software. Boundary condition is fixed at the bottom of the model in *x, y* and *z* direction to restrict the vertical movement while keeping the 4 side of the model unfix in any directions which is shows in Figure 5-7. Initial stress state is set according to the in-situ stresses. Strain-softening model is chosen to be constitutive model. The mechanic properties of potash seam are applied into the model. As mentioned in the previous section, strain-softening model requires tables that represent the change of cohesion and friction angle with shear strain which can be defined from the result of input parameters estimation. The model is stepped until the unbalance force is equilibrium to let the initial state well distributed in the model before fixing the top of the model as well. After that, two difference sets of fish function are coded for this estimation. The first fish is for estimating the average stress acting on pillar while the second fish is for monitoring and recording the strain result from the simulated test. The model is continued stepping while the fish history of pillar stress and strain is monitored until the complete strength curve is obtained in Figure 5-8.

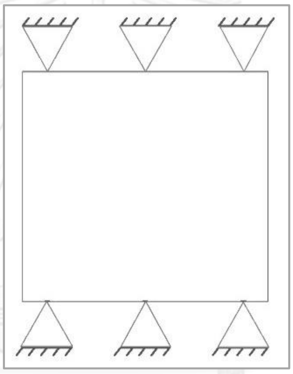

Figure 5-7 Boundary conditions of pillar strength

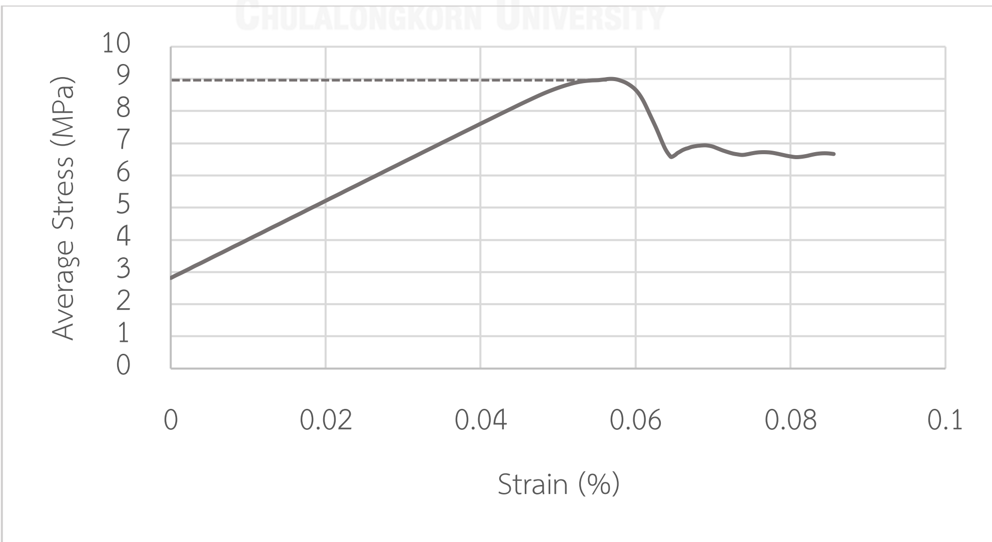

Figure 5-8 The complete failure behavior of pillar (h=5m, w/h=1, e=0.4)

CHAPTER 6

RESULTS AND DISCUSSIONS

6.1. Preliminary Study

It is crucial to note that the results from this section are utilized in all research scope. The purpose of this preliminary study is to eliminate the error that might occur in the research work during the part of numerical simulation. In general, the common errors in the numerical simulation of pillar design are mesh size, input parameter, material size effect.

6.1.1. Mesh Sensitivity

As mentioned above, the examination of mesh sensitivity is divided into two main dimensional groups. The first group is for any geometry that is less than 5m and the second group is for any geometry from 5m and above. The results from this analysis are shown in Figure 6-1 and Figure 6-2.

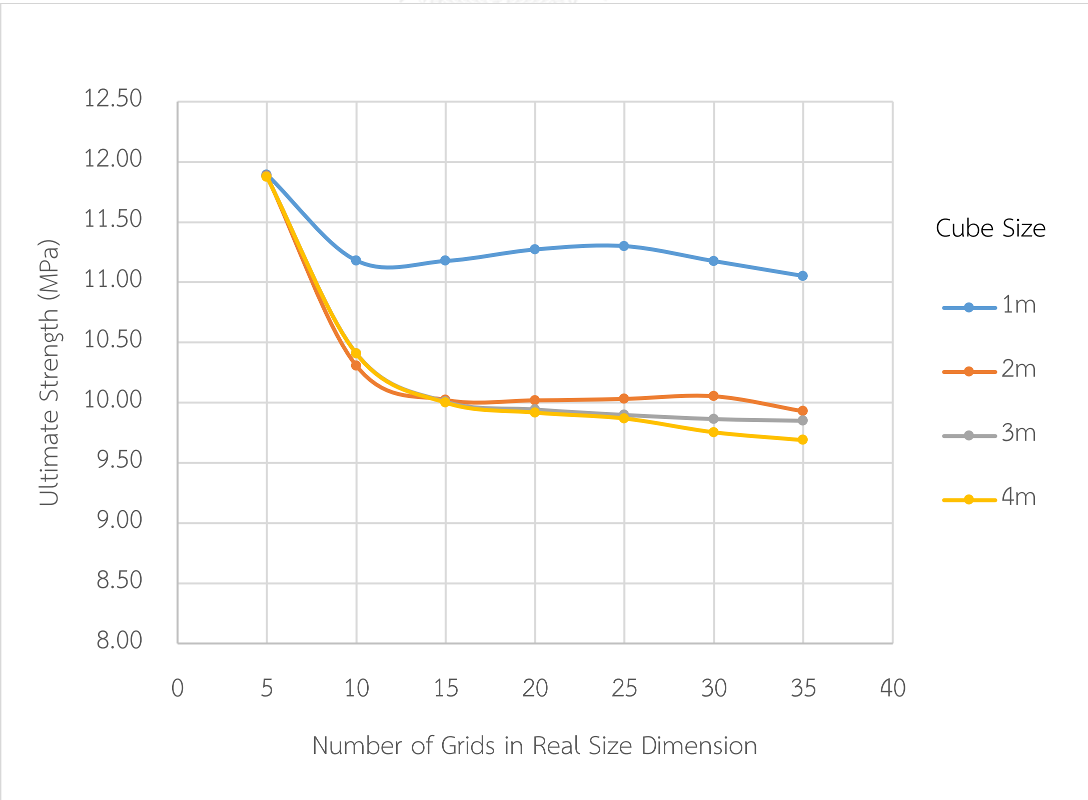

Figure 6-1 Result from mesh sensitivity analysis for group less than 5m

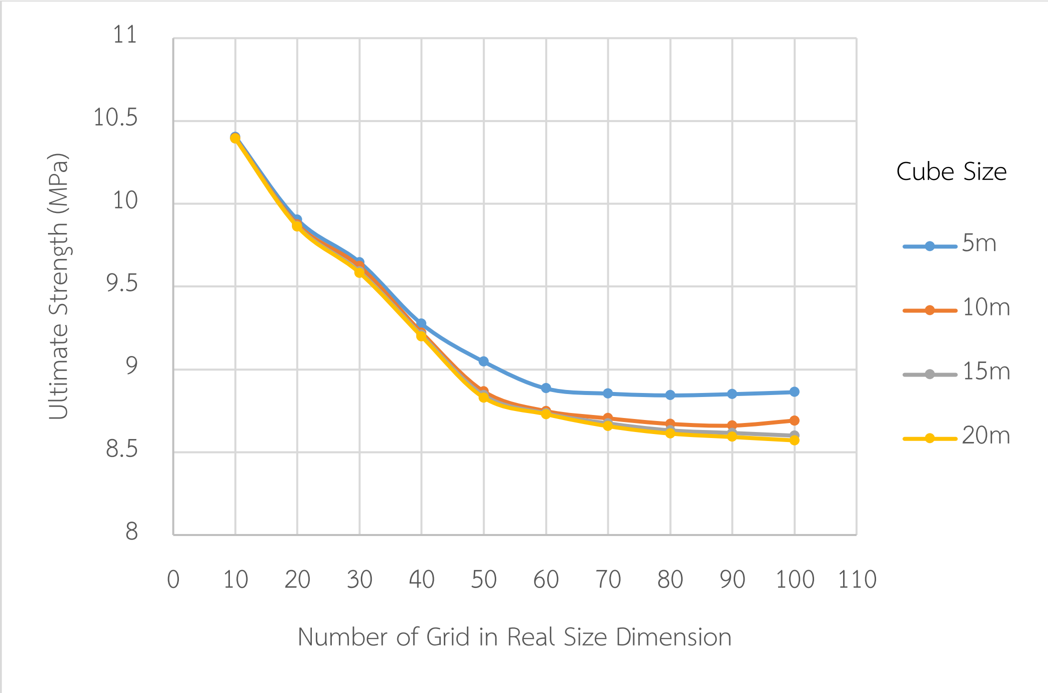

Figure 6-2 Result from mesh sensitivity analysis for group from 5m and above

The results above can be observed that for dimension group less than 5m, the ultimate strength of the material become almost constant from the number of grid per real dimension equal to 15. For dimension group from 5m above, the strength tends to stabilize from the number of grid equal to 50. This study of mesh sensitivity has led to the decision that in order to eliminate the effect from mesh error, for any dimensional size under 5m, the scale of the mesh should be equal to 1/15 of the real dimension size. Other case where the dimension is equal to 5m or above the scale of the mesh should be equal to 1/50 of the real dimensional size.

6.1.2. Input Parameters Estimation

The ultimate strengths from this simulated model are used to compare with the strength from the real UCS test. The decision of selected friction angle and cohesion for each core sample is based on the closest value of ultimate strength of the real UCS test. The selected friction angle and cohesion from each sample are calculated to be the average value which can be represented as the universal ϕ and c of Thailand potash. The results from these estimations are presented in Figure 6-3 and Table 6-1.

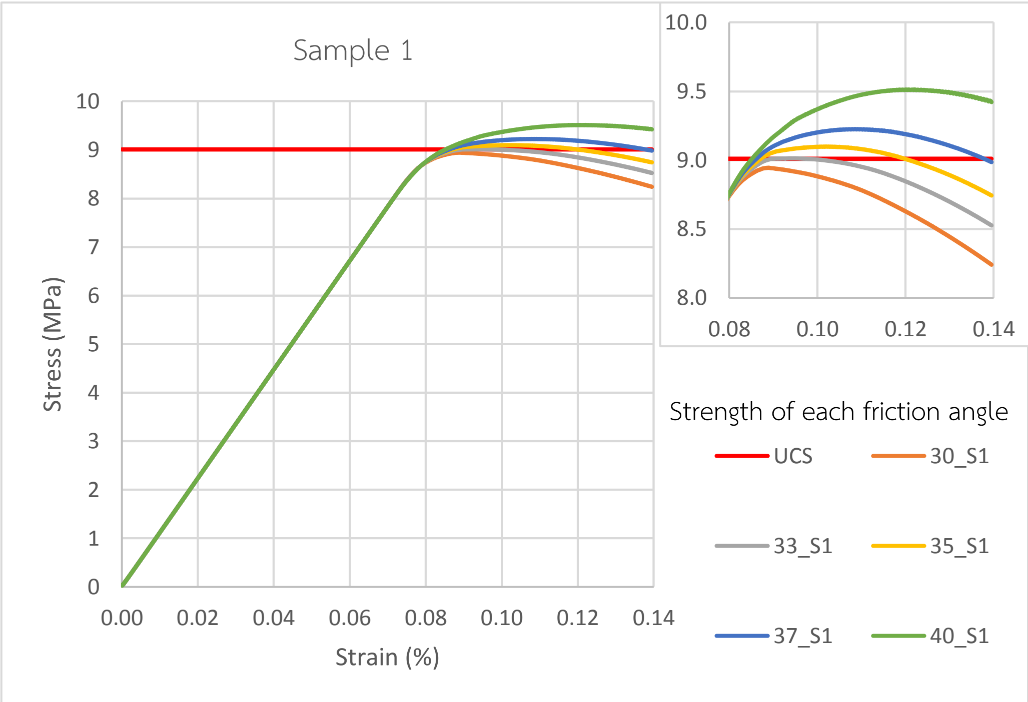

Figure 6-3 Ultimate strength result from core sample 1

Table 6-1 Summary results from simulated friction and cohesion determination

Sample	1	2	3	4	5	Average
UCS (MPa)	9.01	12.51	10.44	5.34	6.41	8.74
Friction (Degree)	33	47	42	37	33	38.4
Cohesion (MPa)	2.45	2.46	2.32	1.33	1.74	2.06

The result in Figure 6-3 shows that ϕ = 33° and c = 2.45MPa (applied ϕ = 33° with UCS of sample 1 to equation 2-11 to obtain c) provided the closest ultimate peak strength to the real test. As a result, these mechanical properties are selected for sample 1. The same concept is applied to other samples. The result in Table 6-1 represents from all the simulation for this identification. The average value of friction angle and cohesion are used for all simulated models in this paper as mechanical properties of potash. Tensile strength (σ_t) is equaled to 1/10 of UCS. Because of the similarity, the model uses same mechanical properties for upper and lower halite.

6.1.3. Size Effect

Size effect of one material can be identified by the UCS test on cubic sample with different sizes. The results from this identification are illustrated in Figure 6-4. These results offer vital evidence for size effect. Based on these outcome results, it cans be observed that the strengths from the samples whose width are greater than 5m, have almost identical value. This finding confirms that the side of potash material have no effect on the pillar strength from the size above 5m. The non-size-effected strength is equal to 8.82 MPa which is really similar to the average strength from actual the UCS 8.74 MPa. As the result, the strength of UCS that use in empirical analysis is taken from the value of strength from the actual UCS test to make this input parameter as realistic as possible. Table 6-2 summarizes all the mechanical input parameters of mechanic properties for every models. Piecewise function for the model is represented in the Table 6-3.

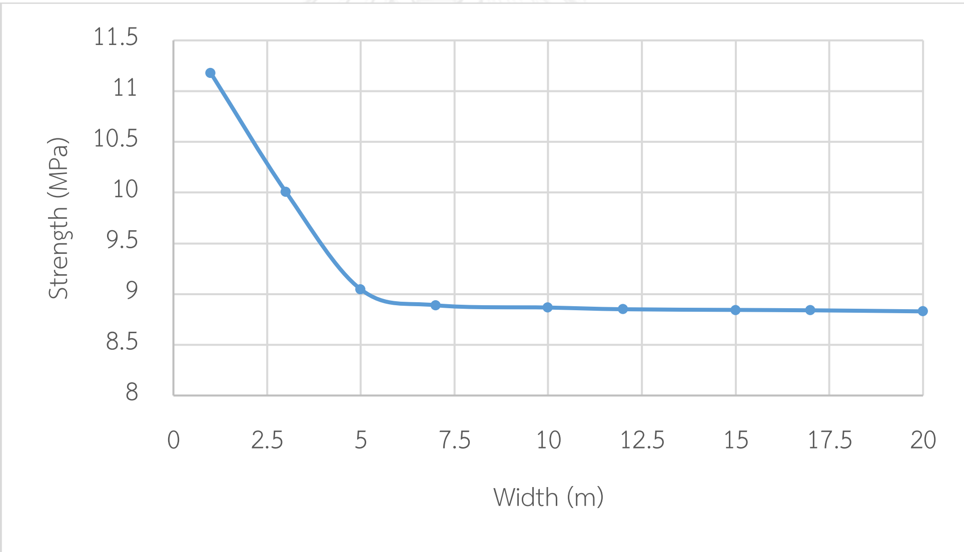

Figure 6-4 Size effect of potash sample on strength

Table 6-2 Mechanical properties of rock strata

Rock	UCS (MPa)	E (GPa)	υ	ϕ (Degree)	c (MPa)	σ_t (MPa)
Halite	29.00	19.11	0.41	-	-	2.90
Claystone	2.12	0.48	0.33	-	-	0.21
Potash	8.74	10.48	0.36	38.4	2.06	0.87

Table 6-3 Piecewise function: change of cohesion and friction vs. shear strain

Shear Strain	Cohesion (MPa)	Friction Angle (Degree)
0.000	2.06	38.4
0.005	0.41	35.9
0.010	0	33.4
0.050	0	33.4

6.1.4. In-situ Stresses

Vertical in-situ stresses are obtained from the study of drilled-hole information from potash exploration. Drilled-hole data is categorized based on the depth of the potash seam. There are three groups of drilled-hole data included potash seam approximately at 200m, 250m and 300m depth. The value of vertical in-situ stress for the simulation are the average value from each group of drilled-hole. Table 6-4 shows the value of vertical in-situ stress together with the calculated horizontal in-situ stress. These values of in-situ stress are utilized in all model simulation based on the depth of the model.

Table 6-4 Vertical and horizontal in-situ stresses

<table>
<tr><th>DH</th><th>Depth (m)</th><th>Vertical Stress (MPa)</th><th>Approximate Depth (m)</th><th>Average Verical Stress σ_v (MPa)</th><th>Horizontal Stress σ_h (MPa)</th></tr>
<tr><td>1</td><td>212.2</td><td>4.34</td><td rowspan="3">200</td><td rowspan="3">4.17</td><td rowspan="3">2.35</td></tr>
<tr><td>2</td><td>184.0</td><td>3.81</td></tr>
<tr><td>3</td><td>212.4</td><td>4.37</td></tr>
<tr><td>4</td><td>258.0</td><td>5.33</td><td rowspan="2">250</td><td rowspan="2">5.31</td><td rowspan="2">2.99</td></tr>
<tr><td>5</td><td>259.5</td><td>5.29</td></tr>
<tr><td>6</td><td>326.6</td><td>6.71</td><td rowspan="2">300</td><td rowspan="2">6.31</td><td rowspan="2">3.55</td></tr>
<tr><td>7</td><td>288.6</td><td>5.92</td></tr>
</table>

6.2. Pillar Design

6.2.1. Relation Between Extraction Ratio with Pillar Load

The results from complementary study in the relationship between extraction ratio and pillar load are shown in Figure 6-5. Table 6-5 shows the actual values of each case. Based on this observation, the difference between the result from each case is as small as 0.01 MPa. It is confident to say that same extraction will provide the same pillar load.

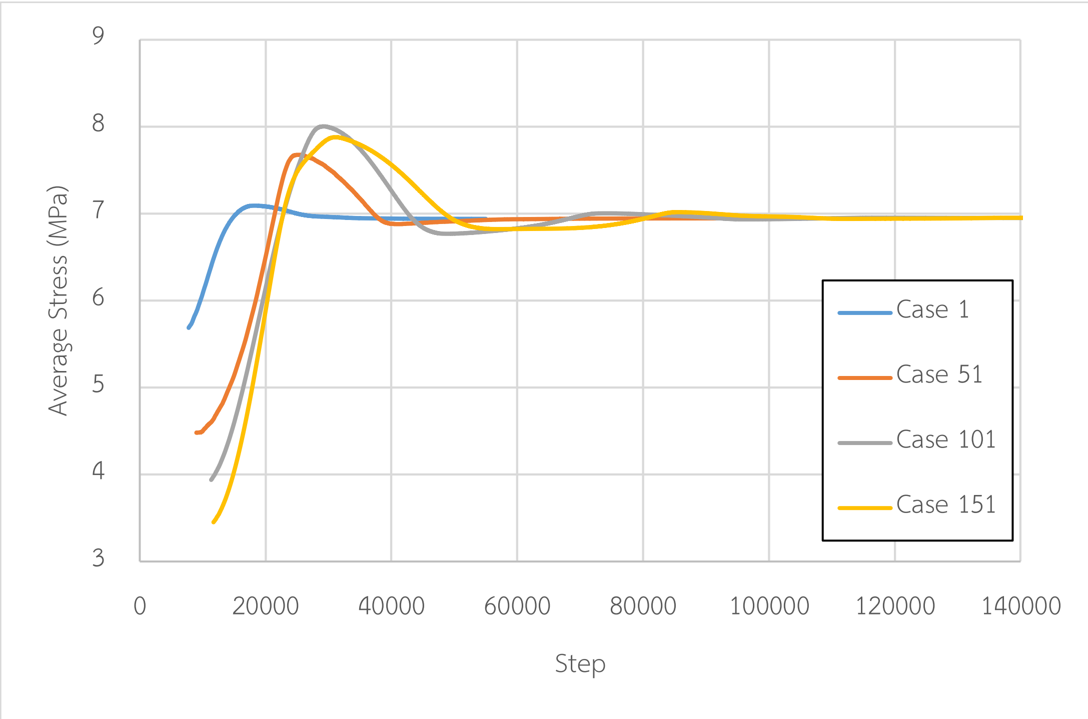

Figure 6-5 Comparison: estimated pillar loads with same extraction ratio but different dimensions

Table 6-5 Relation between extraction ratio with pillar load (e=40%)

Case Study	Average Pillar Stress (MPa)
Case 1 (h=5m, w/h=1)	6.940
Case 51(h=10m, w/h=1.5)	6.946
Case 101 (h=15m, w/h=2)	6.949
Case 151 (h=20m, w/h=2.5)	6.950

6.2.2. Stress Estimation of Pillar

Pillar loads, also known as pillar stress, are estimated using two methods: numerical simulation and empirical analysis. Figure 6-6 offers an illustration of estimated stress results with different extraction ratio from FLAC3D. The model is stepped until the average stress become stable. The stable value of average stress is considered as pillar load. The result from this method is used to compare with the result of pillar stress estimation in empirical analysis which is indicated in Table 6-6.

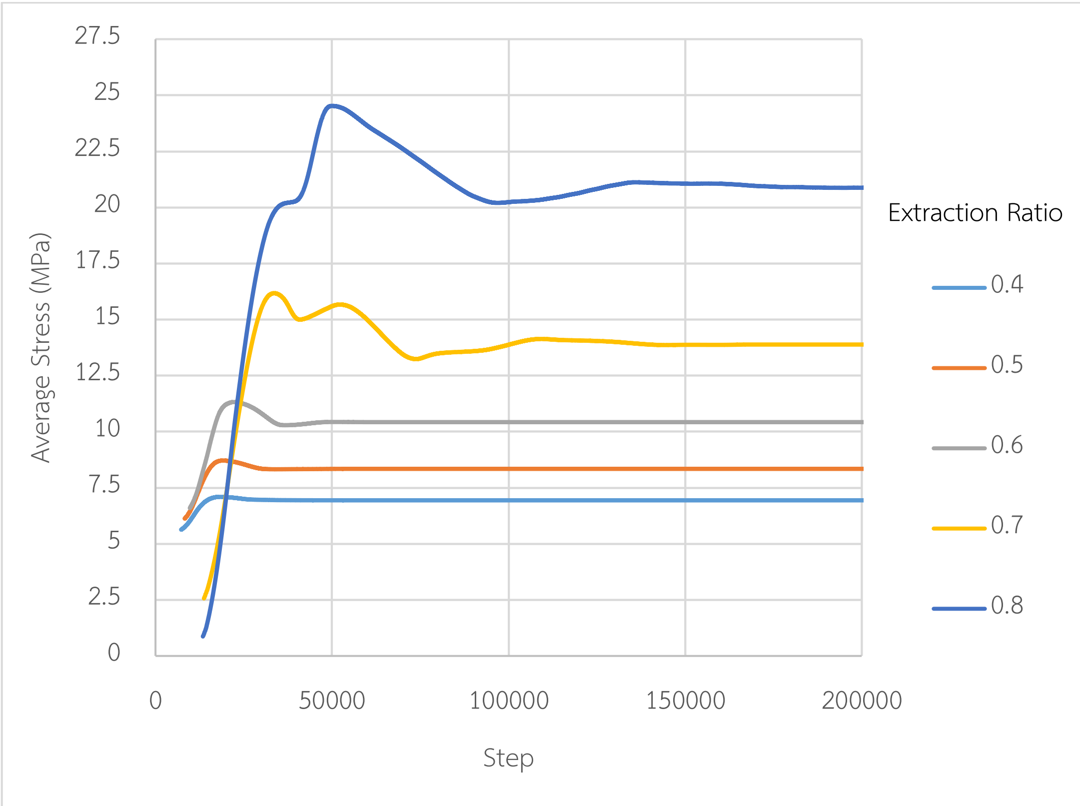

Figure 6-6 Result of simulated pillar stress from FLAC3D (H=200m)

The most remarkable observation emerging from this result is that the estimated value of stress for each extraction ratio from numerical simulation is almost identical to the value of stress from the empirical analysis. The difference is barely distinguishable. From this it can be confirmed that this empirical equation can be used effectively for estimating pillar stress for potash in Thailand as well.

Table 6-6 Comparison result pillar stress: empirical analysis vs. numerical simulation

Depth of Potash (m)	Extraction Ratio	Stress from Empirical (MPa)	Stress from Numerical (MPa)
200	0.4	6.95	6.94
	0.5	8.34	8.34
	0.6	10.43	10.42
	0.7	13.90	13.89
	0.8	20.85	20.87
250	0.4	8.85	8.84
	0.5	10.62	10.62
	0.6	13.28	13.27
	0.7	17.70	17.70
	0.8	26.55	26.60
300	0.4	10.52	10.50
	0.5	12.62	12.62
	0.6	15.78	15.78
	0.7	21.03	21.03
	0.8	31.55	31.55

6.2.3. Strength Estimation of Pillar

For numerical simulation, strength of the pillar is obtained in a way similar to the strength determining in UCS test. History plot between the average pillar stress and pillar strain shows the peak value of stress that represent the strength of the pillar. Figure 6-7 shows the outcome results of strength estimation from numerical simulation for cases that have mining height equal to 5m. Pillar strength is also estimated by empirical analysis. The value of peak strength in numerical simulation is determined to complete the table which represent the whole results of strength estimation from both empirical and numerical.

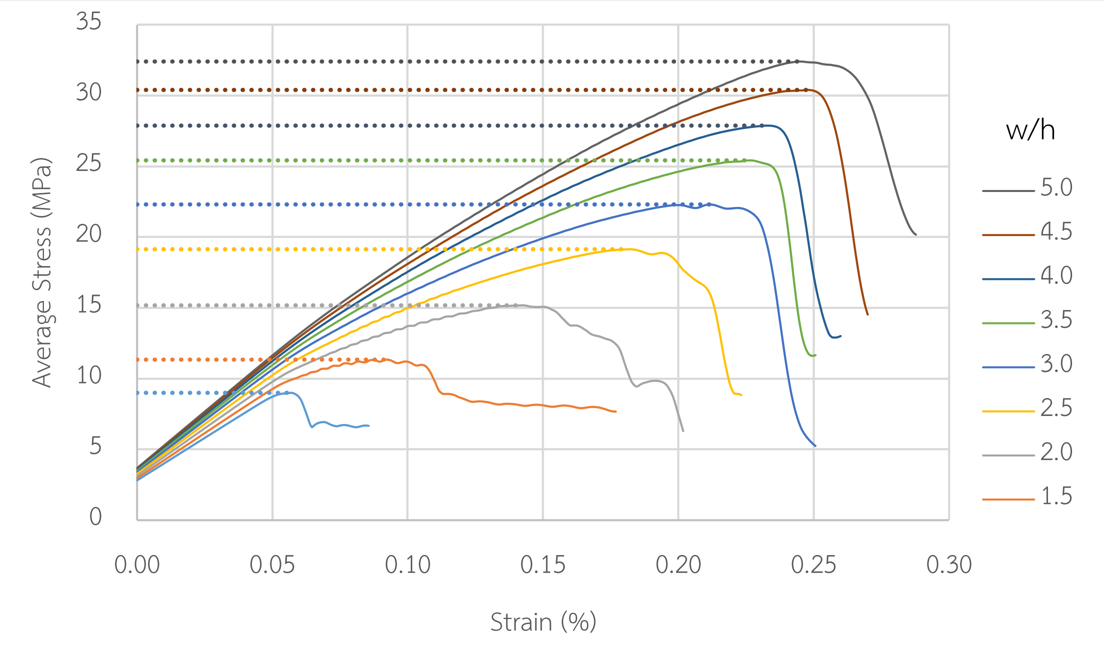

Figure 6-7 Results of peak strength from FLAC3D (h = 5m)

Table 6-7 Estimated strength comparison: numerical vs empirical analysis

w/h Ratio	Numerical Strength (MPa)				Empirical Strength (MPa)
	h = 5m	h = 10m	h = 15m	h = 20m	
1.0	9.00	8.80	8.79	8.78	8.74
1.5	11.34	10.04	11.02	11.01	10.31
2.0	15.18	14.58	14.52	14.46	11.89
2.5	19.15	18.39	18.33	18.19	13.46
3.0	22.31	21.51	21.44	21.32	15.03
3.5	25.43	24.54	24.26	24.12	16.60
4.0	27.88	26.93	26.64	26.47	18.18
4.5	30.4	29.20	28.92	29.08	19.75
5.0	32.41	31.25	31.33	31.56	21.32

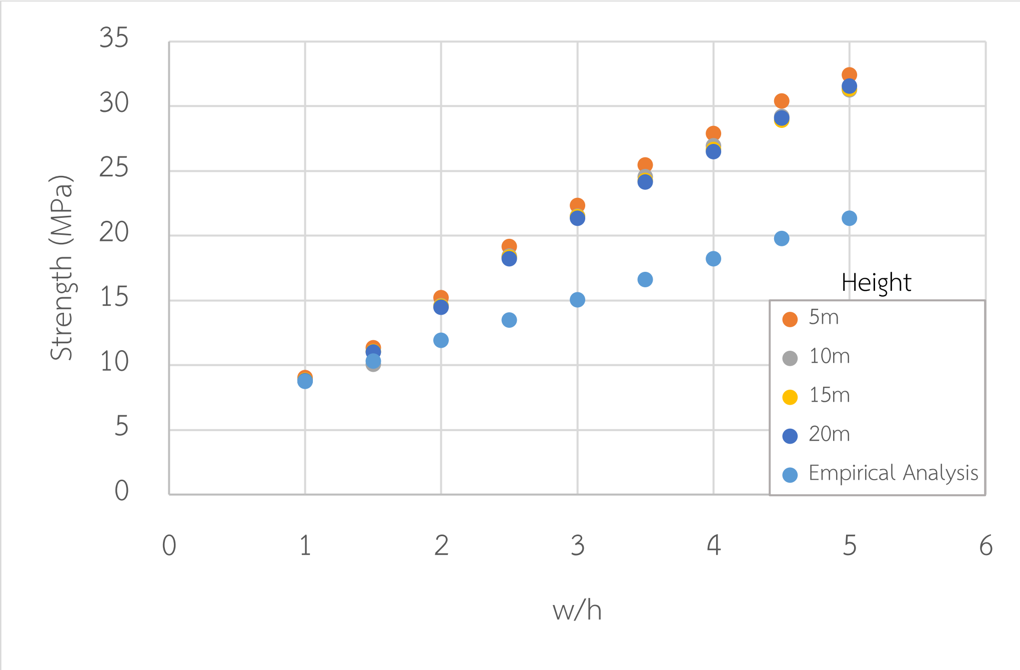

Figure 6-8 Summary results of estimated strength

Based on the result comparison in Table 6-7 and Figure 6-8, utilization of empirical analysis using Equation 2-9 tends to under estimate the value of pillar strength. The difference between these estimated values become even more noticeable when the value of w/h ratio increase. This finding confirms that empirical analysis using this equation is not yet suitable for estimated potash pillar strength. The equation required some modification to fit Thailand potash properties in order to be able to effectively estimated the pillar strength.

6.2.4. Formula Modification for Potash Pillar

The keys criteria of modifying Equation 2-9 to fit with the properties of Thailand's potash are slenderness constant which have a significant impact on empirical estimation of pillar strength. The strength results are categorized and plotted based on the mining height. Figure 6-9 shows relationship between pillar strength and w/h ratio. Slenderness constants can be found from the trendline's equation. Because of the height differences, the four plots give 4 equations however the difference between each equation is significantly small. The value of σ_s is the strength of the average UCS which is 8.74MPa. Table 6-8 expresses the value of slenderness constants that is taken out from each trendline's equation. The average constants will be used as a general slenderness constant for pillar design of potash in Thailand.

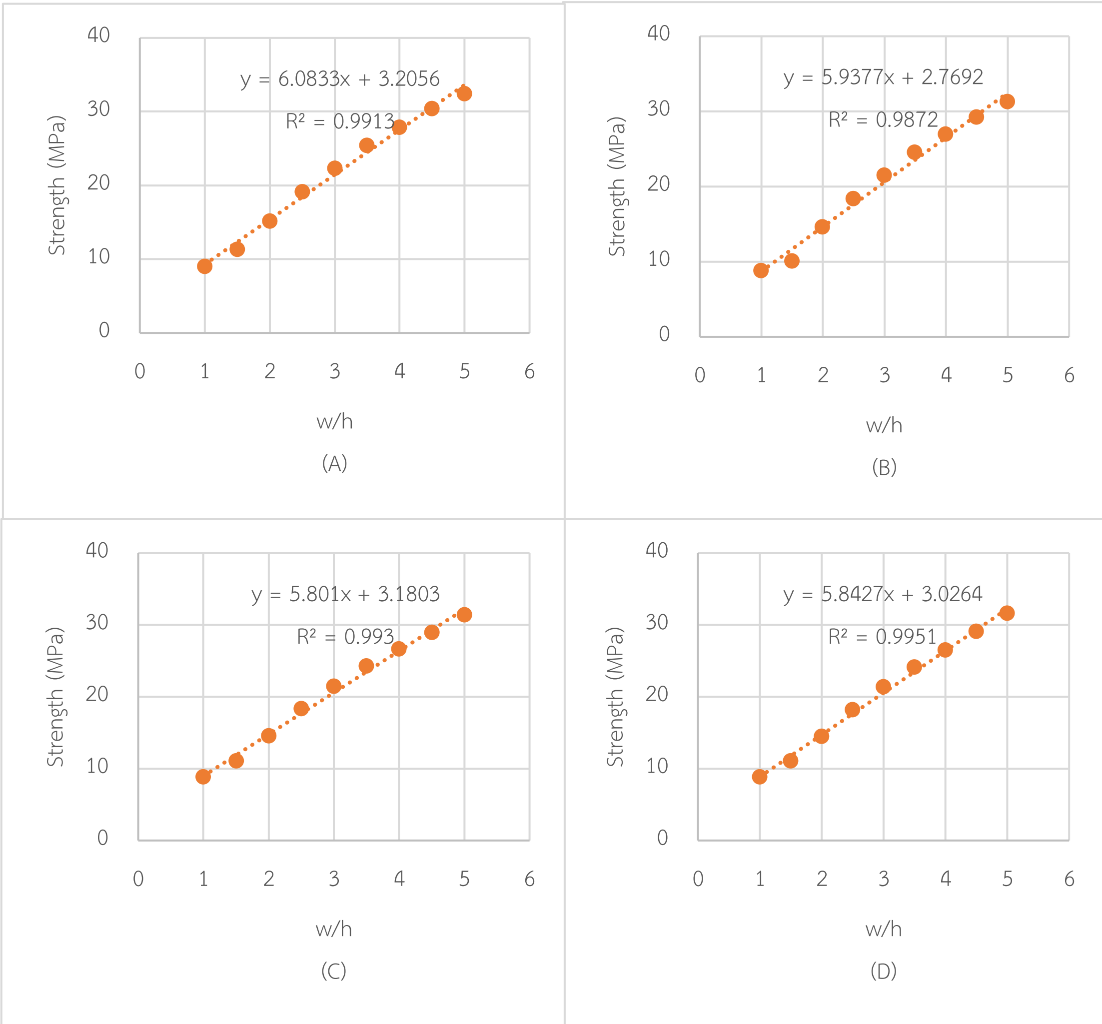

Figure 6-9 Relationship: strength and w/h (A: h=5, B: h=10, C: h=15, D: h=20m)

Table 6-8 Slenderness constants

Height	Trendline's Equation	Format Equation 2-8	α	β
5m	$\sigma_p = (3.2056 + 6.0833 \times \frac{w}{h})$	$\sigma_p = 8.74 \times (0.366 + 0.696 \times \frac{w}{h})$	0.366	0.696
10m	$\sigma_p = (2.7692 + 5.9377 \times \frac{w}{h})$	$\sigma_p = 8.74 \times (0.316 + 0.679 \times \frac{w}{h})$	0.316	0.679
15m	$\sigma_p = (3.1803 + 5.801 \times \frac{w}{h})$	$\sigma_p = 8.74 \times (0.363 + 0.663 \times \frac{w}{h})$	0.363	0.663
20m	$\sigma_p = (3.0264 + 5.8427 \times \frac{w}{h})$	$\sigma_p = 8.74 \times (0.346 + 0.668 \times \frac{w}{h})$	0.346	0.668
Average			0.348	0.677

Based on Table 6-8, the average slenderness constants are α = 0.348 and β = 0.677. By applying these constants to Equation 2-8, we can formulate an empirical pillar strength estimation that is suitable for potash in Thailand. Equation 6-1 is a modified equation of Obert and Duvall. All the results of numerical strength estimation together with the strength estimated from Equation 6-1 are plotted together as illustrated in Figure 6-10 to confirm the applicability of formula for potash in Thailand. The results of comparison in Figure 6-10 are in good agreement as the values of strength are correlated satisfactorily.

$$\sigma_P = \sigma_S (0.348 + 0.677 \frac{w}{h}) \qquad \textit{Equation 6-1}$$

From this relationship demonstration, Equation 6-1 cans be used to estimate the strength of pillar with the conditions of parameter range below:

- Barrier pillar width to height *w/h*: 1 to 5
- Mining height *h*: 5m to 20m

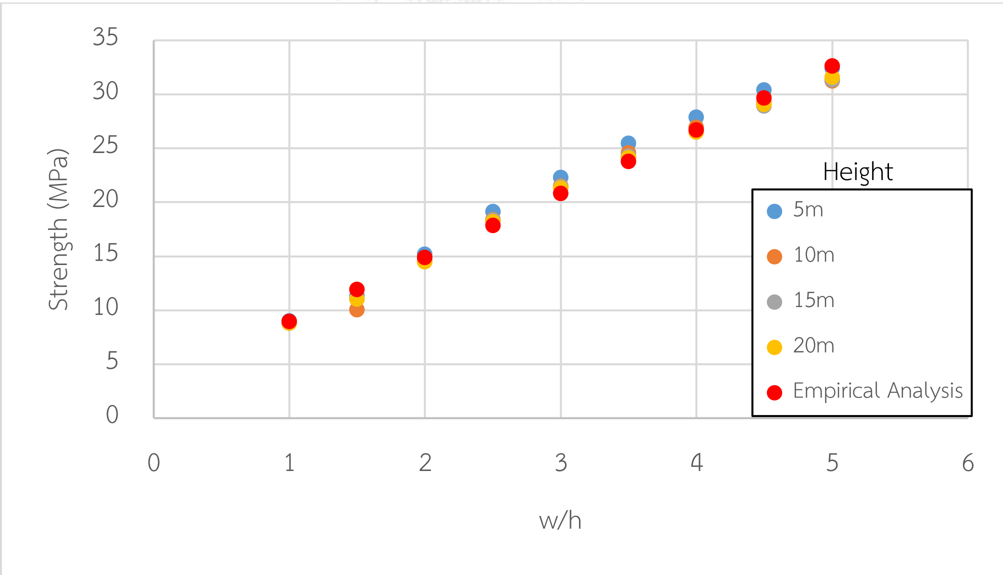

Figure 6-10 Estimated strength: numerical analysis vs modified Obert & Duvall

6.2.5. Safety Envelope of Pillar Design

In order to make it easy to understand, all results from every cases in numerical strength estimation, together with corresponding stress for each case, are calculated into safety factor using Equation 2-12. The result is plotted in graph with w/h ratio based on series of extraction ratios as illustrated in Figure 6-11. There are 4 plotted graphs according to the height of the mine. The value of safety factor is selected to be 1.3 for pillar design as this value is widely used for many previous researches as well as adopted by many other commercial mine companies. When safety factor 1.3 is applied to the graph, the value of extraction ratio and corresponding *w/h* ratio can be defined. It means that if these two corresponding parameters are selected for pillar design, it will provide the safety factor of 1.3.

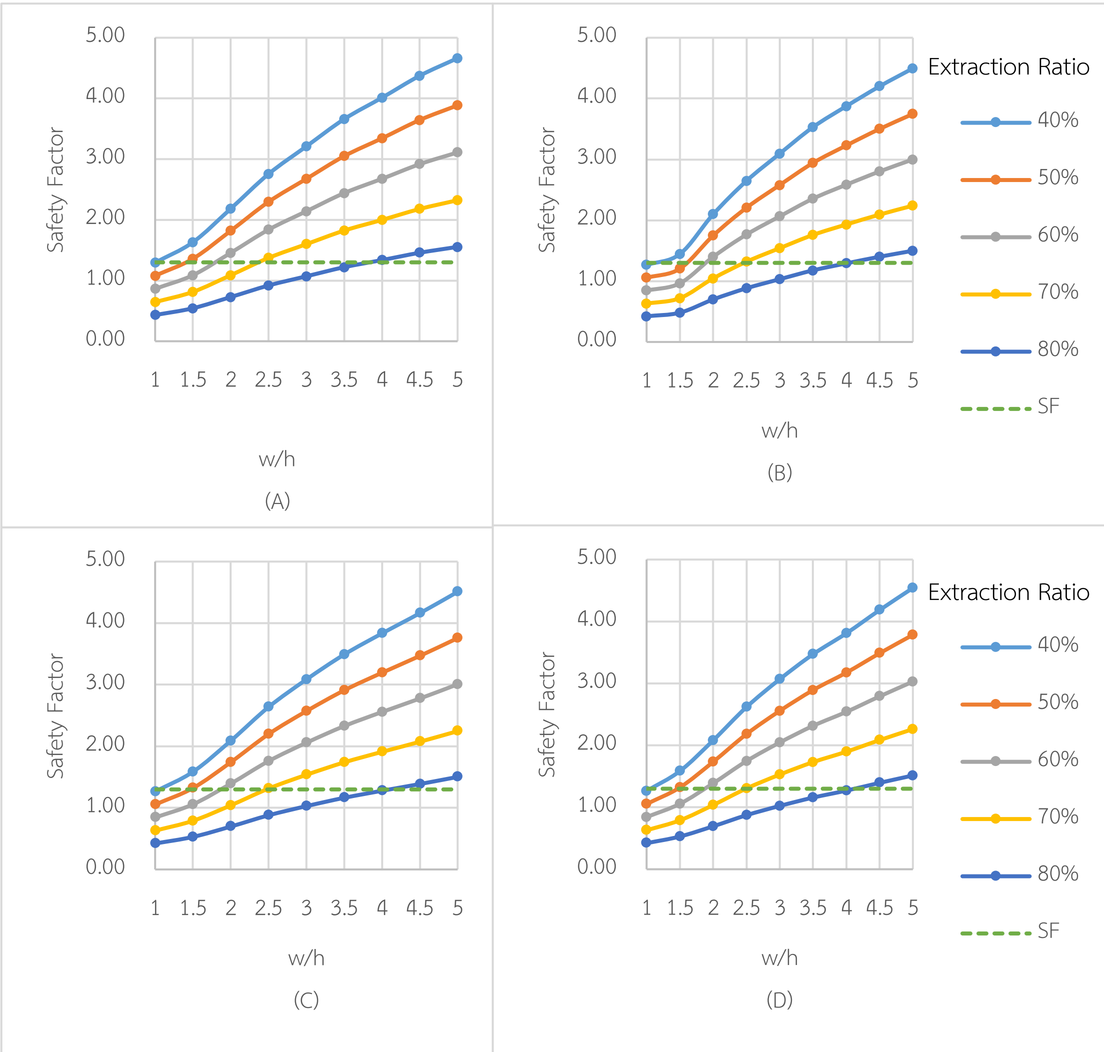

Figure 6-11 Comparison SF with w/h ratio based on extraction ratio for depth 200m (A: h=5m, B: h=10m, C: h=15m D: h=20m)

The results from all 4 graphs provide the optimum value of extraction ratio correlated with w/h ratio which can be utilized to construct a safety envelope for the pillar design. Because the case studies are involving with the change of three different depths of potash seam (200m, 250m, and 300m), the overburden stress will be affected. The change of overburden stress will also affect safety envelope. As a result, safety envelope is required for each depth. The same steps of analysis are applied for other two depths. Table 6-9 summarizes components for constructing safety envelope. These components are obtained from the study of four plots in Figure 6-11. The three safety envelope for each depth are presented in Figure 6-12, Figure 6-13, and Figure 6-14. The optimum dimension should be located on the curve of safety envelope. The zone under the curve is the safety zone in which all potash pillar design should be in this zone.

Table 6-9 Optimum value of extraction ratio correlated with w/h ratio for SF=1.3

Extraction Ratio	w/h Ratio		
	200m	250m	300m
0.4	1.0	2.0	2
0.5	1.5	2.0	2.5
0.6	2.0	2.5	3
0.7	2.5	3.0	4
0.8	4.0	-	-

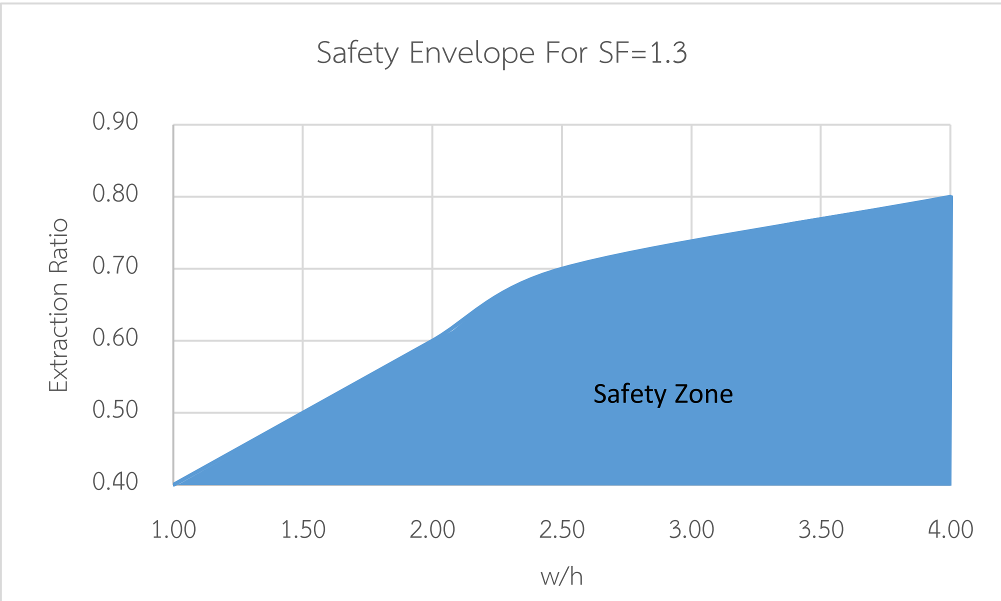

Figure 6-12 Safety envelope for potash pillar design for 200m depth

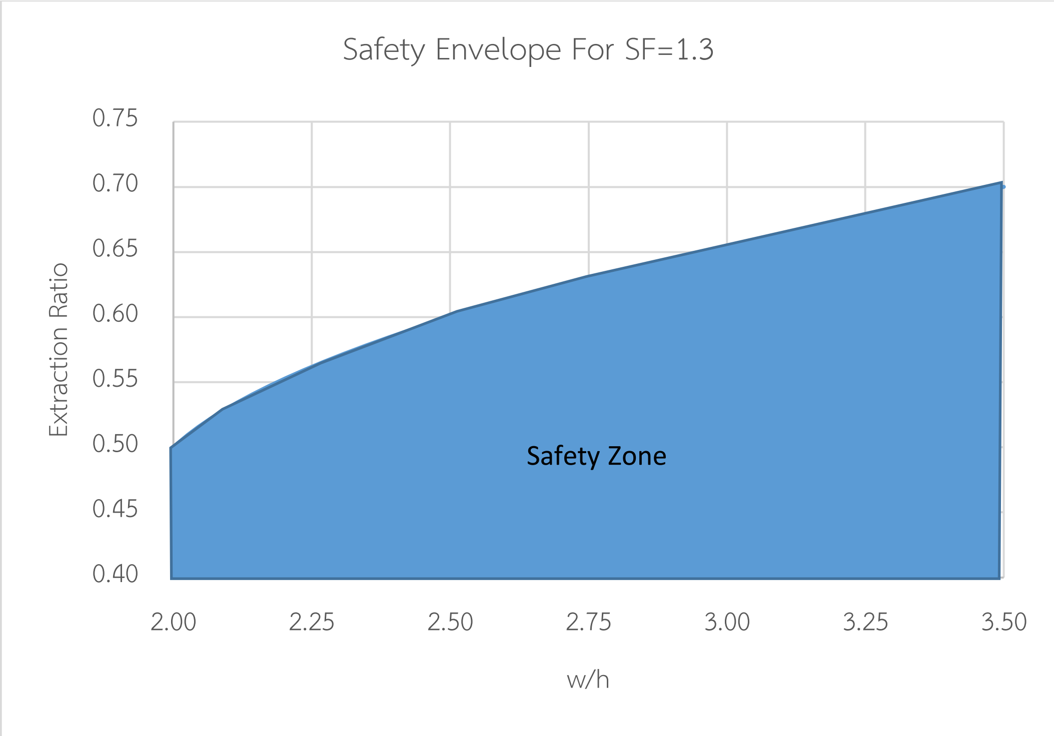

Figure 6-13 Safety envelope for potash pillar design for 250m depth

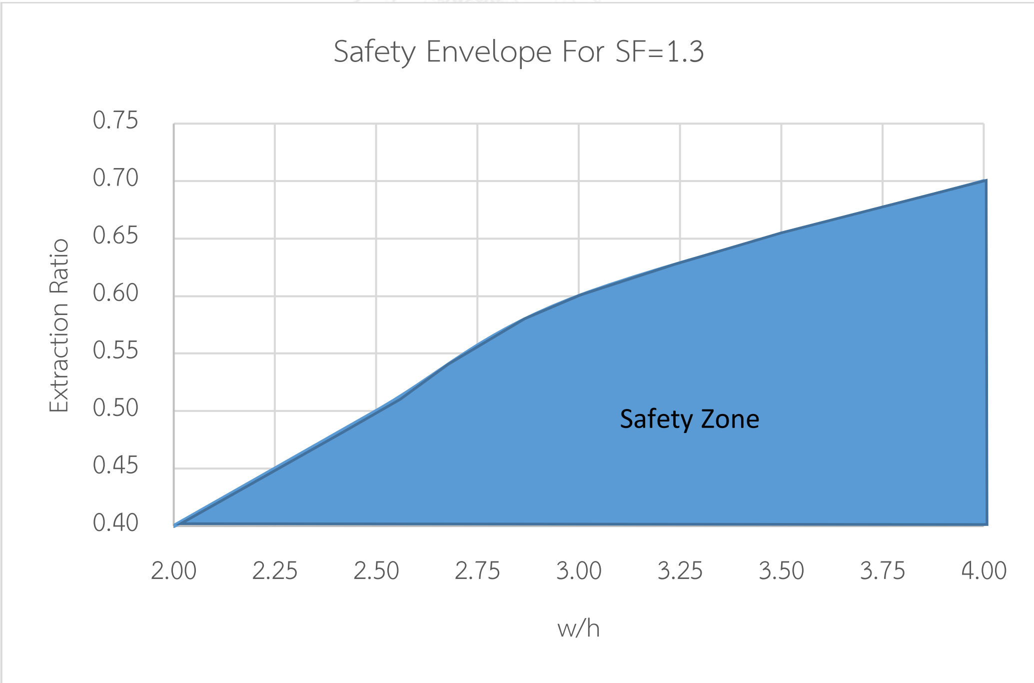

Figure 6-14 Safety envelope for potash pillar design for 300m depth

6.3. Barrier Pillar Design

6.3.1. The Effect of Barrier Pillar Length on Pillar Strength

Barrier pillars are long pillars that support the overburden load on the whole panel and act as panel separator. The length of barrier pillar might have some effect on its strength. So the study in this section is to identify the effect of barrier pillar length on strength. The results from this study are plotted in Figure 6-15.

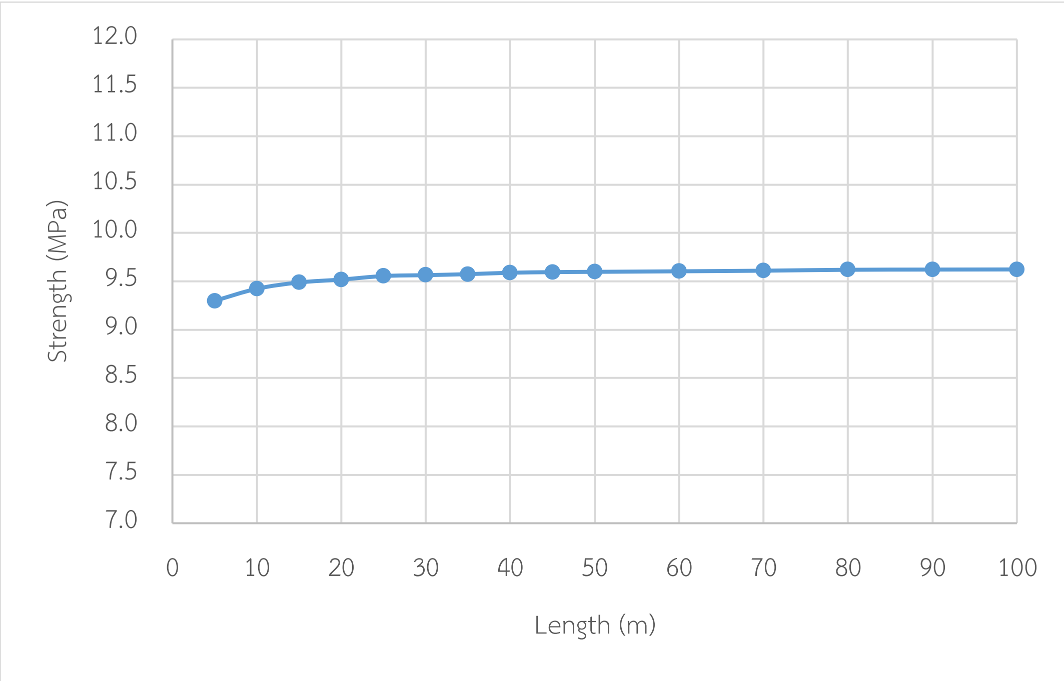

Figure 6-15 The effect of barrier pillar length on its strength (h = 5m, w = 5m)

The observation from Figure 6-15 confirmed that when the length become much longer than the width of the barrier pillar, the strength of the pillar is convergent into a constant value. This mean the length is no longer have an effect on barrier pillar strength. However, because of the running time and the computer capacity, it is not possible to run model with very long length. Pillar length of 10m is selected for this 5m width model as it is compatible with computer capacity with acceptable running time while providing a significantly small error only about 2 percent. For other cases which have difference barrier pillar width, the same concept is applied. As a result, during the estimation of barrier pillar strength, the models should be twice as much length as width.

6.3.2. Stress Estimation of Barrier Pillar

The stresses acting on barrier pillar are estimated similarly to those of the normal pillar. Based on the results from previous section, it is confident that Equation 2-1 can be used for estimating the stress on pillar. However, because of some differences in pillar dimension, it is required to simulate some models of barrier pillar to confirm the capabilities of Equation 2-1 for estimating the stress on barrier pillar.

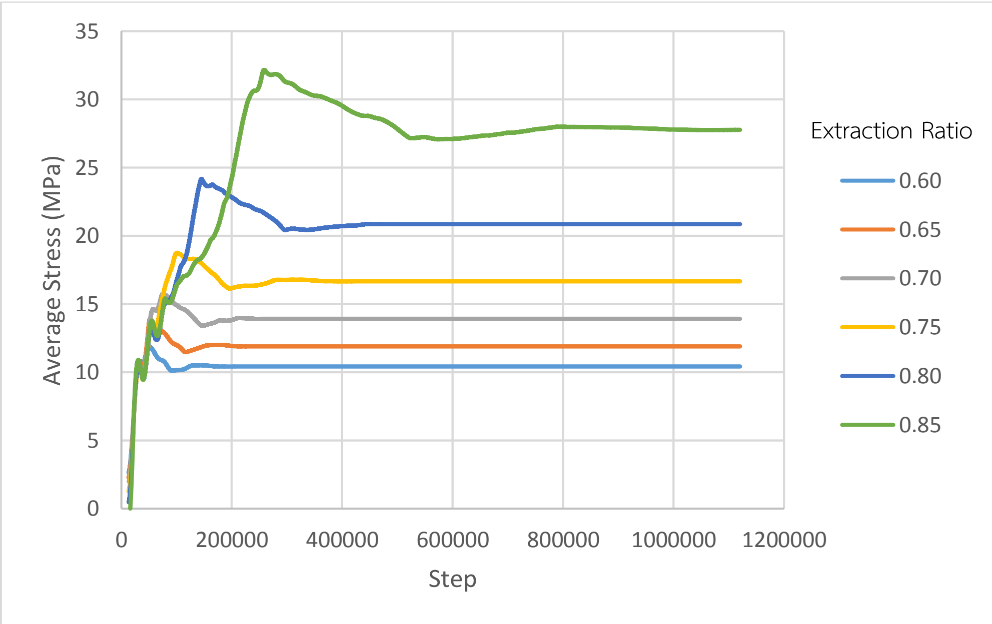

Figure 6-16 Result of simulated barrier pillar stress from FLAC3D (H=200m)

Table 6-10 Comparison barrier pillar stress: empirical analysis vs numerical simulation

Depth of Potash (m)	Extraction Ratio	Stress from Empirical (MPa)	Stress from Numerical (MPa)
200	0.60	10.42	10.42
	0.65	11.91	11.89
	0.70	13.90	13.91
	0.75	16.68	16.66
	0.80	20.85	20.85
	0.85	27.80	27.76

The observation on Figure 6-16 and Table 6-10 of barrier pillar stress estimation shows an identical result to those of the regular pillar. It confirms that Equation 2-1 is also applicable for stress estimation of barrier pillar. Thus, in order to save some running time for stress estimation of barrier pillar. The numerical stress value for the depth of 250 and 300m is confidently assumed to equal to empirical stresses. The estimation result for 250m and 300m are highlighted in Table 6-11.

Table 6-11 Barrier pillar stress for depth 250m and 300m

Depth of Potash (m)	Extraction Ratio	Barrier Pillar Stress (MPa)
250	0.60	13.27
	0.65	15.17
	0.70	17.70
	0.75	21.24
	0.80	26.55
	0.85	35.40
300	0.60	15.77
	0.65	18.03
	0.70	21.03
	0.75	25.24
	0.80	31.55
	0.85	42.06

6.3.3. Strength Estimation of Barrier Pillar

The models for estimating barrier pillar strength is simulated based on the study of length effect mentioned in the section above. In addition to the boundary conditions, barrier pillar model is fixed in one vertical plan at the back of the model which represent the continuities and unlimited length of the barrier pillar. The results of all cases of strength estimation with mine of height of 5m are represented in Figure 6-17. Table 6-12 shows the results comparison from both numerical and empirical analysis using Equation 2-10. Similar, to results of regular pillar, the outcome from both methods are plotted as illustrated in Figure 6-18 to summarize and compare them together. As presumed, the results from empirical barrier pillar strength estimation show a similar to those from regular pillar. Equation 2-10 provided an under-estimated value for each barrier strength estimation. As a result, this equation also need to be modified in order to effectively estimated the strength of barrier pillar strength.

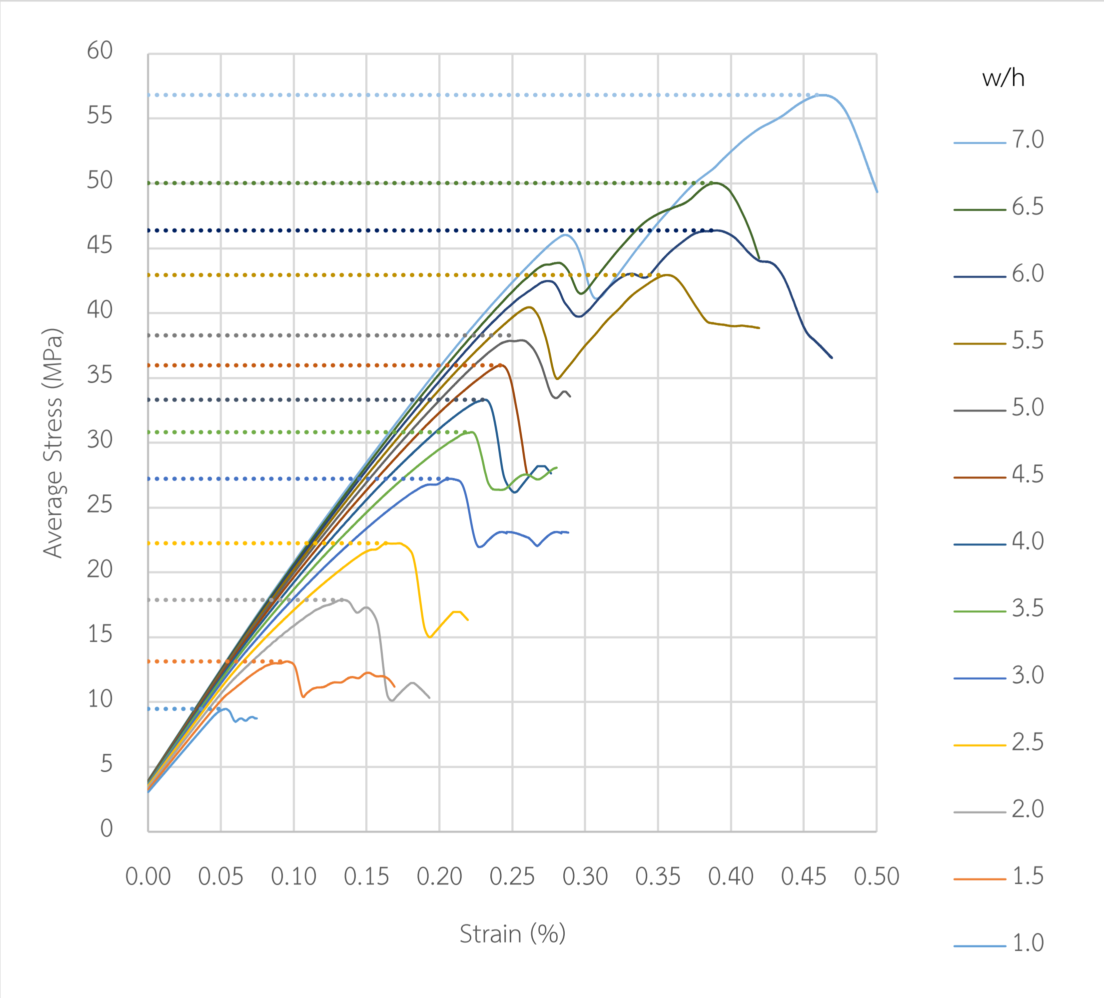

Figure 6-17 Results of barrier pillar peak strength from FLAC3D (h = 5m)

Table 6-12 Estimated barrier pillar strength: numerical vs. empirical analysis

w_B/h Ratio	Numerical Strength (MPa)				Empirical Strength (MPa)
	h = 5m	h = 10m	h = 15m	h = 20m	
1.0	9.48	9.16	9.12	9.10	10.31
1.5	13.14	12.69	12.66	12.64	12.67
2.0	17.88	17.18	17.13	17.04	15.03
2.5	22.25	21.51	21.31	21.25	17.39
3.0	27.22	26.17	25.34	24.83	19.75
3.5	30.82	29.50	29.00	28.24	22.11
4.0	33.32	32.25	31.91	32.12	24.47
4.5	35.97	35.35	35.55	35.81	26.83
5.0	38.28	39.77	37.91	38.09	29.19
5.5	42.94	43.43	42.85	43.29	31.55
6.0	46.38	46.33	44.68	44.75	33.91
6.5	50.03	47.30	47.74	45.63	36.27
7.0	56.82	51.46	51.43	49.30	38.63

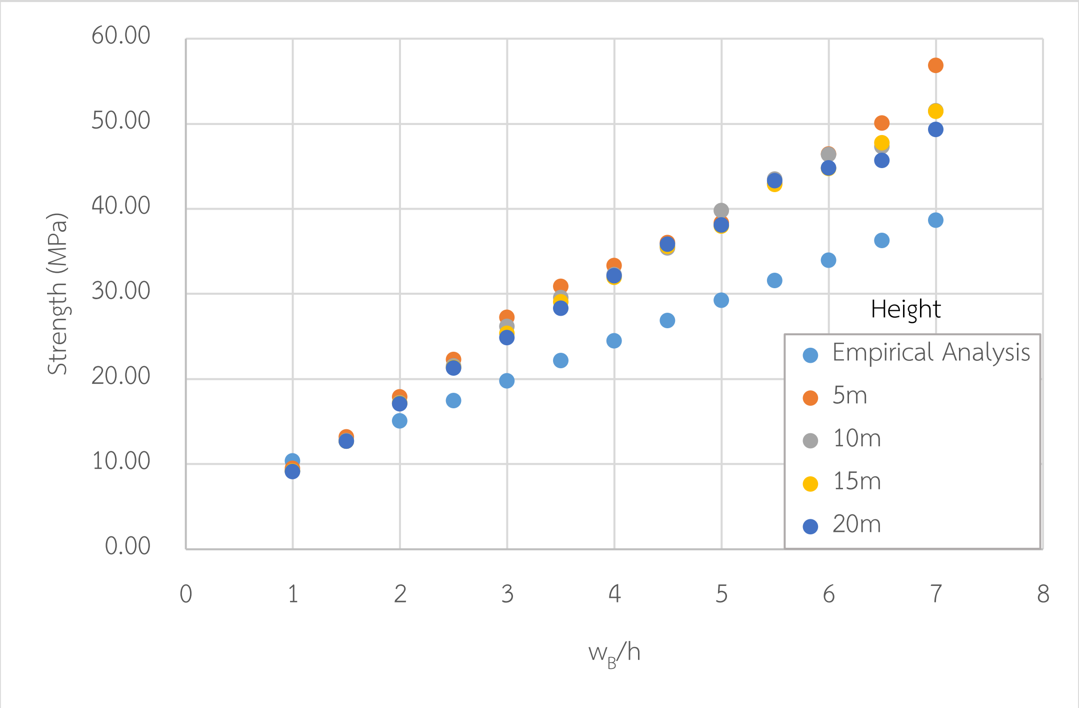

Figure 6-18 Summary results of estimated barrier pillar strength

6.3.4. Formula Modification for Potash Barrier Pillar

The modified Equation 2-10 can be used as the formula for barrier pillar strength estimation as the previous study had already eliminated the length effect. Slenderness constant will be defined for barrier pillar to modify this equation. The same process of identification of slenderness constant for barrier pillar is similar to regular pillar. All the results from numerical barrier pillar strength estimation are plotted separately based on the height as shown in Figure 6-19.

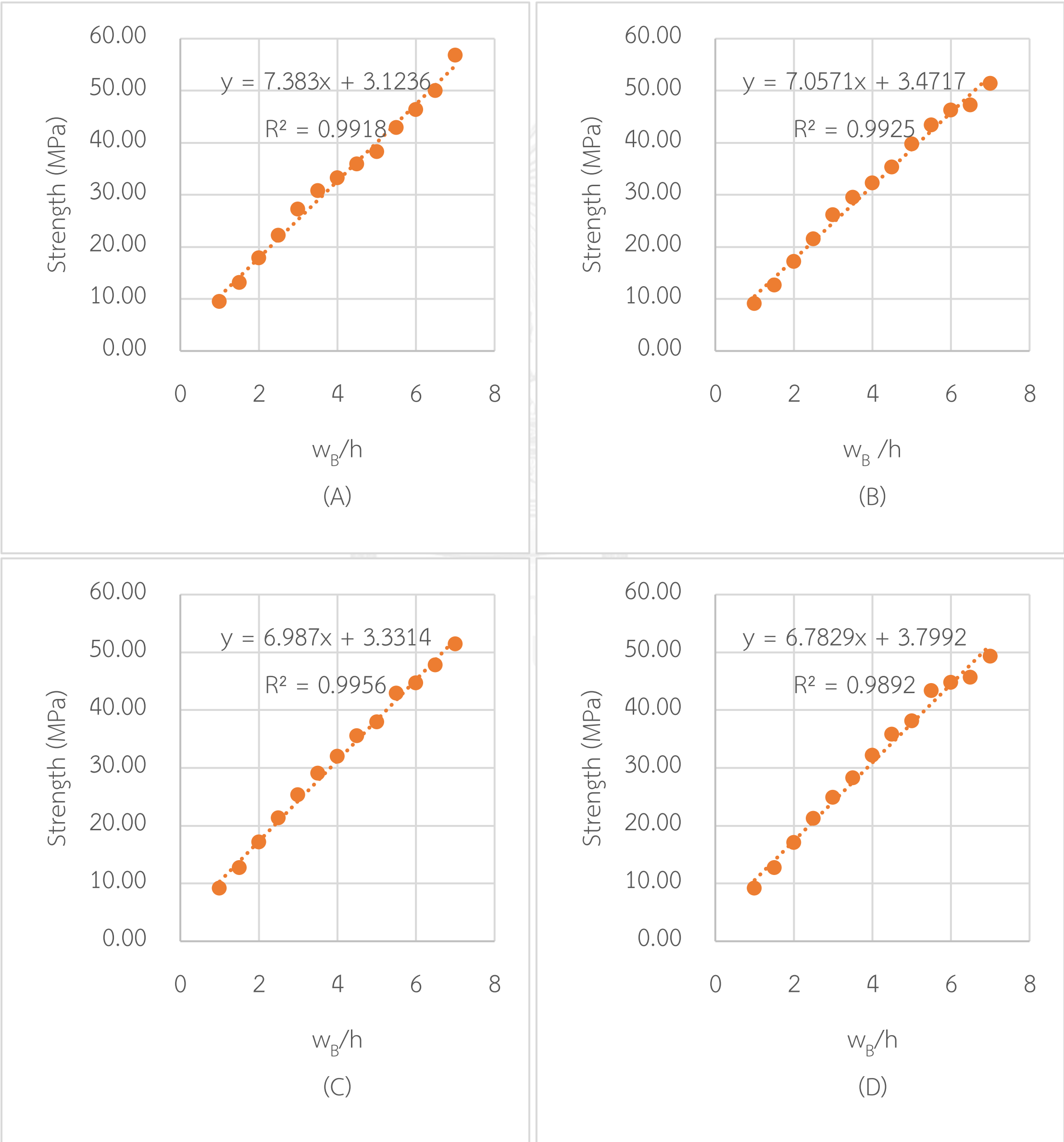

Figure 6-19 Relationship between barrier pillar strength and w_B/h (A: h=5, B: h=10, C: h=15, D: h=20m)

Identical to regular pillar, the values of slenderness constants are taken out from trendline's equations. Because of the unique equations of barrier pillar, slenderness constants for barrier pillar are also differ from those of regular pillar. Table 6-13 summarized the equation and slenderness constants for each height. The average values among these are taken to represent the universal values for estimation the strength of potash barrier pillar.

Table 6-13 Slenderness constants of barrier pillar

Height	Trendline's Equation	Format Equation 2-8	α	β
5m	$\sigma_P = (3.1236 + 7.3830 \times \frac{w_B}{h})$	$\sigma_P = 8.74 \times (0.357 + 0.845 \times \frac{w_B}{h})$	0.357	0.845
10m	$\sigma_P = (3.4717 + 7.0571 \times \frac{w_B}{h})$	$\sigma_P = 8.74 \times (0.397 + 0.807 \times \frac{w_B}{h})$	0.397	0.807
15m	$\sigma_P = (3.3314 + 6.9870 \times \frac{w_B}{h})$	$\sigma_P = 8.74 \times (0.381 + 0.799 \times \frac{w_B}{h})$	0.381	0.799
20m	$\sigma_P = (3.7992 + 6.7829 \times \frac{w_B}{h})$	$\sigma_P = 8.74 \times (0.435 + 0.776 \times \frac{w_B}{h})$	0.435	0.776
Average			0.393	0.807

In order to modify a suitable formula for effectively estimated strength of potash barrier pillar, result of slenderness constants from Figure 6-19 and Table 6-13 is applied into the format of Equation 2-8. The final result is expressed in Equation 6-2 which would be suitable for this estimation.

$$\sigma_P = \sigma_S (0.393 + 0.807 \times \frac{w_B}{h}) \qquad \textit{Equation 6-2}$$

From this relationship demonstration, Equation 6-2 cans be used to estimate the strength of barrier pillar with the conditions of parameter range below:

- Barrier pillar width to height w_B/h: 1 to 7
- Mining height h: 5m to 20m

For confirming the applicability of the formula for estimating the strength of barrier pillar, the empirical analysis is adopted the equation above for estimation. The results from the above analysis are compared again with the results from numerical simulation by plotting them together. As illustrated in Figure 6-20, values of strength from both methods are correlated satisfactorily well with each other. This finding is further support the idea of using this empirical equation for estimating the strength of barrier pillar of underground potash mine in Thailand.

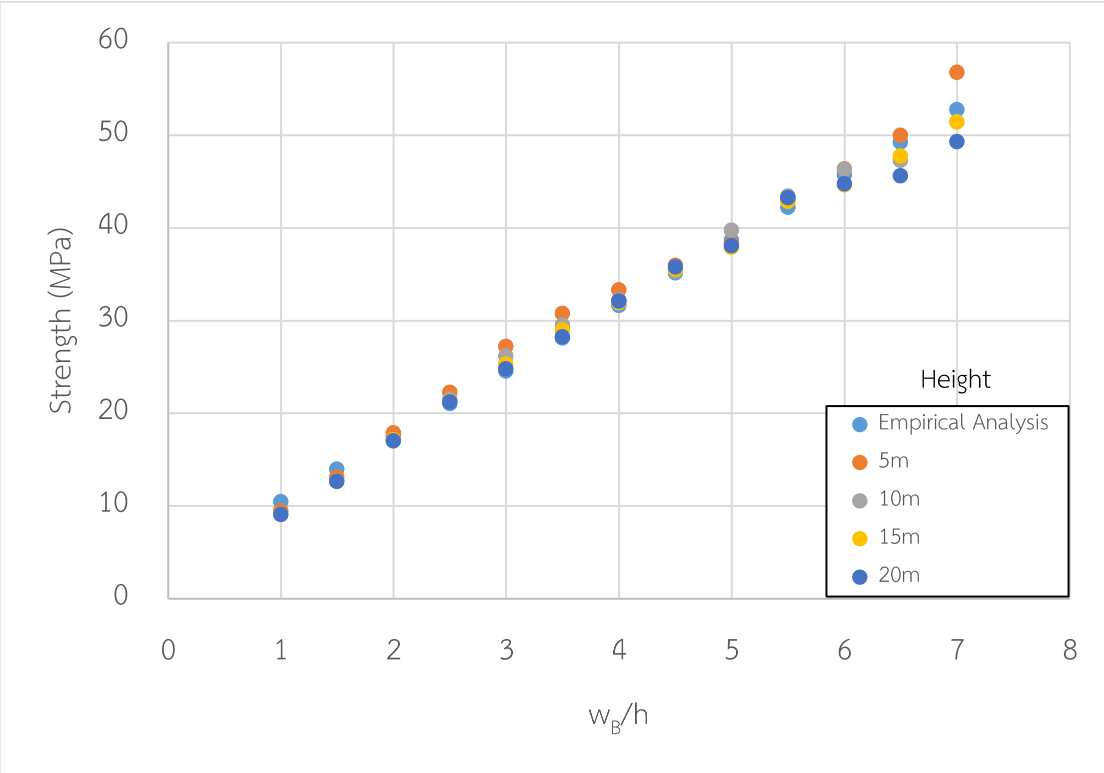

Figure 6-20 Barrier pillar strength: numerical analysis vs modified Obert & Duvall

6.3.5. Safety Envelope of Barrier Pillar Design

Safety envelope of barrier pillar is designed in the same way as the regular pillar. The result from stress and strength estimation is calculated into the values of safety factor and plotted in group based on the height of mine in Figure 6-21. During modeling barrier pillar, all the pillar in the panel are assumed to be already failed. As the result, the value of safety factor for barrier pillar can be as low as 1.3. By applied the value of safety factor equal to 1.3 to the graph, the optimum correlation between w/h ratio and extraction ratio can be defined as represented in Table 6-14.

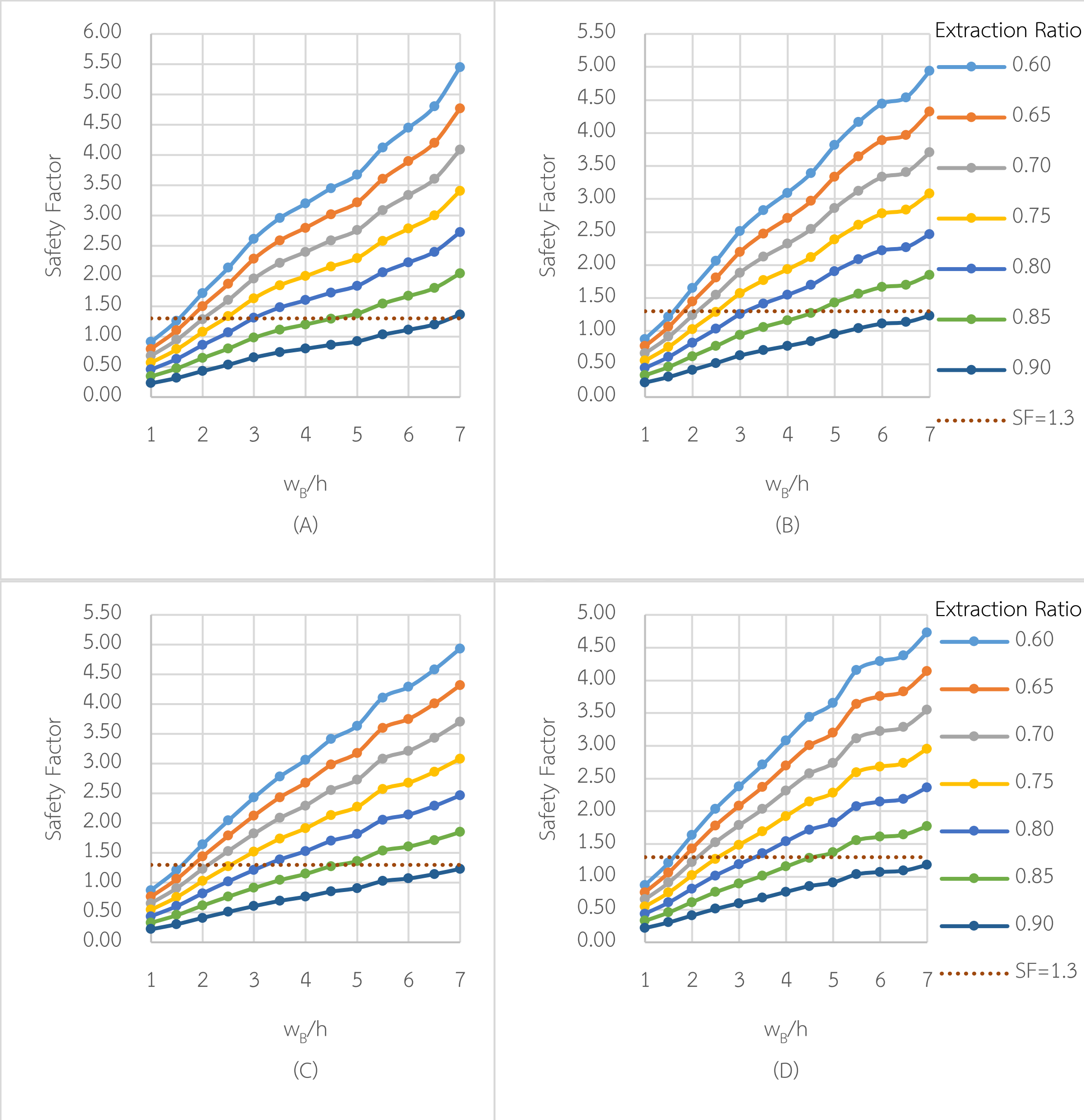

Figure 6-21 Comparison SF with w_B/h ratio of barrier pillar based on extraction ratio for depth 200m (A: h=5m, B: h=10m, C: h=15m D: h=20m)

The result from Table 6-14 can be used for constructing safety envelope for barrier pillar similarly to those for regular pillar. Figure 6-22, Figure 6-23 and Figure 6-24 illustrated the safety envelope for designing barrier pillar for underground potash mine in Thailand. As the purpose of designing barrier pillar is for figuring out how big is the panel that barrier pillar can support, relationship between width of barrier pillar with the panel width is required for a better illustration. This relationship can be determined from each safety envelope. Because there are 4 values of mining height and each height require different relation, each safety envelope can generate 4 different relations between barrier pillar and panel width. Figure 6-25, Figure 6-26 and Figure 6-27 show the final result for barrier pillar design which presented the relation between barrier pillar width and panel width based on the depth of the mine.

Table 6-14 Optimum correlation between extraction ratio and w_B/h ratio for SF=1.3

Extraction Ratio	w_B/h Ratio		
	200m	250m	300m
0.60	1.5	2.0	2.5
0.65	2.0	2.5	3.0
0.70	2.0	3.0	3.5
0.75	2.5	3.5	4.5
0.80	3.5	4.5	5.5
0.85	4.5	6.5	-
0.90	-	-	-

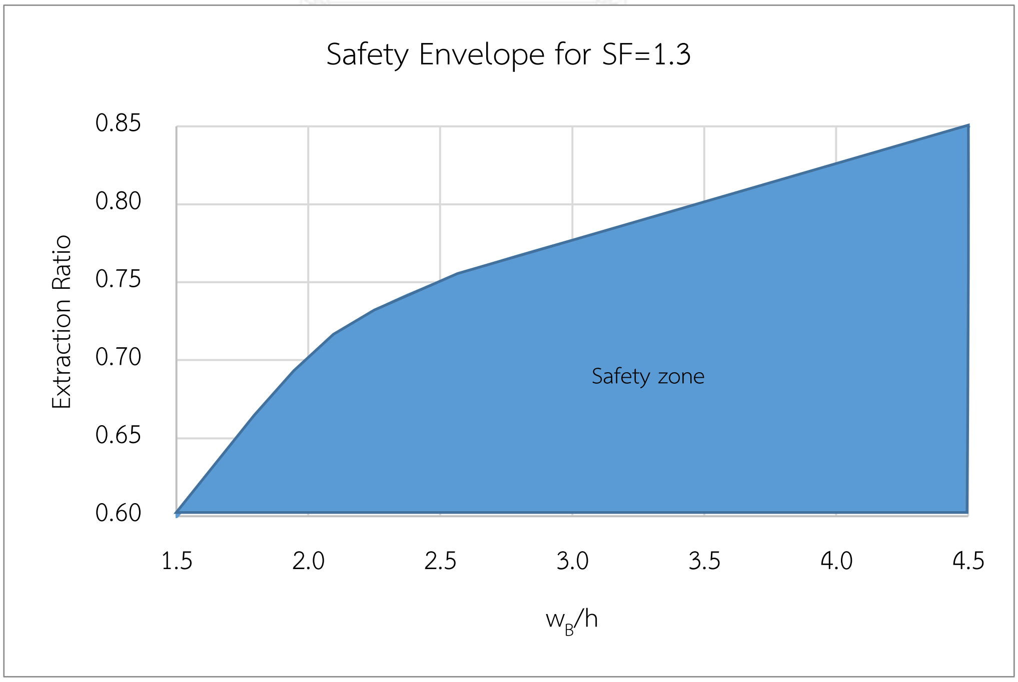

Figure 6-22 Safety envelope for potash barrier pillar design for 200m depth (SF=1.3)

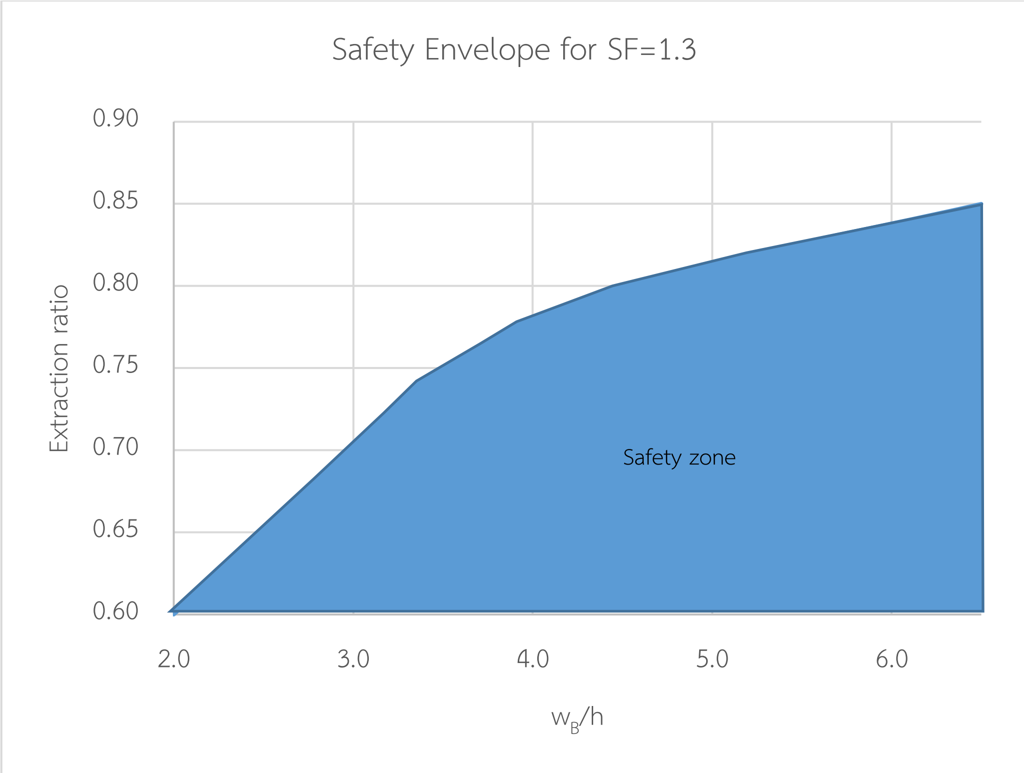

Figure 6-23 Safety envelope for potash barrier pillar design for 250m depth (SF=1.3)

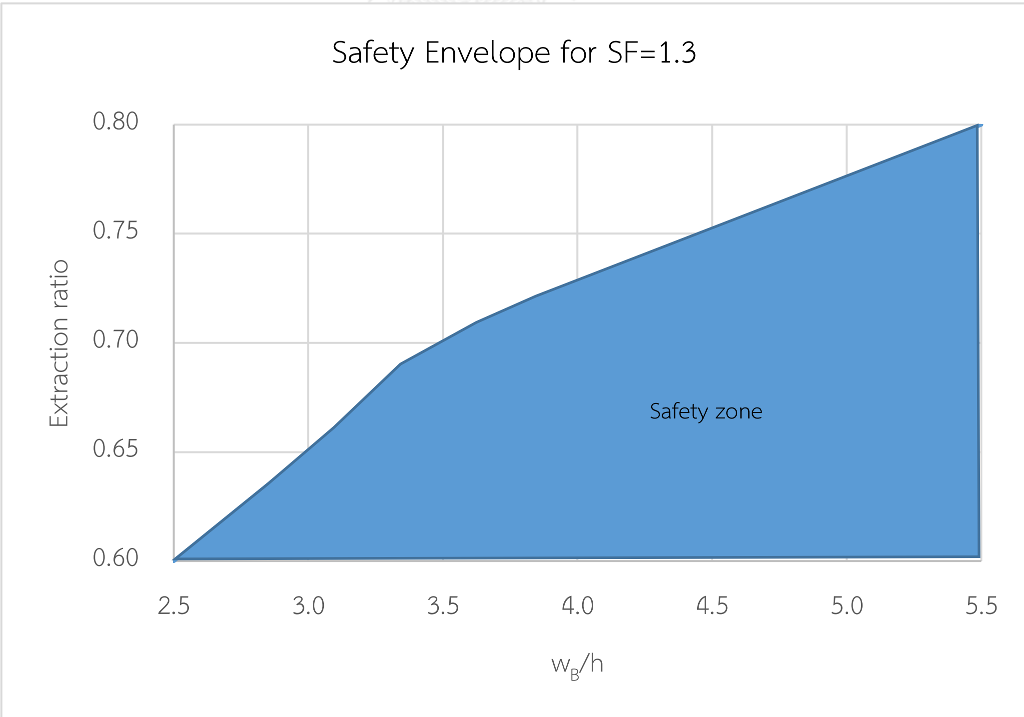

Figure 6-24 Safety envelope for potash barrier pillar design for 300m depth (SF=1.3)

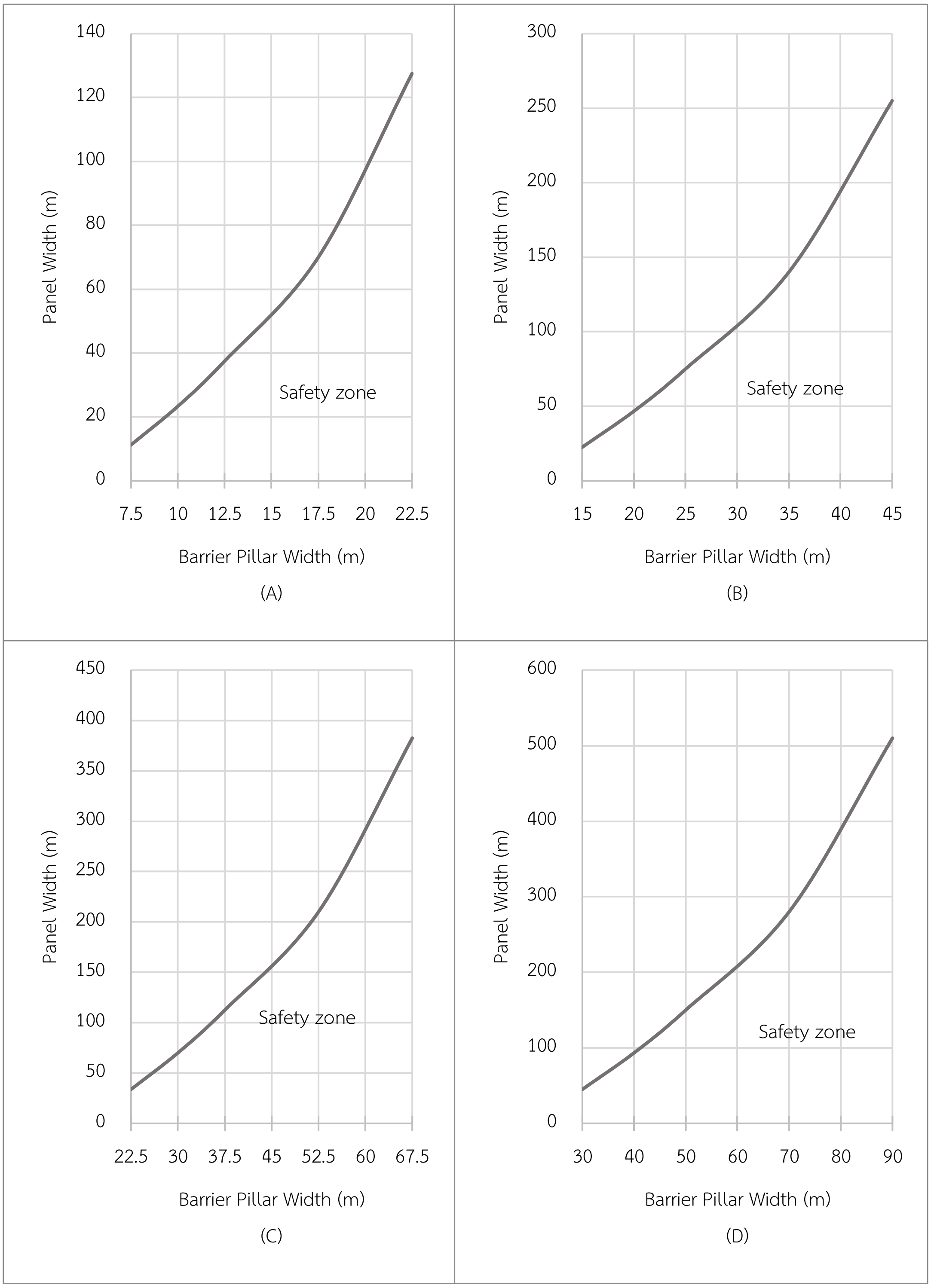

Figure 6-25 Relationship between barrier pillar width and panel width for 200m depth A: h=5m, B: h=10m, C: h=15m D: h=20m)

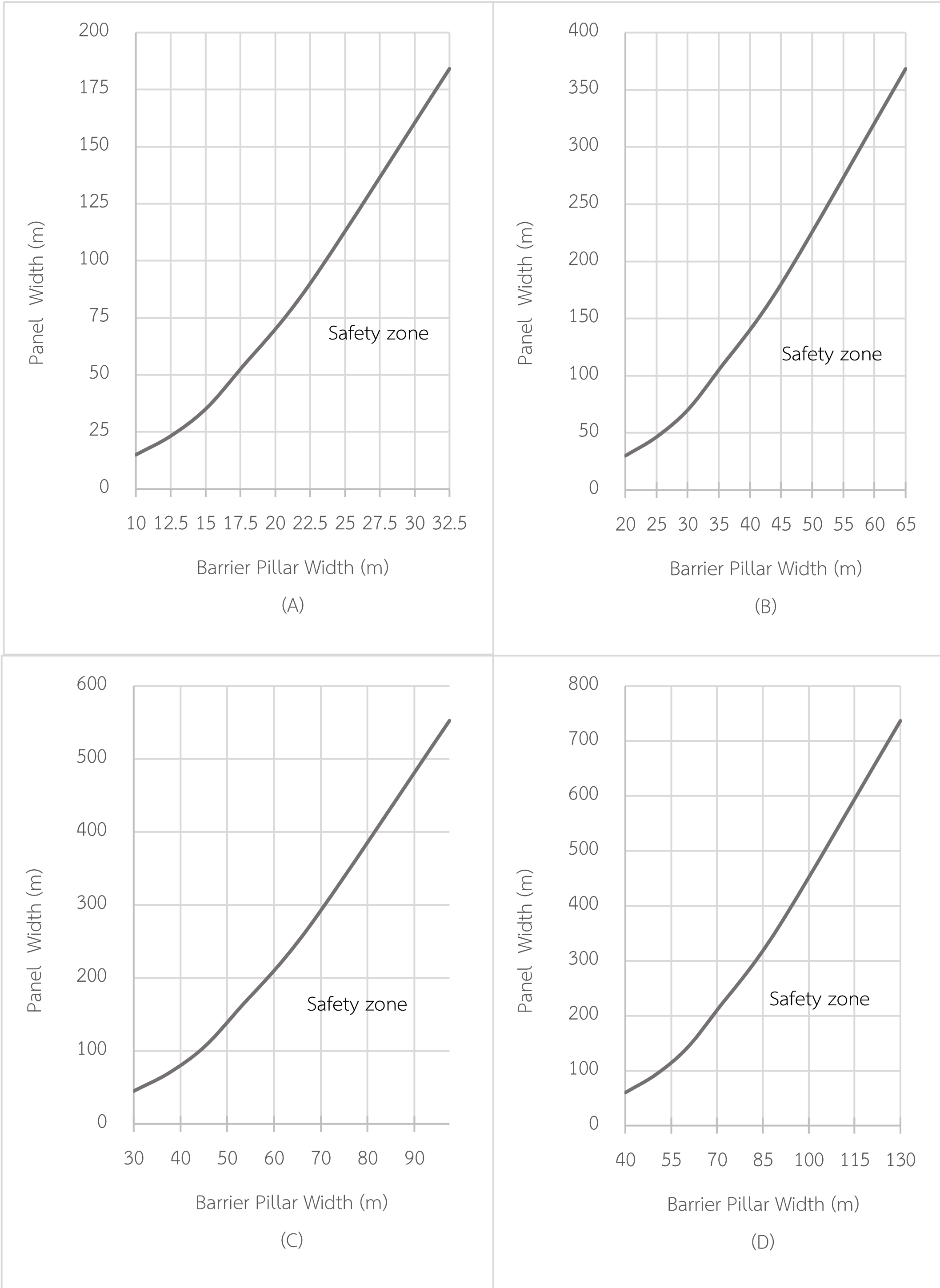

Figure 6-26 Relationship between barrier pillar width and panel width for 250m depth (A: h=5m, B: h=10m, C: h=15m D: h=20m)

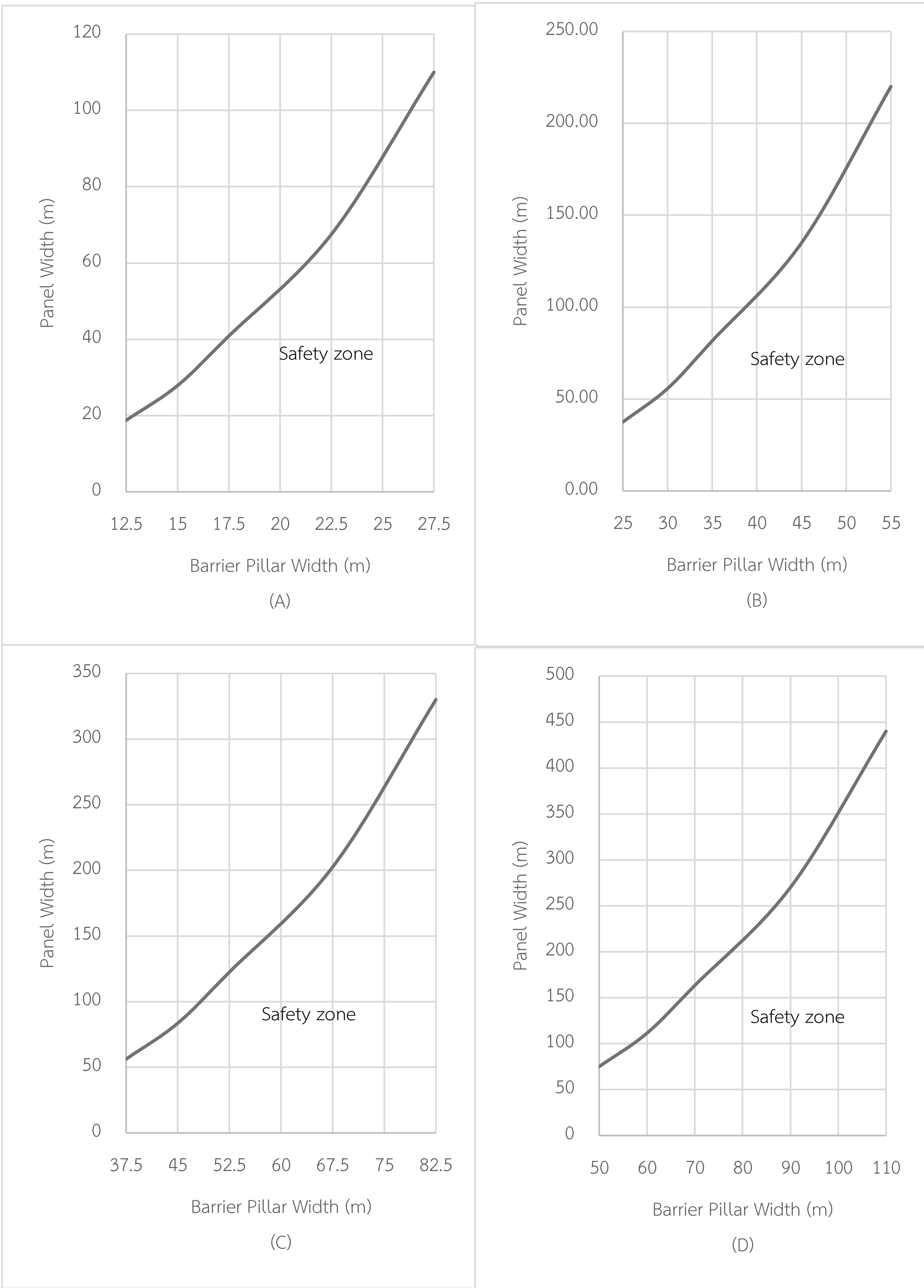

Figure 6-27 Relationship between barrier pillar width and panel width for 300m depth (A: h=5m, B: h=10m, C: h=15m D: h=20m

The relationship between barrier pillar width w_B and panel width w_{Pn} can be found for the depth of 200m by using graph normalization method of the four graphs in Figure 6-25. As the relation between four graphs in Figure 6-25 are based on mining height, the normalized graph for this figure can be generated by dividing the panel width and barrier pillar width by the mining height. The value of panel wide to height ration and barrier pillar width to height ratio from each graph in Figure 6-25 are identical. These two ratios are plotted into a graph as shown in Figure 6-28. The trendline's equation in Equation 6-3 from the normalized plot which can be rewritten into Equation 6-4 to show the relation between panel width, barrier pillar width and mining height for depth 200m.

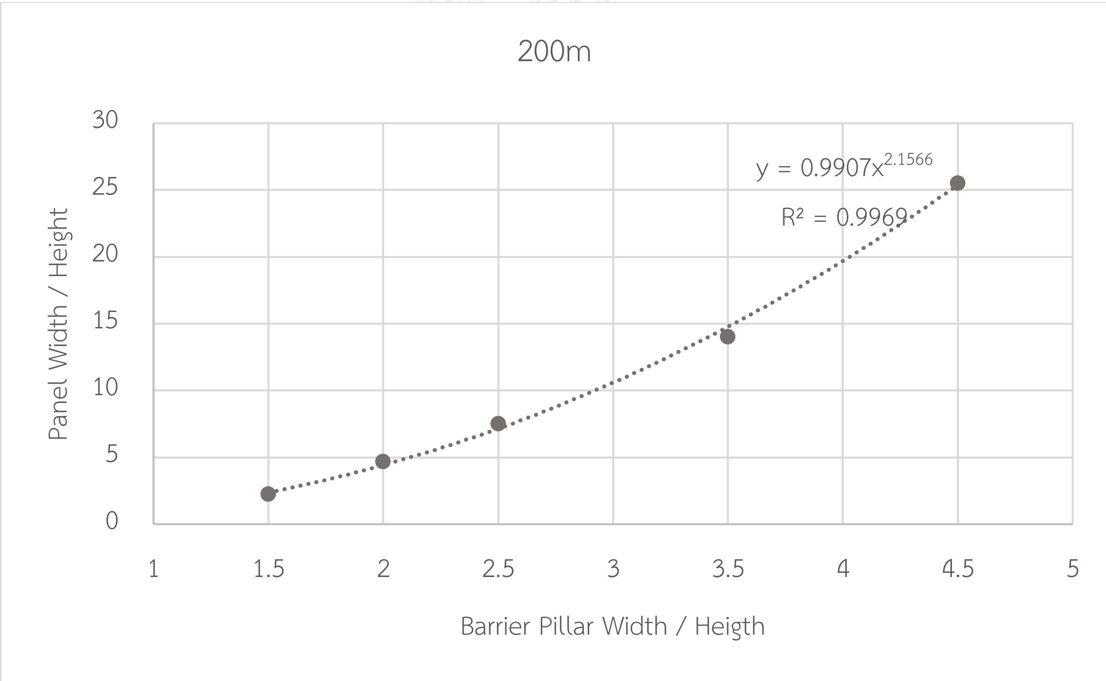

Figure 6-28 Relation between barrier pillar width and panel width for 200m depth

$$\frac{w_{Pn}}{h} = 0.9906\left(\frac{w_B}{h}\right)^{2.1566} \qquad \text{Equation 6-3}$$

$$w_{Pn} = \frac{0.9906 \times w_B^{\,2.1566}}{h^{1.1566}} \qquad \text{Equation 6-4}$$

By applying the same concept to 250m depth in Figure 6-26 and 300m depth in Figure 6-27, the relationship between barrier pillar width and panel width can be normalized based on mining height. The value of panel width to height ratio and barrier panel width to height ratio is plotted in Figure 6-29 for 250m and Figure 6-30 for 300m. The trendline's equation in Equation 6-5 and 6-7 from the normalized plot which can be rewritten into Equation 6-6 and 6-8 to show the relation between panel width, barrier pillar width and mining height for depth 250m and 300m respectively.

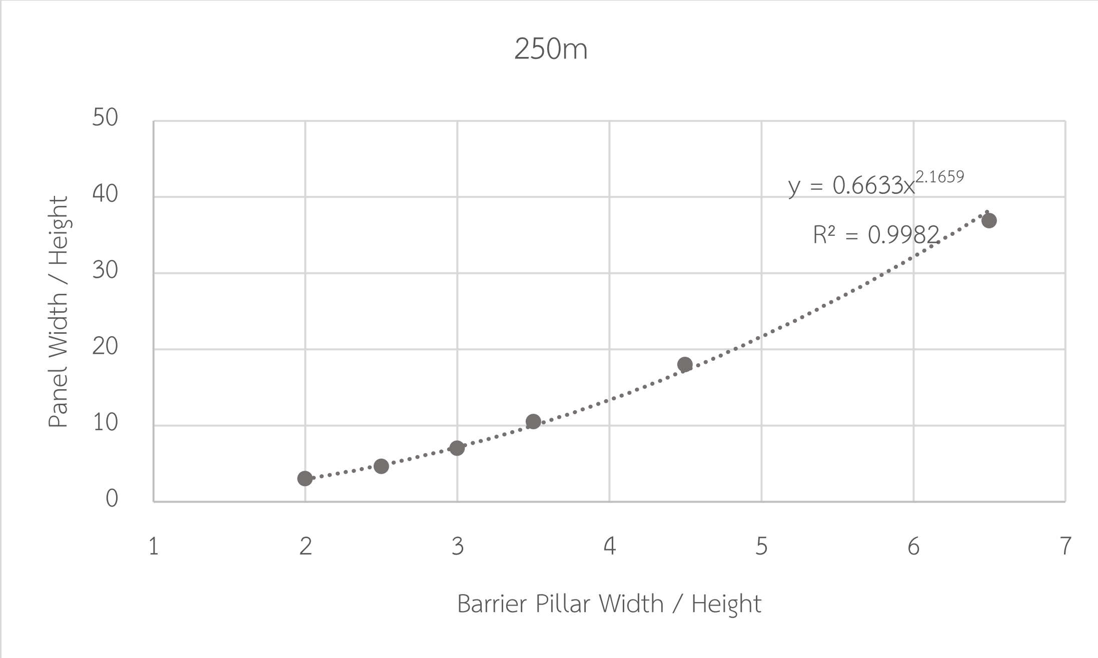

Figure 6-29 Relation between barrier pillar width and panel width for 250m depth

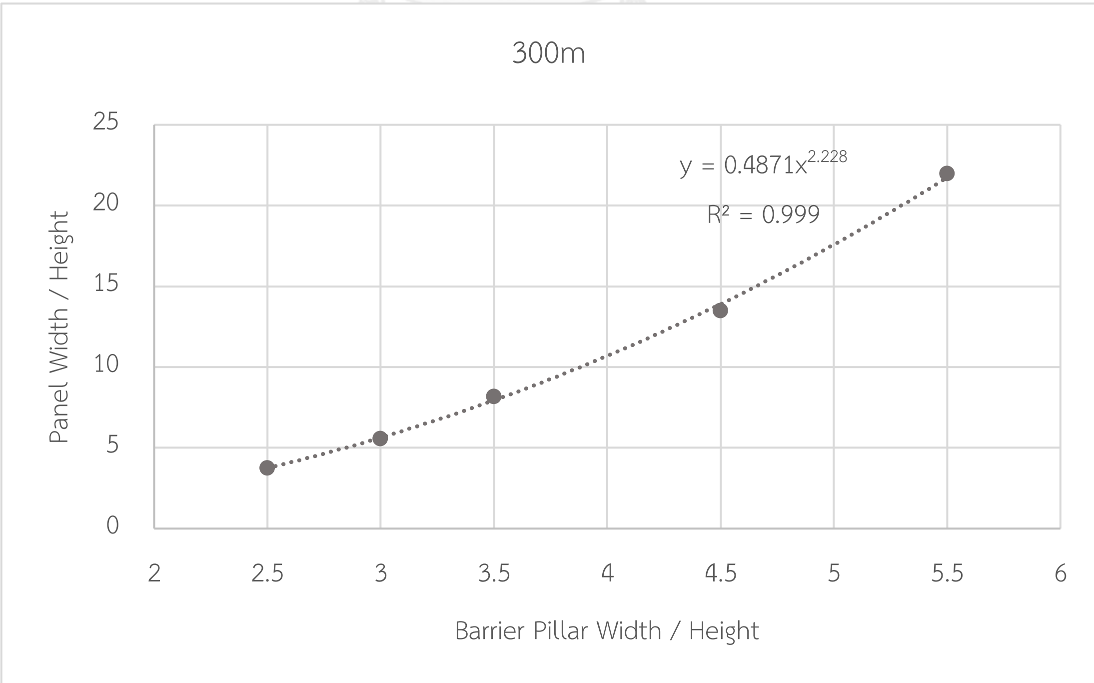

Figure 6-30 Relation between barrier pillar width and panel width for 300m depth

$$\frac{w_{Pn}}{h} = 0.6633\left(\frac{w_B}{h}\right)^{2.1659}$$ Equation 6-5

$$w_{Pn} = \frac{0.6633 \times w_B^{2.1659}}{h^{1.1659}}$$ Equation 6-6

$$\frac{w_{Pn}}{h} = 0.4871\left(\frac{w_B}{h}\right)^{2.2280}$$ Equation 6-7

$$w_{Pn} = \frac{0.4871 \times w_B^{2.2280}}{h^{1.2280}}$$ Equation 6-8

$$w_{Pn} = \frac{f(H) \times w_B^{f'(H)}}{h^{f''(H)}}$$ Equation 6-9

The formula of panel width can be further generalized based on the depth of the of the deposit. By study on the Equation 6-4, 6-6 and 6-8, there are three different depth functions included *f(H), f'(H)* and *f"(H).* These depths related functions are determined separately by plotting depth related constants from each function with the depth as shown in Figure 6-31, 6-32 and 6-33.

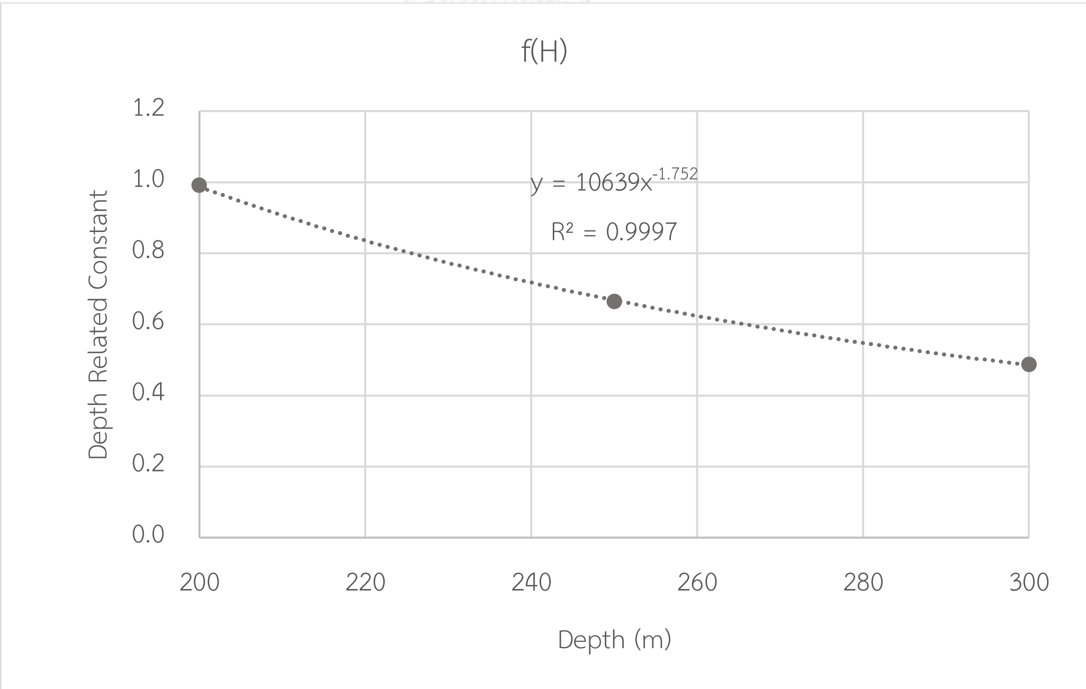

Figure 6-31 Demonstration of f(H)

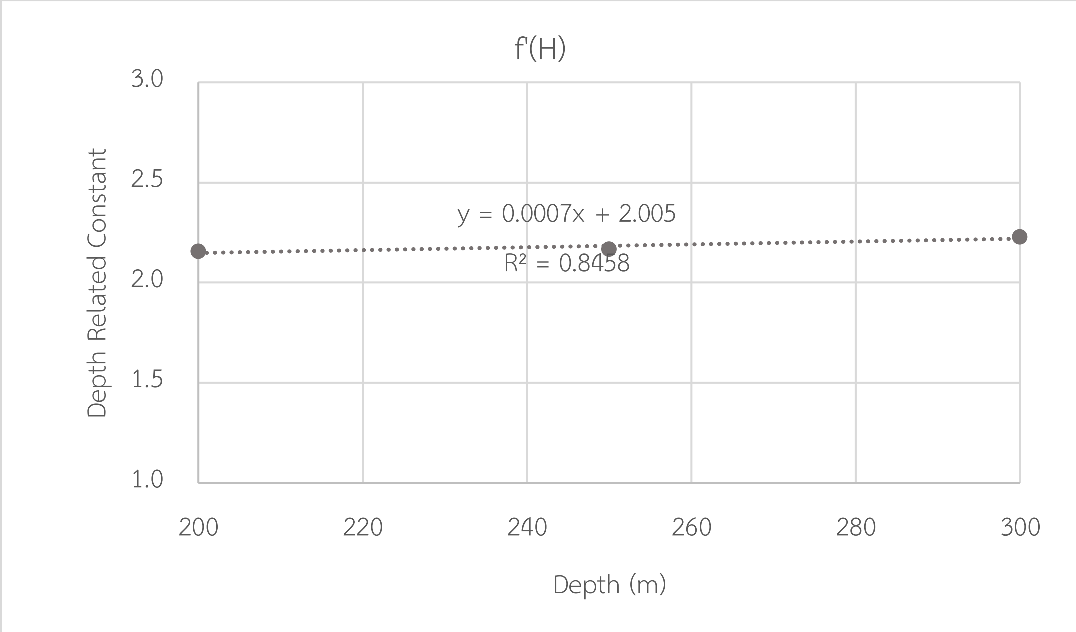

Figure 6-32 Demonstration of f'(H)

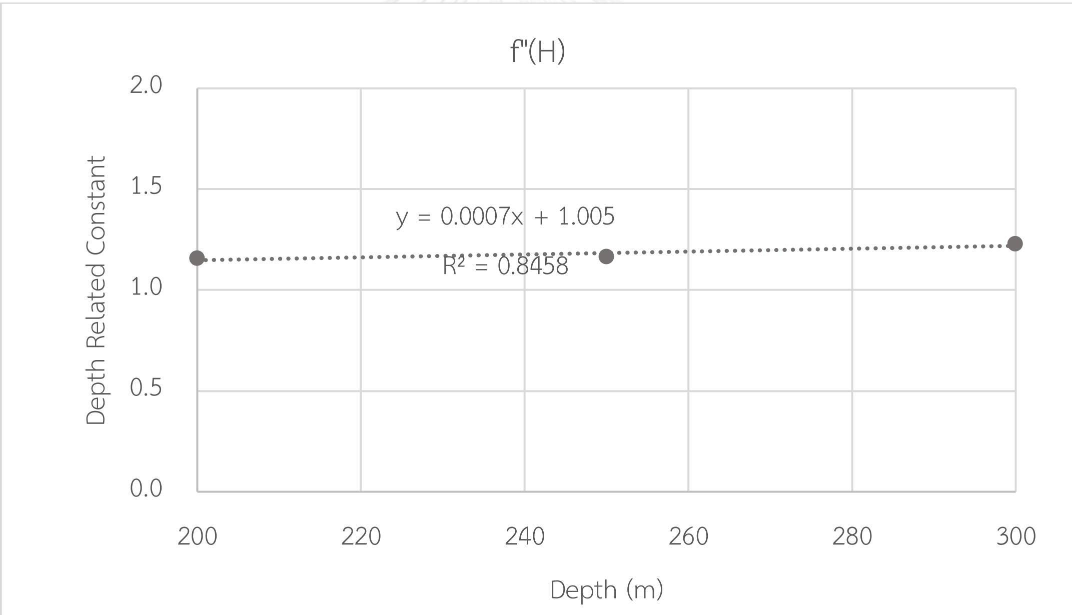

Figure 6-33 Demonstration of f"(H)

The outcome from the demonstration of the depth functions in figure above, show the three different depth function equations which are shown in Equation 6-10, 6-11 and 6-12. Supposing a depth related constant *k* is equal to $7 \times 10^{-4} \times H$, each depth function is simplified into equation 6-13, 6-14 and 6-15. By applying these functions in to the Equation 6-9, general form of panel width formula can be obtained, which is expressed in Equation 6-16.

$$f(H)=\frac{1.06\times10^{4}}{H^{1.75}} \qquad \text{Equation 6-10}$$

$$f'(H)=\left(7\times10^{-4}\times H\right)+2 \qquad \text{Equation 6-11}$$

$$f''(H)=\left(7\times10^{-4}\times H\right)+1 \qquad \text{Equation 6-12}$$

$$f(H)=\frac{7.42}{kH^{0.75}} \qquad \text{Equation 6-13}$$

$$f'(H)=k+2 \qquad \text{Equation 6-14}$$

$$f''(H)=k+1 \qquad \text{Equation 6-15}$$

$$w_{Pn}=\frac{7.42\times w_{B}^{(k+2)}}{kH^{0.75}h^{(k+1)}} \qquad \text{Equation 6-16}$$

where $k=7\times10^{-4}\times H$

From this relationship demonstration, Equation 6-16 cans be used to define the width of panel from barrier pillar width w_b, mining height h and depth of the potash deposit H with the conditions of parameter range below:

- Barrier pillar width to height w_B/h: 1 to 7
- Mining height h: 5m to 20m
- Depth of the deposit H: 200m to 300m

6.4. Comparison Empirical Strength Formulation with Previous Formula

6.4.1. Square Pillar

Table 6-15 Comparison of empirical strength formulation for square pillar between research work and Bieniawski work

		Research Work	Bieniawski Work
Square Pillar	Formula	$\sigma_P=\sigma_S(0.348+0.677\frac{w}{h})$	$\sigma_P=\sigma_S(0.64+0.36\frac{w}{h})$
	Material	Potash in Thailand	Coal
	Testing Method	Model Simulation FLAC3D	Field Investigation
	w/h Ratio	1 to 5	0.5 to 3.4
	Mining Height	5m to 20m	Any height

The empirical strength formulation from this research for square pillar is compared with the previous work of Bieniawski. Slenderness constants are varied based on material properties. Method of testing is different for both work. The previous work used the experience of mine observation while this research used numerical simulation which lead to the wider range of *w/h* ratio. Mining height from the previous work is not specified however for empirical strength formulation form this work should be used in the mining height range between 5m to 20m.

6.4.2. Rectangular Pillar

Table 6-16 Comparison of empirical strength formulation for rectangular pillar between research work and Mark-Bieniawski work

		Research Work	**Mark-Bieniawski Work**
Rectangular Pillar	**Formula**	$\sigma_P = \sigma_S(0.393 + 0.807\frac{w}{h})$	$\sigma_P = \sigma_S(0.64 + 0.54\frac{w}{h})$
	Material	Potash in Thailand	Coal
	Testing Method	Model Simulation FLAC3D	Model Simulation ARMPS
	w/h Ratio	1 to 7	1 to 20
	Mining Height	5m to 20m	Up to 20m

The comparison of empirical formula for estimating strength of rectangular pillar from this research with the previous research also shows that the slenderness constant is related with the material properties. Both work use the simulation model as the analytical method. The previous work covered a wider of *w/h* ratio. As strength of potash is higher compared to those of coal, the design of potash pillar can be effectively work in a smaller range of *w/h* ratio. Empirical strength formulation from both work is recommended for similar mining height which is up to 20m.

CHAPTER 7

CONCLUSIONS AND RECOMMENDATIONS

7.1. Conclusions

Numerical simulation is a powerful tool for underground pillar design. However, in order to obtain the best result, it required input parameters as realistic as possible. The equation for strength estimation from Obert and Duvall is not suitable for estimating pillar strength of potash in Thailand as it tends to underestimate the strength value. In underground pillar design, the wider width is required when the mine go deeper. There is no specific optimum dimension that fit all underground pillar design as the geometry of the deposit differ from one another. The optimum dimension can only be represented by using safety envelope. Through this research work, it can be concluded as the following:

A. Pillar design

a. Equation 2-1, which is used for estimating the stress on pillar, can be effectively used for potash underground pillar design in Thailand as it provides an undistinguishable value of stress compared with numerical simulation.

b. Based on numerical analysis of pillar strength estimation, Obert and Duvall equation has been modified into Equation 6-1. This modified formula is in good agreement with all numerical simulation as the values of estimated strength are correlated satisfactorily. This confirms the capability of Equation 6-1 for estimating potash pillar strength with the specific range of parameter condition that is mentioned in Section 6.2.4 of Chapter 6.

c. Safety envelope can be used as a primary tool for designing pillar as it shows the optimum w/h ratio corresponding to extraction ratio. Based on the safety envelope, in the range of studied *w/h* ratio, the maximum extraction ratio tends to decrease from 80% to 70% as the depth increase from 200m to 300m.

B. Barrier pillar design

a. Barrier pillar stress estimation also follows the rule of Equation 2-1 even if the barrier pillar shape is different from pillar. Barrier Pillar stress can also be estimated effectively using this equation.

b. Based on numerical analysis of barrier pillar strength estimation, the modification of Obert and Duvall equation for barrier pillar provides different slenderness constants from those of the normal pillar since the results are varied according to the different shapes. Obert and Duvall equation has been modified into Equation 6-2. This modified formula is confirmed its capability for estimating potash barrier pillar strength with the specific range of parameter condition that is mentioned in Section 6.3.4 of Chapter 6.

c. The optimum barrier pillar design is also represented by safety envelope. The same conclusion can be drawn out from barrier pillar safety envelope in which the maximum extraction ratio decreases about 10% while the depth increase 100m.

d. Relationship between panel width and barrier pillar width based on mining height can be generated from the safety envelope of barrier pillar. This relationship can be further generalized base on depth of the deposit which are expressed in the Equation 6-16. This equation can be utilized to define the panel width from barrier pillar width, mining height and depth of the deposit with the specific range of parameter condition that is mentioned in Section 6.3.5 of Chapter 6.

7.2. Recommendations

In addition to the simulated input parameters, the future study should perform more tests on the real potash sample in order to obtain input parameters as realistic as possible. The study of field test from real potash underground mine is also another key factor to increase the confidence of the utilization of this empirical formulation.

The height of the mine can be limited by technology and equipment. As a result, some of the mine cannot excavate the material to their optimum extraction because of the height limit. As the matter of fact, the future study should also focus on double or multiple seams mining or underground benching in order to increase the extraction ratio to the optimum point.

REFERENCES

[1] Garrett, D.E., *Potash: Deposits, Processing, Properties and Uses*. 1996. Netherlands. Springer

[2] Suwanich, P., *Potash-evaporite deposits in Thailand*. in *Geo_Thai Proceedings of the International Conference on Geology of Thailand*. 2007.

[3] Japakasetr, T., and Workman, D., *Evaporite deposits of northeast Thailand.* SG 12: Energy Resources of the Pacific Region, 1981.

[4] Bartlett, R.W., *Solution Mining: Leaching and Fluid Recovery of Materials*. Vol. 2. 1998. Gordon and Breach Science Publishers.

[5] Hamrin, H., *Underground Mining Methods and Applications*. Underground Mining Methods: Engineering Fundamentals and International Case Studies, ed. W.A. Hustrulid and R.L. Bullock. 2001. Society for Mining, Metallurgy, and Exploration. 3-14.

[6] Livingstone, P., Purcell, J., Morehouse, D., and Waugh, D., *Mining at IMC Potash Carlsbad.* Underground Mining Methods: Engineering Fundamentals and International Case Studies. Society of Mining, Metallurgy and Exploration, 2001. p. 131-136.

[7] Lau, L.I.H., *Performance of Pillars in Rock Salt Mines.* 2010.

[8] Sheorey, P.R., *A theory for in situ stresses in isotropic and transverseley isotropic rock*. in *International journal of rock mechanics and mining sciences & geomechanics abstracts*. 1994. Elsevier.

[9] Esterhuizen, G., Dolinar, D.R., and Ellenberger, J.L., *Pillar strength and design methodology for stone mines*. in *Proceedings of the 27th international conference on ground control in mining. Morgantown WV: West Virginia University*. 2008.

[10] Zipf, R.K., *Pillar design to prevent collapse of room-and-pillar mines.* Underground Mining Methods: Engineering Fundamentals and International Case Studies, 2001. p. 493-511.

[11] Jeremic, M.L., *Rock Mechanics in Salt Mining*. 1994. Taylor & Francis.

[12] Obert, L., and Duvall, W.I., *Rock Mechanics and the design of structures in rock.* 1967.

[13] Bieniawski, Z.T., *Rock mechanics design in mining and tunneling*. 1984. A.A. Balkema.

[14] Mark, C., Chase, F.E., and Campoli, A.A., *Analysis of retreat mining pillar stability*. 1995. West Virginia Univ., Morgantown, WV (United States).

[15] Vermeer, P.A., and De Borst, R., *Non-associated plasticity for soils, concrete and rock.* HERON, 1984.

[16] Mohan, G.M., Sheorey, P., and Kushwaha, A., *Numerical estimation of pillar strength in coal mines.* International Journal of Rock Mechanics and Mining Sciences, 2001. 38(8). p. 1185-1192.

[17] Arthur, F., and Ge, M., *Numerical Estimation of the Strength of St. Peter Sandstone Pillars–A Case Study at Iowa*. in *49th US Rock Mechanics/Geomechanics Symposium*. 2015. American Rock Mechanics Association.

[18] Verma, C.P., Porathur, J.L., Thote, N.R., Roy, P.P., and Karekal, S., *Empirical Approaches for Design of Web Pillars in Highwall Mining: Review and Analysis.* Geotechnical and Geological Engineering, 2014. 32(2). p. 587-599.

[19] Kolano, M., and Flisiak, D., *Comparison of geo-mechanical properties of white rock salt and pink rock salt in Kłodawa salt diapir.* Studia Geotechnica et Mechanica, 2013. 35(1). p. 119-127.

APPENDIX A

Drilled-holes Information

DH2				
Rock Strata	**Density**	**Thickness**	**Unit Weight**	**Stress**
	(Kg/m^3)	**(m)**	**kN/m^3**	**MPa**
Topsoil	1600	2	15.70	0.03
Siltstone	2000	84.5	19.62	1.66
Anhydrite	2400	3.7	23.54	0.09
Claystone	2100	36.5	20.60	0.75
Halite	2110	109.3	20.70	2.26
Claystone	2100	19.1	20.60	0.39
Anhydrite	2400	4.4	23.54	0.10
Total		259.5	**Average**	5.29

DH3				
Rock Strata	**Density**	**Thickness**	**Unit Weight**	**Stress**
	(Kg/m^3)	**(m)**	**kN/m^3**	**MPa**
Topsoil	1600	2	15.70	0.03
Siltstone	2000	104	19.62	2.04
Anhydrite	2400	5	23.54	0.12
Claystone	2100	29	20.60	0.60
Anhydrite	2400	13.5	23.54	0.32
Halite	2110	114.3	20.70	2.37
Claystone	2100	26.2	20.60	0.54
Anhydrite	2400	10	23.54	0.24
Halite	2110	22.6	20.70	0.47
Total		326.6	**Average**	6.71

DH4				
Rock Strata	Density	Thickness	Unit Weight	Stress
	(Kg/m^3)	(m)	kN/m^3	MPa
Topsoil	1600	3.5	15.70	0.05
Siltstone	2000	46.5	19.62	0.91
Anhydrite	2400	5.8	23.54	0.14
Claystone	2100	34.5	20.60	0.71
Halite	2110	103.5	20.70	2.14
Claystone	2100	35.8	20.60	0.74
Halite	2110	59	20.70	1.22
Total		288.6	**Average**	5.92

DH5				
Rock Strata	Density	Thickness	Unit Weight	Stress
	(Kg/m^3)	(m)	kN/m^3	MPa
Topsoil	1600	2.5	15.70	0.04
Siltstone	2000	48.5	19.62	0.95
Claystone	2100	36.8	20.60	0.76
Anhydrite	2400	6.2	23.54	0.15
Halite	2110	91.5	20.70	1.89
Claystone	2100	22.3	20.60	0.46
Halite	2110	4.4	20.70	0.09
Total		212.2	**Average**	4.34

DH6				
Rock Strata	Density	Thickness	Unit Weight	Stress
	(Kg/m^3)	(m)	kN/m^3	MPa
Topsoil	1600	7	15.70	0.11
Claystone	2100	16.5	20.60	0.34
Siltstone	2000	18.5	19.62	0.36
Anhydrite	2400	6.6	23.54	0.16
Claystone	2100	21.4	20.60	0.44
Anhydrite	2400	15.3	23.54	0.36
Halite	2110	87.6	20.70	1.81
Claystone	2100	10.1	20.60	0.21
Halite	2110	1	20.70	0.02
Total		184	**Average**	3.81

DH7				
Rock Strata	Density	Thickness	Unit Weight	Stress
	(Kg/m^3)	(m)	kN/m^3	MPa
Topsoil	1600	1.8	15.70	0.03
Siltstone	2000	53.7	19.62	1.05
Anhydrite	2400	6.8	23.54	0.16
Claystone	2100	27.7	20.60	0.57
Anhydrite	2400	7.5	23.54	0.18
Halite	2110	98.9	20.70	2.05
Claystone	2100	12.1	20.60	0.25
Halite	2110	3.9	20.70	0.08
Total		212.4	**Average**	4.37

APPENDIX B

Input Parameters Estimation Results

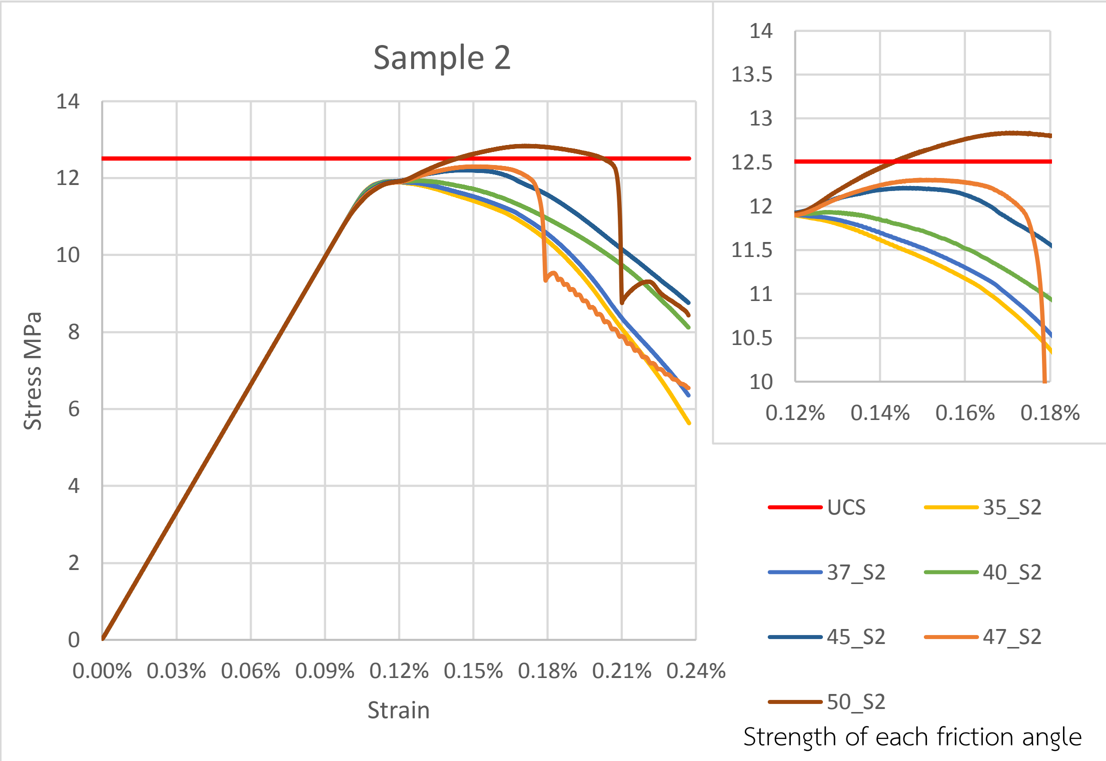
Sample 2
Stress MPa
Strain
0
2
4
6
8
10
12
14
0.00%
0.03%
0.06%
0.09%
0.12%
0.15%
0.18%
0.21%
0.24%
10
10.5
11
11.5
12
12.5
13
13.5
14
0.12%
0.14%
0.16%
0.18%
UCS
35_S2
37_S2
40_S2
45_S2
47_S2
50_S2
Strength of each friction angle

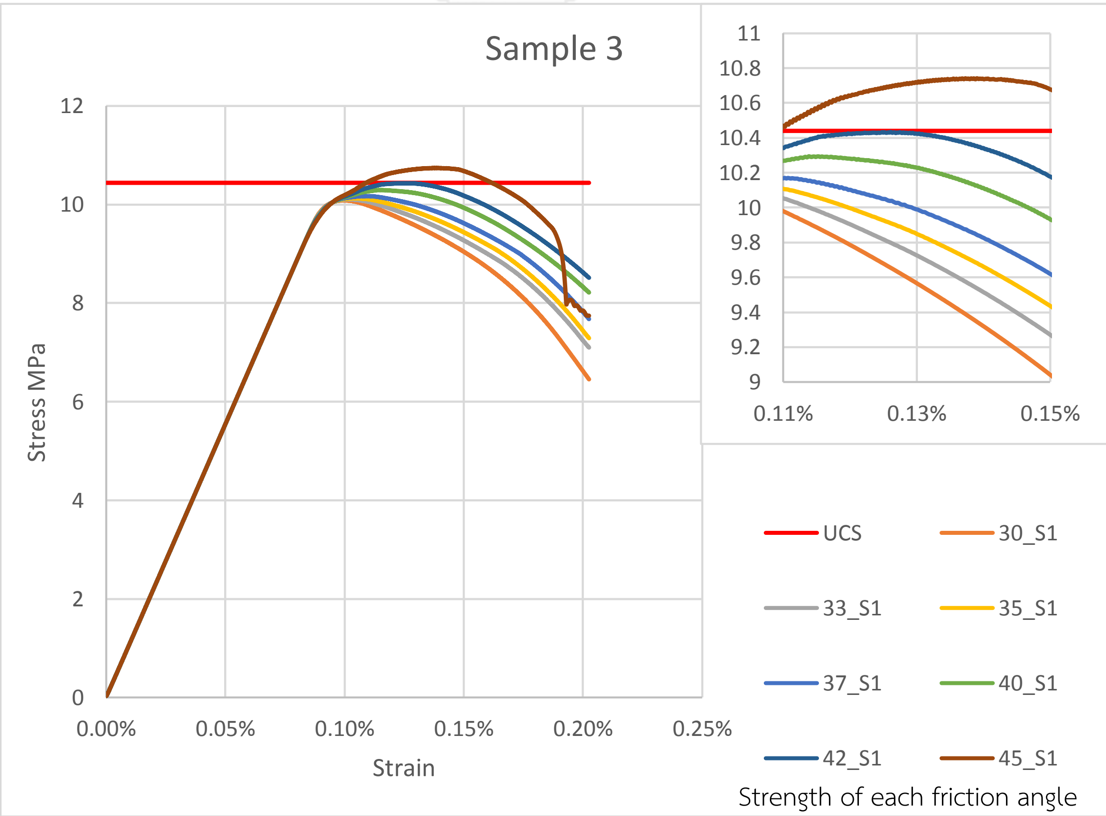
Sample 3
Stress MPa
Strain
0
2
4
6
8
10
12
0.00%
0.05%
0.10%
0.15%
0.20%
0.25%
9
9.2
9.4
9.6
9.8
10
10.2
10.4
10.6
10.8
11
0.11%
0.13%
0.15%
UCS
30_S1
33_S1
35_S1
37_S1
40_S1
42_S1
45_S1
Strength of each friction angle

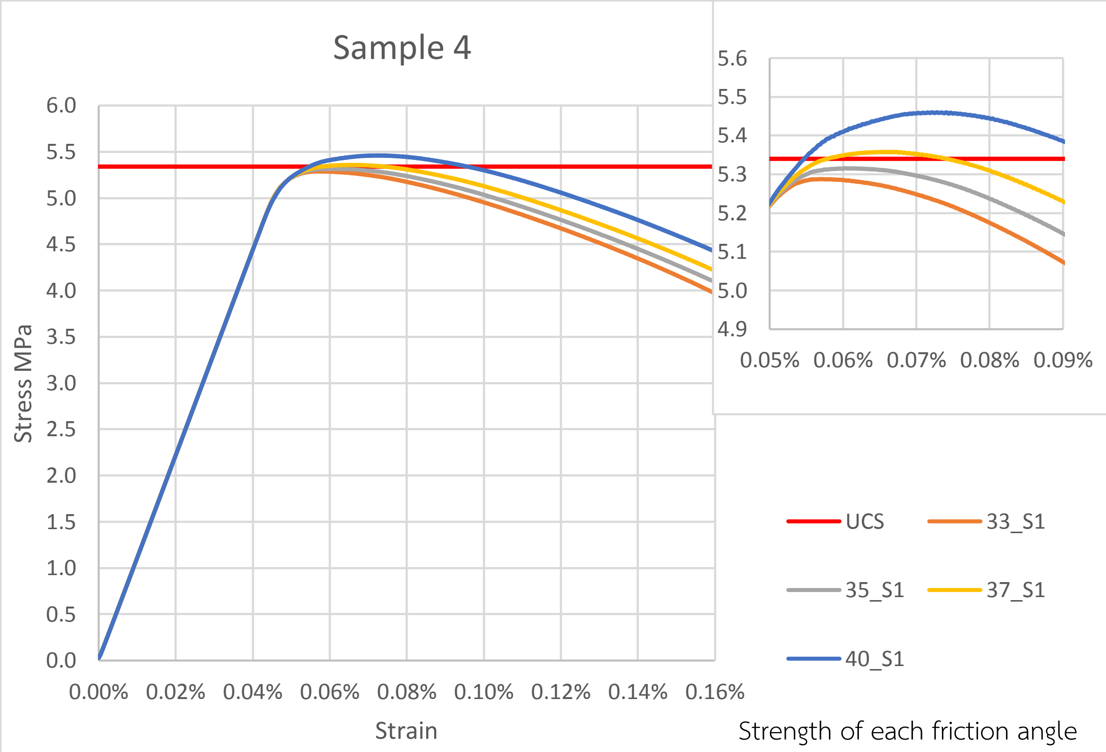
Sample 4
Stress MPa
6.0
5.5
5.0
4.5
4.0
3.5
3.0
2.5
2.0
1.5
1.0
0.5
0.0
0.00% 0.02% 0.04% 0.06% 0.08% 0.10% 0.12% 0.14% 0.16%
Strain
5.6
5.5
5.4
5.3
5.2
5.1
5.0
4.9
0.05% 0.06% 0.07% 0.08% 0.09%
UCS
33_S1
35_S1
37_S1
40_S1
Strength of each friction angle

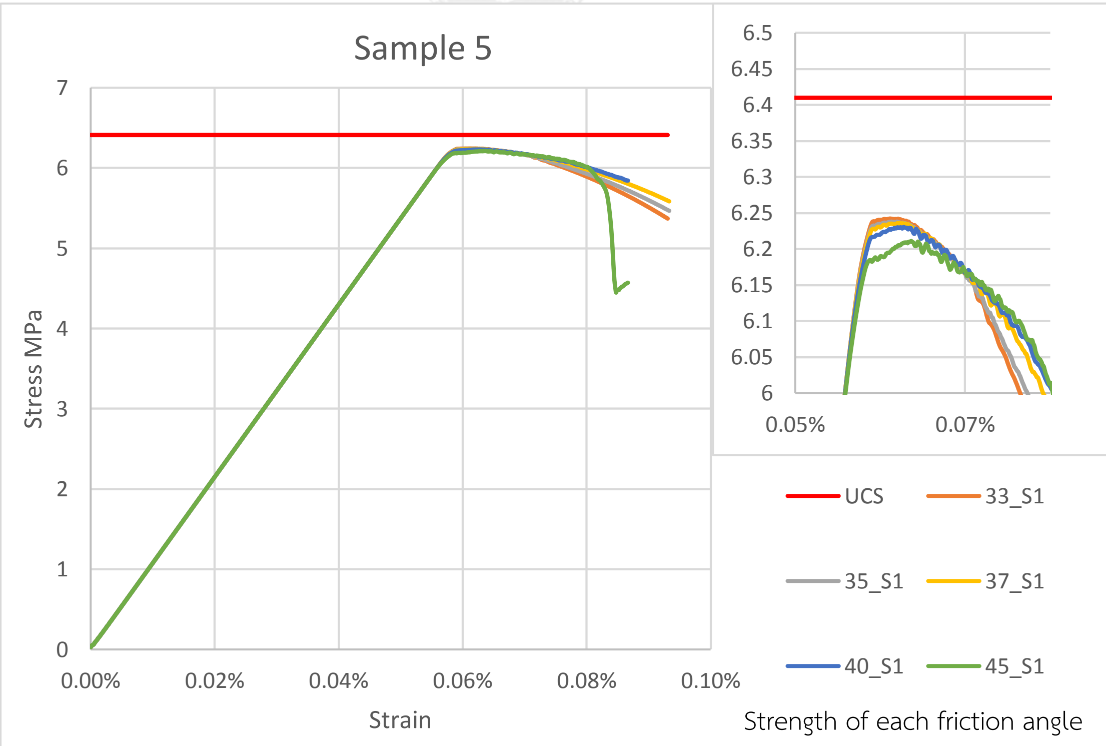
Sample 5
Stress MPa
7
6
5
4
3
2
1
0
0.00% 0.02% 0.04% 0.06% 0.08% 0.10%
Strain
6.5
6.45
6.4
6.35
6.3
6.25
6.2
6.15
6.1
6.05
6
0.05% 0.07%
UCS
33_S1
35_S1
37_S1
40_S1
45_S1
Strength of each friction angle

APPENDIX C

Correlations Between SF and w/h of Pillar

H = 250m

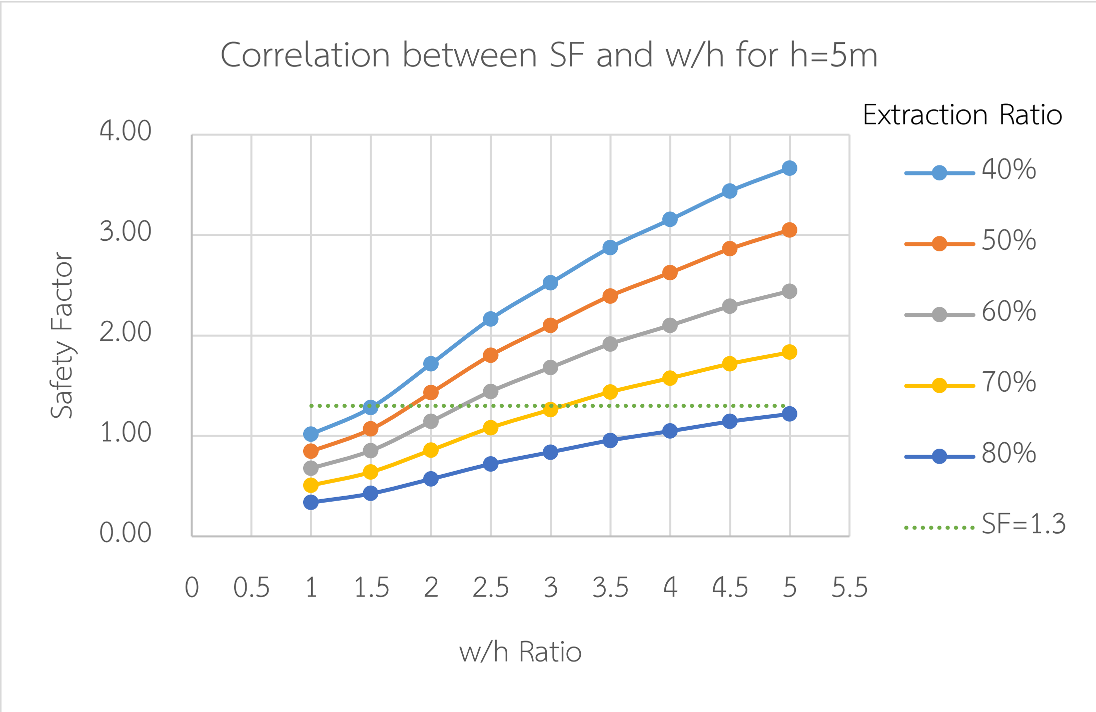
Correlation between SF and w/h for h=5m
Extraction Ratio
40%
50%
60%
70%
80%
SF=1.3
Safety Factor
4.00
3.00
2.00
1.00
0.00
0
0.5
1
1.5
2
2.5
3
3.5
4
4.5
5
5.5
w/h Ratio

H = 250m

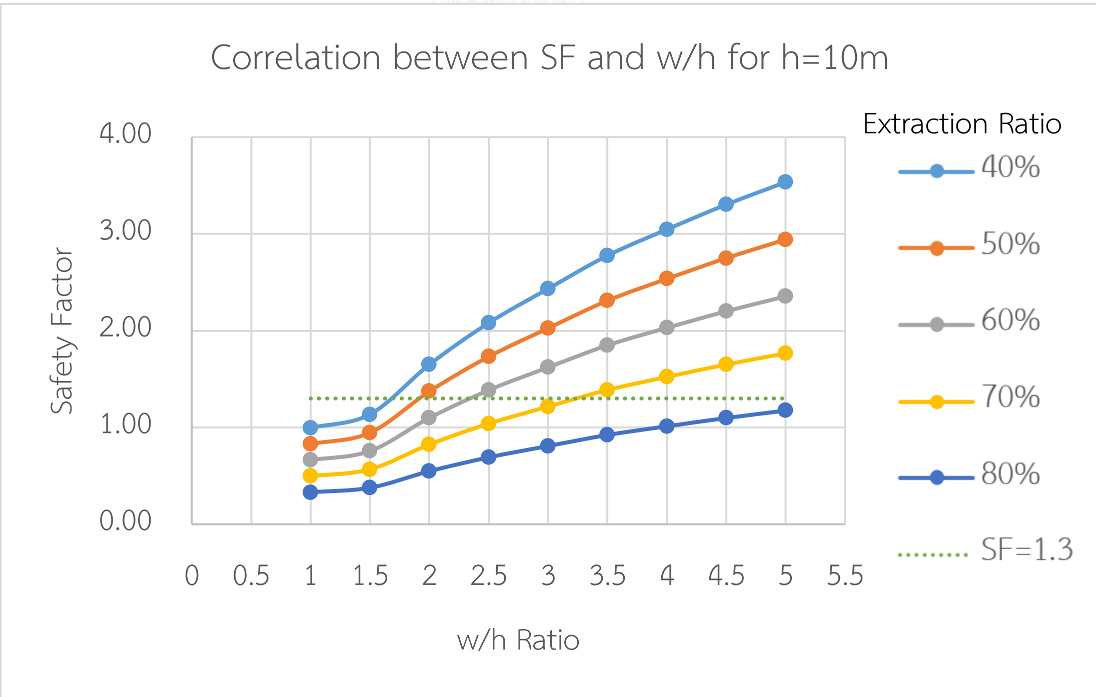
Correlation between SF and w/h for h=10m
Extraction Ratio
40%
50%
60%
70%
80%
SF=1.3
Safety Factor
4.00
3.00
2.00
1.00
0.00
0
0.5
1
1.5
2
2.5
3
3.5
4
4.5
5
5.5
w/h Ratio

H = 250m

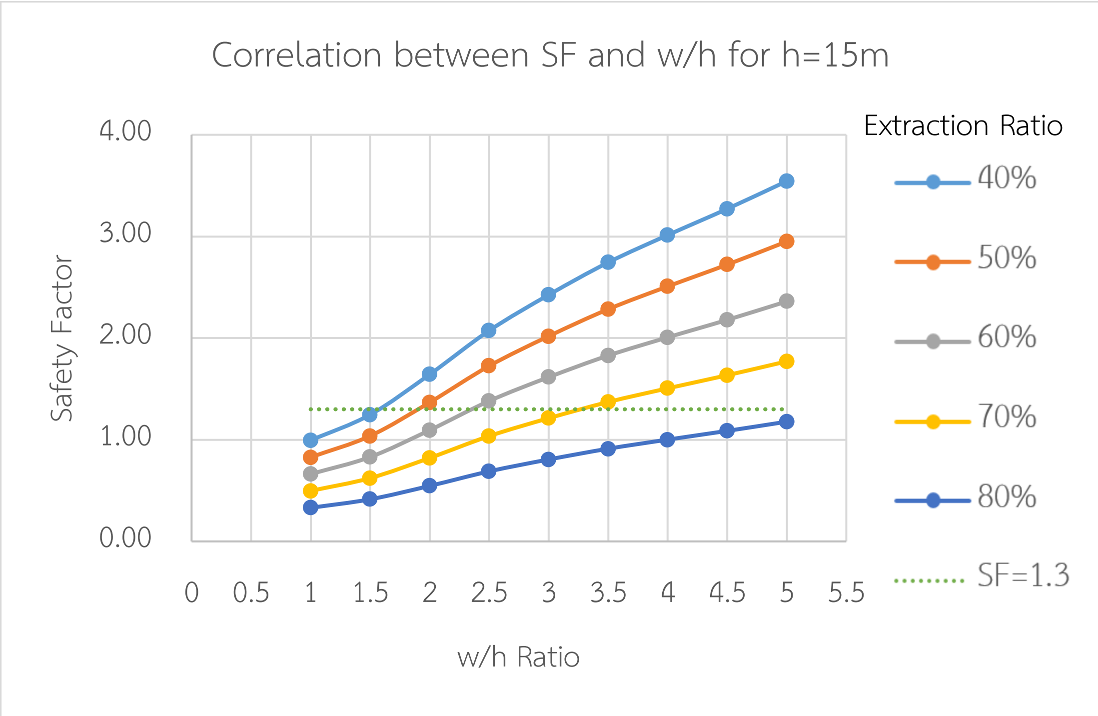

Correlation between SF and w/h for h=15m
Safety Factor
4.00
3.00
2.00
1.00
0.00
0
0.5
1
1.5
2
2.5
3
3.5
4
4.5
5
5.5
w/h Ratio
Extraction Ratio
40%
50%
60%
70%
80%
SF=1.3

H = 250m

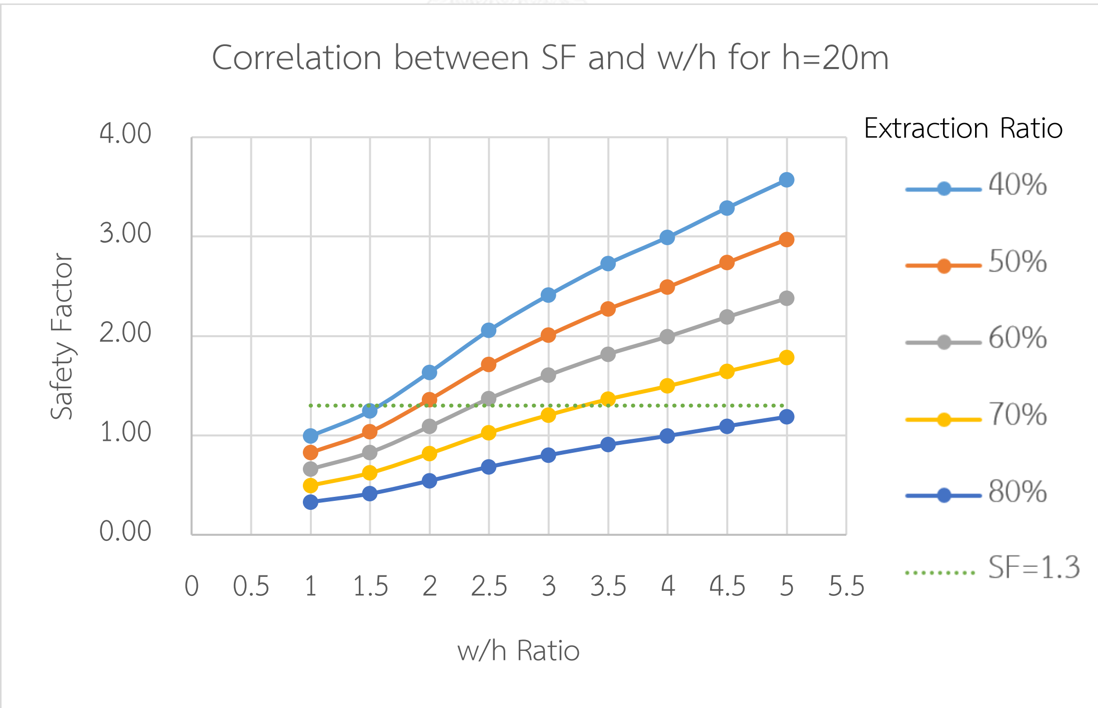

Correlation between SF and w/h for h=20m
Safety Factor
4.00
3.00
2.00
1.00
0.00
0
0.5
1
1.5
2
2.5
3
3.5
4
4.5
5
5.5
w/h Ratio
Extraction Ratio
40%
50%
60%
70%
80%
SF=1.3

H = 300m

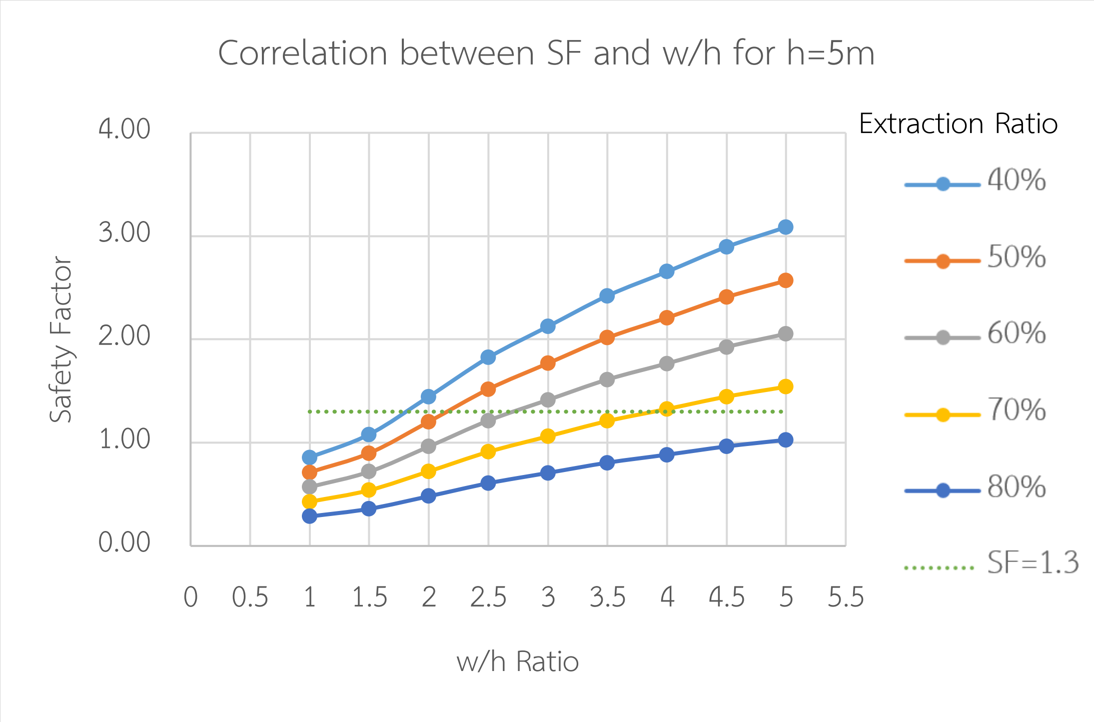
Correlation between SF and w/h for h=5m
Safety Factor
4.00
3.00
2.00
1.00
0.00
0
0.5
1
1.5
2
2.5
3
3.5
4
4.5
5
5.5
w/h Ratio
Extraction Ratio
40%
50%
60%
70%
80%
SF=1.3

H = 300m

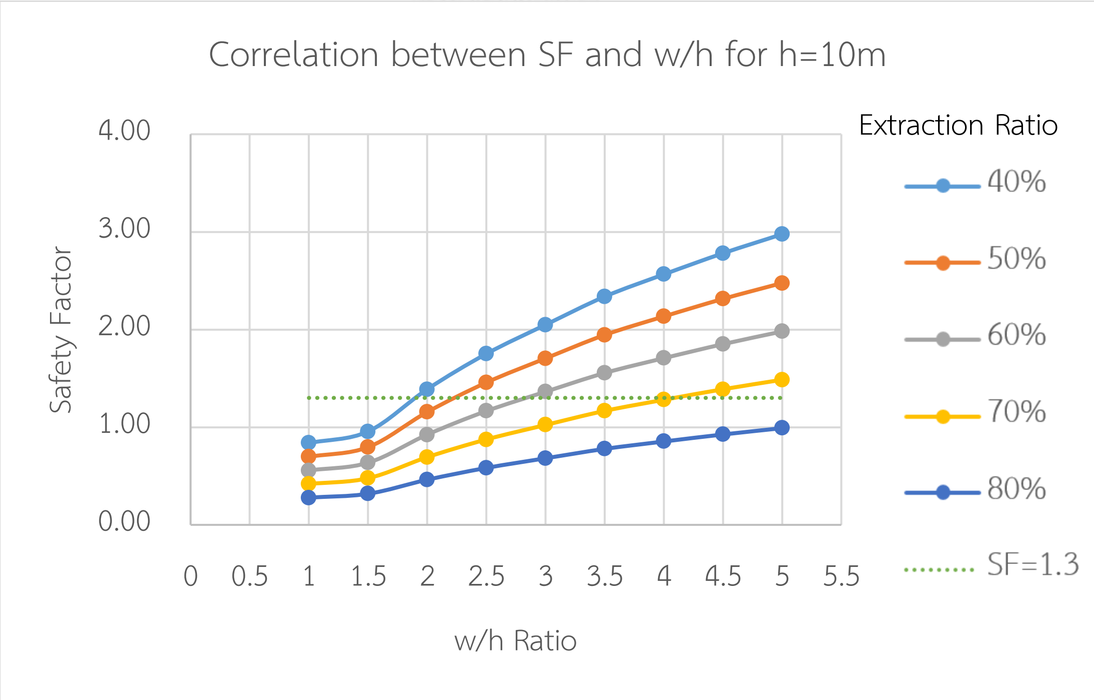
Correlation between SF and w/h for h=10m
Safety Factor
4.00
3.00
2.00
1.00
0.00
0
0.5
1
1.5
2
2.5
3
3.5
4
4.5
5
5.5
w/h Ratio
Extraction Ratio
40%
50%
60%
70%
80%
SF=1.3

H = 300m

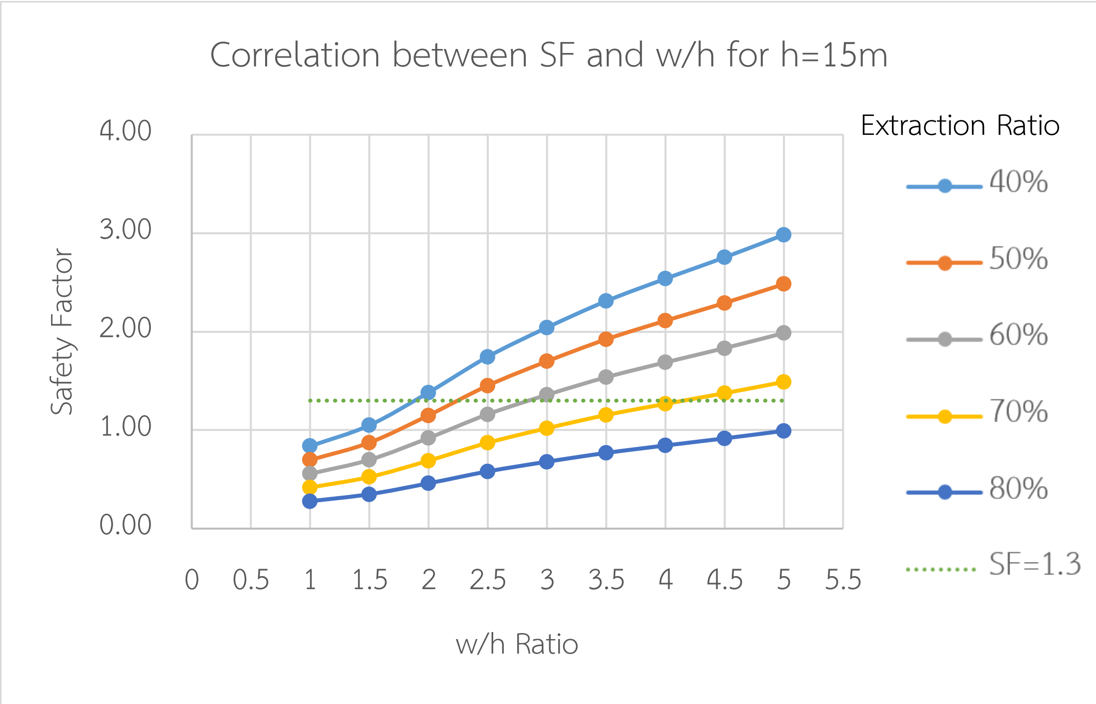
Correlation between SF and w/h for h=15m
Safety Factor
4.00
3.00
2.00
1.00
0.00
0
0.5
1
1.5
2
2.5
3
3.5
4
4.5
5
5.5
w/h Ratio
Extraction Ratio
40%
50%
60%
70%
80%
SF=1.3

H = 300m

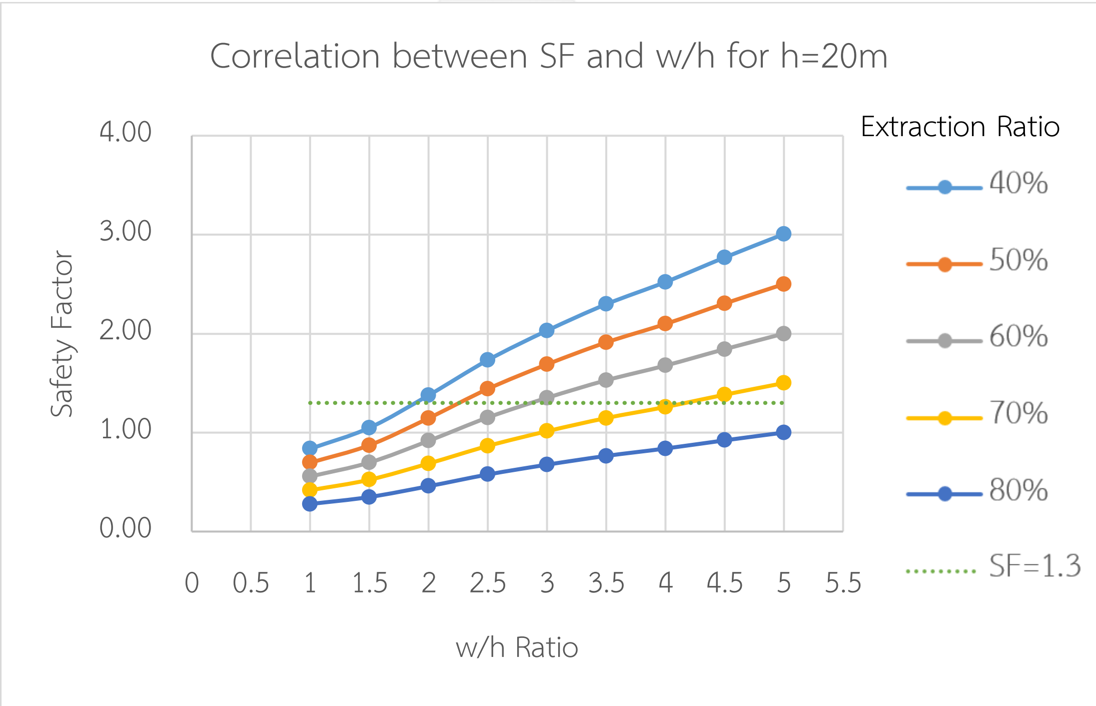
Correlation between SF and w/h for h=20m
Safety Factor
4.00
3.00
2.00
1.00
0.00
0
0.5
1
1.5
2
2.5
3
3.5
4
4.5
5
5.5
w/h Ratio
Extraction Ratio
40%
50%
60%
70%
80%
SF=1.3

APPENDIX D

Correlations Between SF and w/h of Barrier Pillar

H = 250m

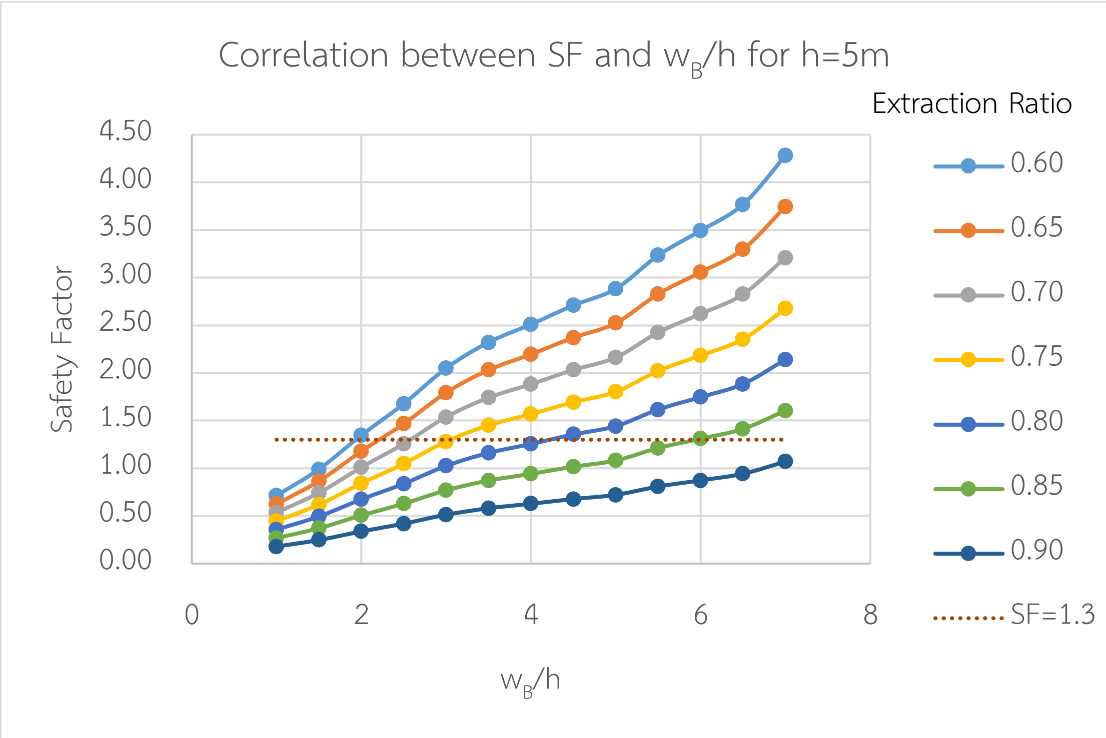

Correlation between SF and w_B/h for h=5m
Extraction Ratio
0.60
0.65
0.70
0.75
0.80
0.85
0.90
SF=1.3
Safety Factor
0.00
0.50
1.00
1.50
2.00
2.50
3.00
3.50
4.00
4.50
0
2
4
6
8
w_B/h

H = 250m

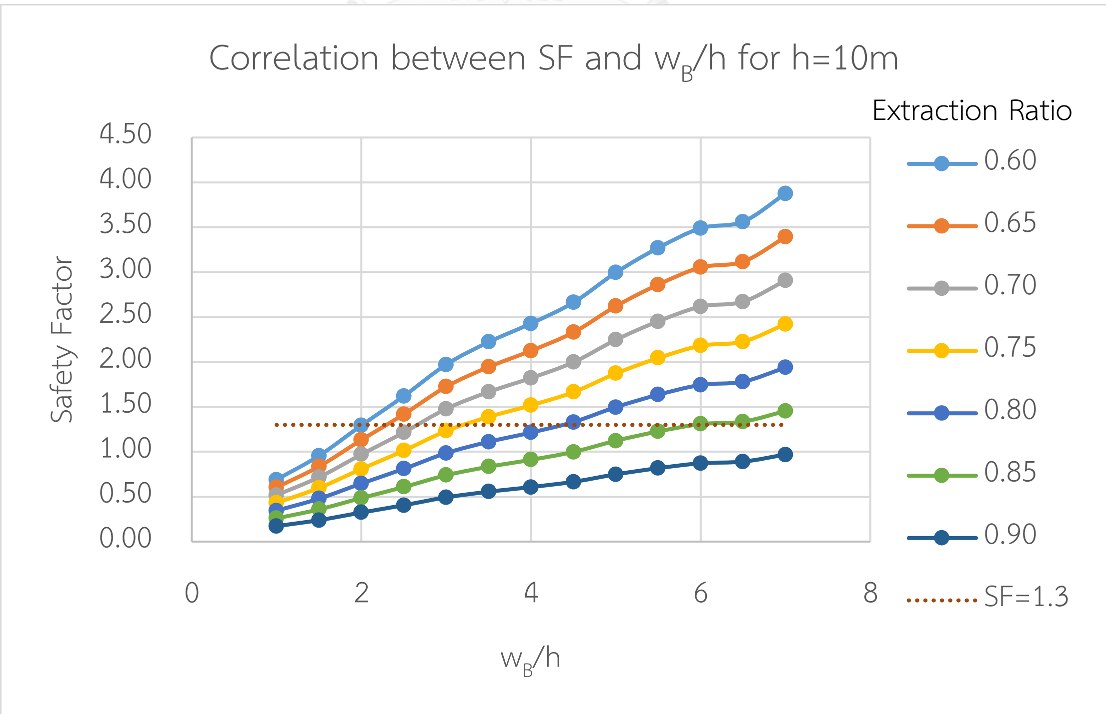

Correlation between SF and w_B/h for h=10m
Extraction Ratio
0.60
0.65
0.70
0.75
0.80
0.85
0.90
SF=1.3
Safety Factor
0.00
0.50
1.00
1.50
2.00
2.50
3.00
3.50
4.00
4.50
0
2
4
6
8
w_B/h

H = 250m

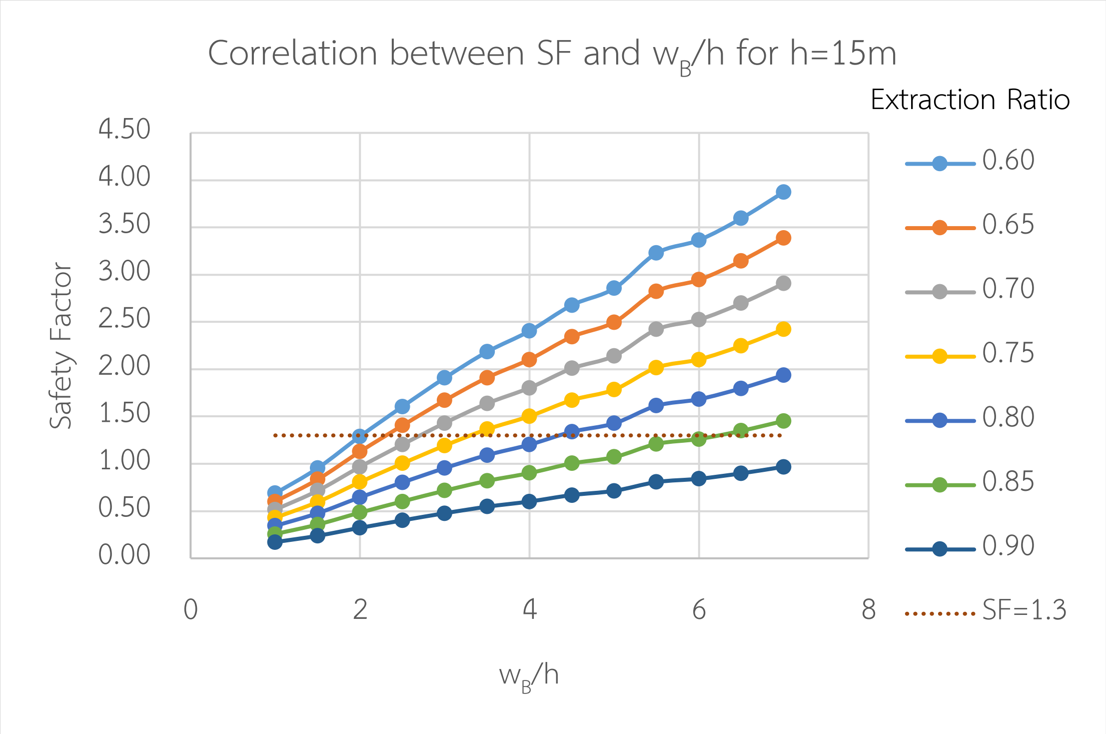

Correlation between SF and w_B/h for h=15m
Extraction Ratio
Safety Factor
4.50
4.00
3.50
3.00
2.50
2.00
1.50
1.00
0.50
0.00
0
2
4
6
8
w_B/h
0.60
0.65
0.70
0.75
0.80
0.85
0.90
SF=1.3

H = 250m

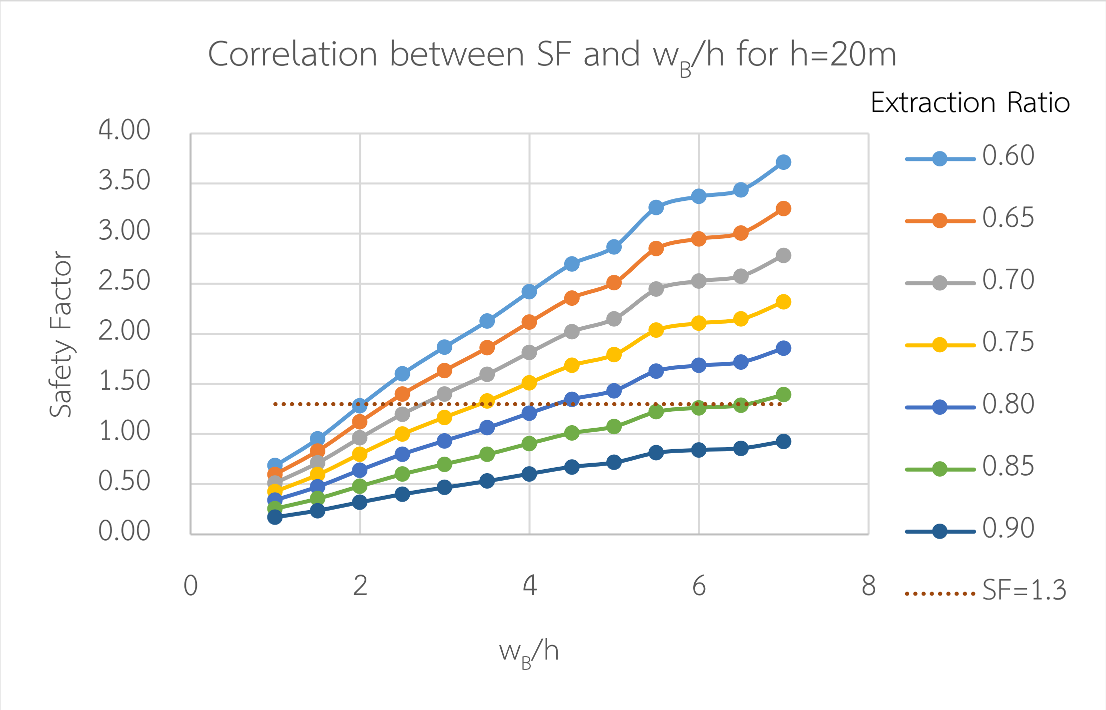

Correlation between SF and w_B/h for h=20m
Extraction Ratio
Safety Factor
4.00
3.50
3.00
2.50
2.00
1.50
1.00
0.50
0.00
0
2
4
6
8
w_B/h
0.60
0.65
0.70
0.75
0.80
0.85
0.90
SF=1.3

H = 300m

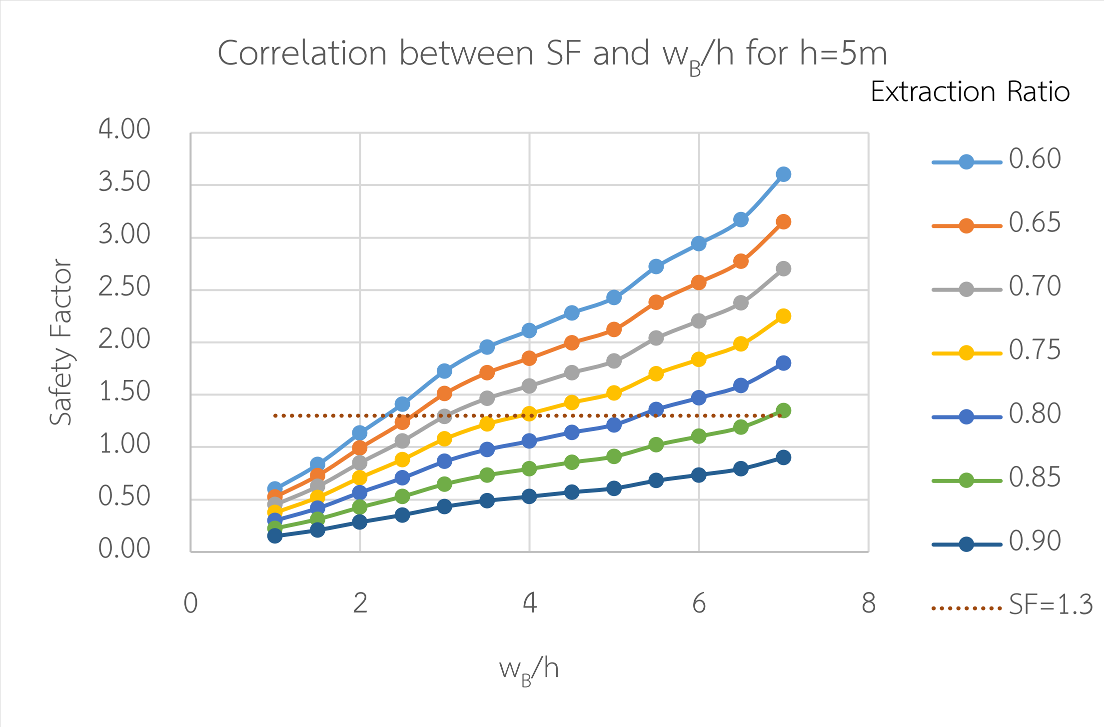

Correlation between SF and w_B/h for h=5m
Extraction Ratio
4.00
3.50
3.00
2.50
2.00
1.50
1.00
0.50
0.00
Safety Factor
0
2
4
6
8
w_B/h
0.60
0.65
0.70
0.75
0.80
0.85
0.90
SF=1.3

H = 300m

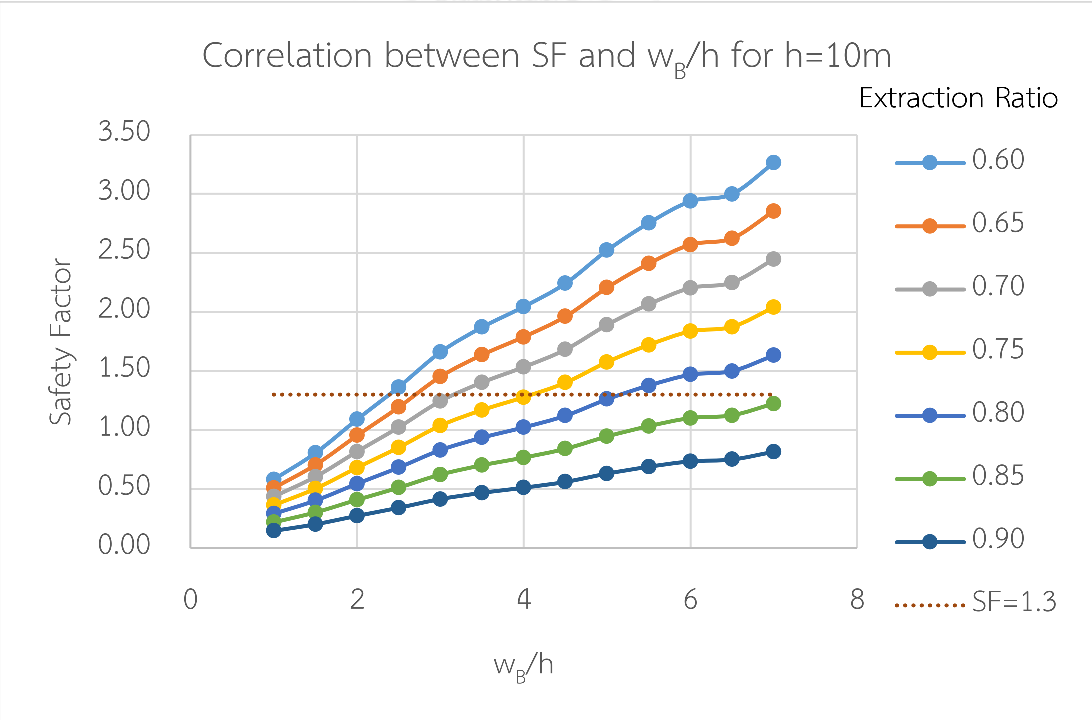

Correlation between SF and w_B/h for h=10m
Extraction Ratio
3.50
3.00
2.50
2.00
1.50
1.00
0.50
0.00
Safety Factor
0
2
4
6
8
w_B/h
0.60
0.65
0.70
0.75
0.80
0.85
0.90
SF=1.3

H = 300m

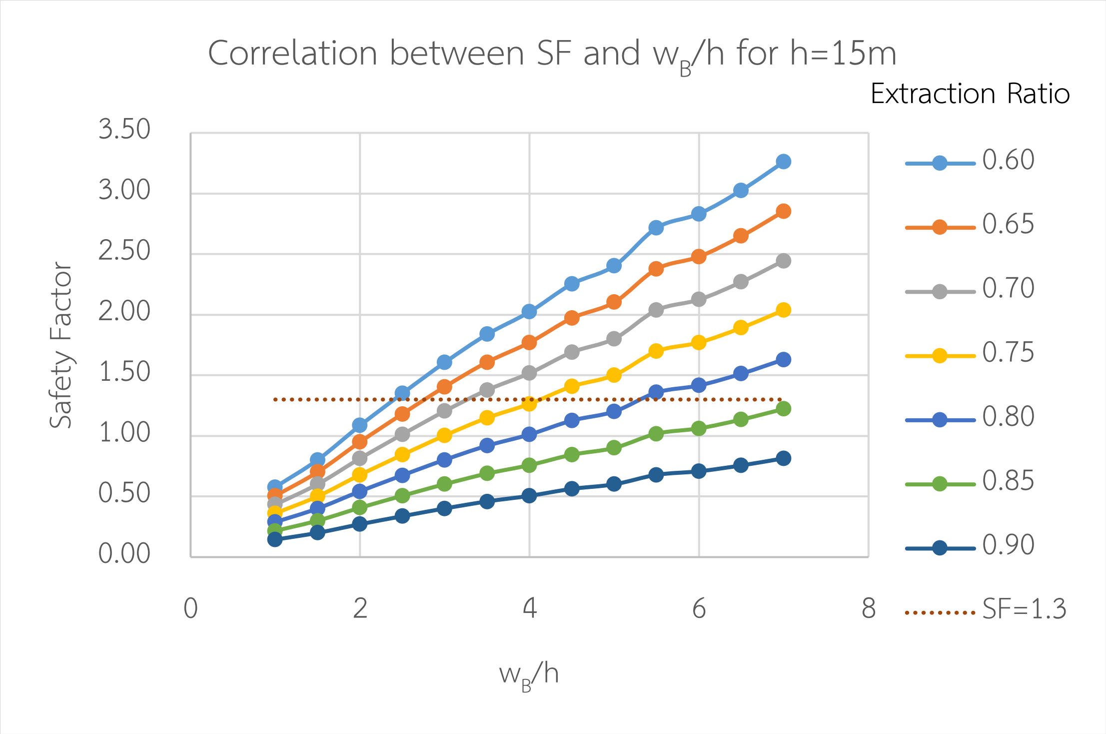
Correlation between SF and w_B/h for h=15m
Extraction Ratio
3.50
3.00
2.50
2.00
1.50
1.00
0.50
0.00
Safety Factor
0
2
4
6
8
w_B/h
0.60
0.65
0.70
0.75
0.80
0.85
0.90
SF=1.3

H = 300m

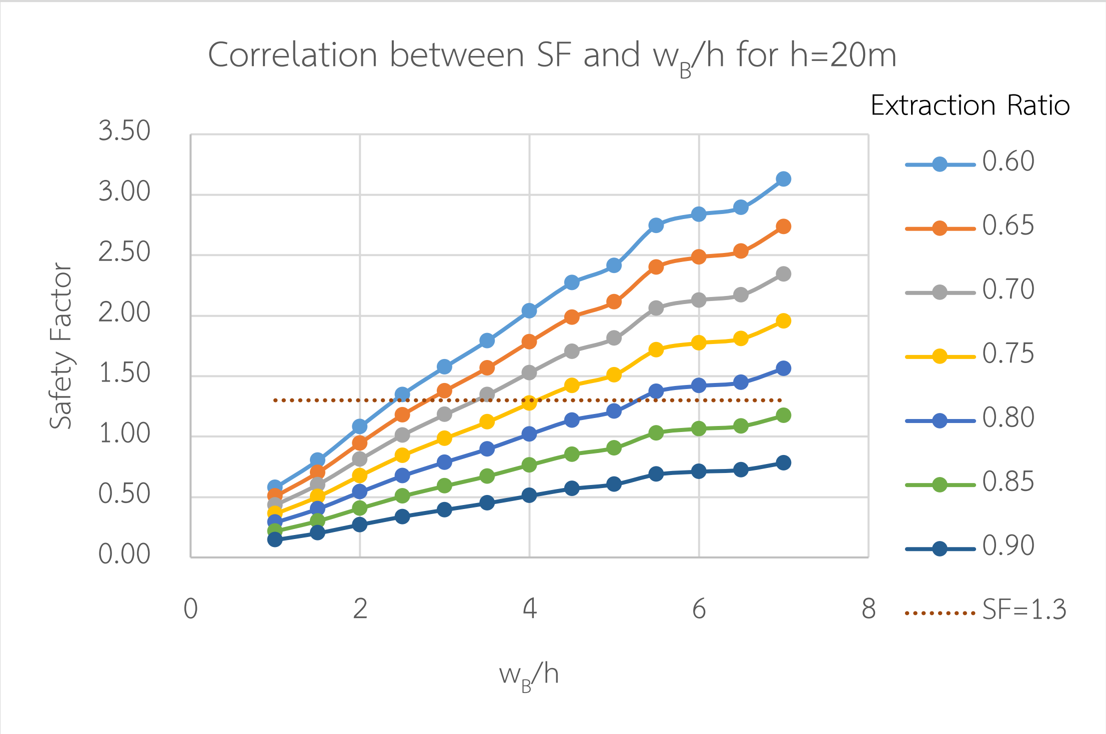
Correlation between SF and w_B/h for h=20m
Extraction Ratio
3.50
3.00
2.50
2.00
1.50
1.00
0.50
0.00
Safety Factor
0
2
4
6
8
w_B/h
0.60
0.65
0.70
0.75
0.80
0.85
0.90
SF=1.3

VITA

Mr. Pisith Mao was born in Phnom Penh, capital city of Cambodia on June 24th, 1992. After graduated from high school in 2009, he had passed the entrance exam and continued his bachelor degree in geo-resources and geotechnical engineering in Institute of Technology of Cambodia (ITC). In 2013, he got an offer from Chulalongkorn University of Thailand for one semester exchange which is sponsored by ASEAN scholarship for neighboring country. He had successfully graduated from ITC in 2014. At that graduation year, he got a scholarship from AUN/SEED-Net program, sponsored by JICA, to study his master degree in geo-resources engineering at Chulalongkorn University for two years. He is now on proceeding as a presenter for “ASEAN++2016 Towards Geo-Resources Education in ASEAN Economic Community” conference.